AN ABSTRACT OF THE THESIS OF

Justin D. Hynicka for the degree of Master of Science in Forest Ecosystems and Society and Soil Science presented on July 30, 2014.

Title: Interactions Between Ecosystem Nitrogen and Bedrock Control Long-term Calcium Sources in Oregon Coast Range Forests

Abstract approved:

Steven S. Perakis Julie Pett-Ridge

Ecosystem nitrogen (N) supply strongly influences the availability and cycling of other essential nutrients in temperate forests, especially calcium (Ca). Short-term additions of N that exceed ecosystem demands often increase dissolved nitrate fluxes and decrease soil pH, which can stimulate soil Ca loss. However, the long-term effects of high N supply on ecosystem Ca availability are more difficult to determine, and may depend on the Ca content of bedrock and mineral soils. To address this, we examined major and trace element concentrations and $^{87}Sr/^{86}Sr$ ratios that trace Ca sources in precipitation, foliage, soil pools, and bedrock at 24 forested sites in the Oregon Coast Range having a wide, natural range of soil N (0.16 – 0.97 % N, 0-10 cm) on contrasting basaltic and sedimentary bedrock. Using a suite of 17 site properties, we also evaluated whether soil N variation across sites was related to the

five major state-factors of soil and ecosystem development: climate, organisms, topography, parent material, and time.

We found that as soil N increased across sites, its $^{15}N/^{14}N$ ratio declined towards atmospheric values, suggesting that soil N variation reflects a biotic legacy of symbiotic N fixation inputs. In contrast, soil N variation was unrelated to 17 other metrics of soil forming factors that represented climate (mean annual precipitation, mean annual temperature, and distance from the coast), topography (slope, soil depth, and abundance of coarse rock fragments), parent material (within bedrock type bulk and 1 M HNO_3 leachable rock Ca chemistry), and proxies of soil age (Hurst's redness rating, effective cation exchange capacity, Ca in non-exchangeable soil residues, chemical index of alteration, weathering index of Parker, Ca in coarse soil fragments, and soil Ca loss relative to bedrock). These analyses highlight symbiotic N-fixing red alder as a keystone organismal state-factor that produces a wide range of soil N accumulation in coastal Oregon forests.

Strontium isotopes ($^{87}Sr/^{86}Sr$) and other geochemical analyses indicate that long-term Ca sources in foliage and exchangeable soil pools in Oregon Coast Range forests depend on an interactive effect between N availability and bedrock. Basaltic rocks contained nearly 20-times more Ca than sedimentary rocks across our sites, and this difference was reflected in Sr-isotope partitioning of base cation sources. Atmospheric sources dominated plant and soil pools in forests overlying Ca-poor sedimentary rock, regardless of variation in soil N, indicating extremely limited capacity of weathering to support forest Ca demands. In contrast, forests overlying

basaltic rock obtained as much as 80% of Ca from rock weathering in low N sites, yet relied to a greater extent on atmospheric Ca as soil N increased, with less than 10% of Ca from rock weathering at sites with the highest soil N. Surprisingly, differences in fresh rock Ca content and base cation sources between sedimentary and basaltic sites was not reflected in ecosystem Ca availability, and instead increasing soil N caused similar declines in foliar and exchangeable Ca across both rock types. This illustrates that nutrient pool sizes do not necessarily reflect long-term nutrient supply, and highlights how coupled biogeochemical cycles within ecosystems can regulate nutrient loss and supply to biota. Broadly, our results highlight how interactions between biological and geologic factors can influence base cation sources in forest ecosystems. The sustainability of base cation supplies to forests may therefore depend greatly on variation in bedrock weathering at low N sites, yet converge to depend on atmospheric inputs in sites that receive high N loading from biological fixation or anthropogenic deposition.

Interactions Between Ecosystem Nitrogen and Bedrock Control Long-term Calcium Sources in Oregon Coast Range Forests

by
Justin D. Hynicka

A THESIS

submitted to

Oregon State University

in partial fulfillment of
the requirements for the
degree of

Master of Science

Presented July 30, 2014
Commencement June 2015

Master of Science thesis of Justin D. Hynicka presented on July 30, 2014.

APPROVED:

Co-Major Professor, representing Forest Ecosystems and Society

Co-Major Professor, representing Soil Science

Head of the Department of Forest Ecosystems and Society

Head of the Department Head of Crop and Soil Science

Dean of the Graduate School

I understand that my thesis will become part of the permanent collection of Oregon State University libraries. My signature below authorizes release of my thesis to any reader upon request.

Justin D. Hynicka, Author

ACKNOWLEDGEMENTS

First and foremost, I would like to thank my co-major professors Steve Perakis and Julie Pett-Ridge for providing and encouraging opportunities to be creative and explore ecosystem science, always making time to discuss data and ideas, and for their continual support. I would also like to thank my other committee members, David Hibbs and Jay Noller, for their feedback throughout this project. I continue to be impressed by the cross-disciplinary and collaboratory environment created by the Forest Ecosystems and Society & Crop and Soil Science departments. The is also true for the Oregon State University community at large, and the scope of this project was greatly expanded due to access of specialized equipment at the W. M. Keck Collaboratory for Plasma Spectrometry in the College of Earth, Ocean, and Atmospheric Sciences.

Secondly, this work would not have been possible without an exceptional support network both in the field and the lab. Chris Catricala is both an exceptional lab manager and outstanding individual, and the success of this project is in no small way due to her support. Thank you to Matthew Holmes for persisting through a rigorous first field season, and to Joshua ‘Eddie’ Harding-Frederick for enduring an even more grueling second field season. Who would have thought that bedrock would be so far down? Thanks also to Lauren Armony, Elise Cowley, Kecia Jones, Roseanne Parker, Amber Ross, and Clarinda Wilson for their assistance with sample

processing, as well as the Pett-Ridge Lab that includes Liz King, Jade Marks, and Matt McClintock for adopting me into their research group.

TABLE OF CONTENTS

TABLE OF CONTENTS (CONTINUED)

LIST OF FIGURES

LIST OF FIGURES (CONTINUED)

LIST OF TABLES

CHAPTER 1 – INTRODUCTION

Calcium (Ca) is an essential element in many biological and ecosystem processes. In plants, it is a key macronutrient that contributes to both plant structure and chemical function (Epstein and Bloom, 2005; Matoh and Kobayashi, 1998). In soils, Ca is often the most abundant base cation (i.e., Ca, Mg, K, Na) on soil exchange sites, and thus buffers against changes in soil acidity while also facilitating soil organic matter aggregation (Brady and Weil, 2010; Essington, 2004). At the ecosystem level, the Ca content of foliage can influence ungulate browsing behavior (Short et al., 1966), organic matter decomposition (Reich et al., 2005), and whole catchment water balances (Green et al., 2013). Globally, the release of Ca through silicate weathering in terrestrial ecosystems, followed by precipitation of calcium-carbonate in ocean basins, contributes to a negative-feedback that regulates concentrations of atmospheric CO_2 over geologic timescales (Walker et al., 1981). The key role of Ca from cellular and organismal levels up to ecosystem and global scales has also been shaped by human activity, both directly through widespread use of Ca in fertilizers and building materials or Ca depletion via biomass harvest, and indirectly through changes to other element cycles that are closely coupled to Ca biogeochemistry (Federer et al., 1989; Huntington et al., 2000; Schlesinger and Bernhardt, 2013).

Geology is a fundamental factor governing Ca supply rates to ecosystems. Calcium is the 5th most abundant element in Earth's crust and enters ecosystems through *in-situ* weathering, and for these reasons is often abundant in forests. Yet,

rates of *in-situ* weathering vary based on mineralogy, with Ca-bearing silicate minerals among the least stable (rapidly weathering) silicate minerals at low temperature and pressure (Goldich, 1938; Nesbitt and Young, 1984; White and Brantley, 1995). Therefore, differences in mineralogy and Ca content in rocks can strongly influence nutrient supply rates to ecosystems (Anderson, 1988), and the ability to buffer against Ca loss from forest harvest and acid deposition (Federer et al., 1989; Likens et al., 1996).

In addition to geology there are four other environmental 'state' factors including climate, organisms, relief, and time that influence mineral weathering and soil formation processes (pedogenesis), and thus nutrient availability in ecosystems (Jenny, 1941). In regions with warm, moist climates mineral weathering and soil formation processes are often rapid compared to regions with cold and/or dry climates. Organisms such as plant roots and associated mycorrhizae influence mineral weathering directly by concentrating exudates at specific mineral surfaces (Bonneville et al., 2009; Landeweert et al., 2001; Van Breemen et al., 2000), and indirectly by modifying soil pH through belowground respiration, by exuding organic acids (Hinsinger et al., 2003), or by modifying soil hydrology (Huxman et al., 2005). Relief is shaped by geomorphic processes such as tectonic uplift and erosion (Rasmussen et al., 2011; Riebe et al., 2001), and glaciation (Blum and Erel, 1995) that promote a continuous supply or maximize the surface area of fresh mineral surfaces. Lastly, Ca supply via weathering decreases with soil age due to the loss of weatherable material

(Colman, 1981; White and Brantley, 2003), which can lead to Ca and P limitation of ecosystems.

While these and other soil forming state factors may influence in-situ weathering rates and Ca availability to ecosystems, isolating the effect of any one state factor can be difficult because processes associated with each factor interact and co-vary in nature. Ideally, environmental gradients can be selected and/or state-factors manipulated to vary only a single state factor while limiting variability in others. For example, contrasts of adjacent forests overlying Ca-poor vs Ca-rich bedrock (Page, 1982), and contrasts of co-occurring tree species with different Ca uptake and recycling rates (Cross and Perakis, 2011) provide evidence of single state-factor regulation of Ca cycling in forest ecosystems.

Despite its generally high abundance in bedrock, Ca is susceptible to leaching and loss from forest soils. Calcium can be a growth-limiting nutrient in forests growing on acidic soils receiving acid precipitation (Hyman et al., 1998; Juice et al., 2006; Likens et al., 1996) or high nitrogen supply (Adams et al., 2007; Mainwaring et al., 2014), growing on stable but ancient landscapes (Laurance et al., 1999), or with repeated biomass removal (Federer et al., 1989). During N-cycling in ecosystems, nitrification of organic N (to nitrate) leads to H^+ production. Yet only where N availability exceeds microbial demand will nitrate leach from soils causing a net production of acidity (decrease in soil pH), the displacement of base cations from soil exchange sites, and coupled leaching of base cations with NO_3^- to groundwater (Aber et al., 1989; Reuss et al., 1986). Concerns of Ca depletion are greatest in regions with

soils that developed from parent materials with low Ca abundance and/or limited acid buffering capacity (Langan et al., 1995; Lawrence et al., 1997). In this way, the risk of Ca depletion and limitation depends on the balance between long-term supplies of Ca from *in-situ* weathering and shorter-term rates of base cation leaching, but may also be influenced by patterns of atmospheric deposition (Hedin et al., 1994).

The key role of N as a limiting nutrient in many forest ecosystems makes interactions with Ca of particular importance especially given the limited evolutionary strategies for Ca conservation when compared to N and P. In the Pacific Northwest, rates of atmospheric N deposition are relatively low, but legacies of symbiotic N fixation by red alder (*Alnus rubra*) lead to among the most N-rich soils worldwide (Perakis and Sinkhorn, 2011). Consequently, these soils are moderately acidic with high rates of nitrate leaching, leading to declines in foliar and soil-exchangeable base-cations (Perakis et al., 2006). Surprisingly, long term variation in N availability in these forests can override the role of parent material (base-poor sedimentary versus base-rich basaltic) in shaping base-cation availability in soils and trees (Perakis et al., 2006). While results from one forest in the Pacific Northwest suggest that actively cycled Sr and Ca can be derived almost exclusively from the atmosphere (ocean aerosols) under high N availability (Perakis et al., 2006), it remains unclear how atmospheric versus weathering sources of Ca vary as both a function of ecosystem N status and across different bedrock types that vary in initial Ca content.

Strontium isotopes ($^{87}Sr/^{86}Sr$) have been widely used to trace long-term sources of Ca to ecosystems (Åberg, 1995; Capo et al., 1998; Gosz et al., 1983;

Graustein, 1989). Strontium is a trace element with similar charge (+2) and hydrated radius (r_{Ca} = 0.272 nm; r_{Sr} = 0.274 nm) to Ca (Marcus and Kertes, 1969), allowing it to substitute for Ca in biologic and mineral structures. Isotopes of Sr are not substantially fractionated during biologic or geologic processes due to their relatively high mass, and the small fractionation that does occur in nature and chemical analysis (instrument mass bias) are corrected by normalizing each sample to $^{86}Sr/^{88}Sr = 0.1194$. ^{84}Sr, ^{86}Sr, and ^{88}Sr are stable isotopes meaning that their abundances and isotope ratios are constant on Earth. In contrast, ^{87}Sr is a radiogenic isotope produced through radioactive decay of ^{87}Rb (β-decay, $t_{1/2}$ = 49 billion years) and is the source of natural variation in $^{87}Sr/^{86}Sr$ ratios that makes them useful as a tracer. Rb is a monovalent cation with a similar hydrated radius to potassium (K). Therefore, minerals that have high concentrations of K will tend to have higher $^{87}Sr/^{86}Sr$ ratios than Ca-bearing minerals, a difference that will increase with increasing geologic age of the minerals.

Rocks and atmospheric deposition are the ultimate sources of Ca in terrestrial ecosystems, and are expected to have distinct $^{87}Sr/^{86}Sr$ ratios in Oregon Coast Range (OCR) forests that allow them to be traced in vegetation and soil pools. OCR sedimentary rocks originate from ancient, K-rich magmas and have $^{87}Sr/^{86}Sr$ ratios > 0.710 (Heller et al., 1985). In contrast, OCR basaltic rocks originate from younger, K-poor magmas and have $^{87}Sr/^{86}Sr$ ratios < 0.704 (Parker et al., 2010). In coastal areas, atmospheric Ca and Sr come largely from ocean aerosols, which have a globally constant $^{87}Sr/^{86}Sr$ ratio = 0.70917 (Berner and Berner, 2012; Dia et al., 1992). In cases where inputs of Sr and Ca from dust and/or volcanism are minimal, $^{87}Sr/^{86}Sr$ ratios in

rocks and atmospheric deposition represent the isotopic end-points or end-members of Sr and Ca entering OCR forests. Therefore, biologically cycled Sr and Ca will have a $^{87}Sr/^{86}Sr$ value that falls between these two values, and represents a quantitative mixture of these two sources.

The main objective of this study was to determine the proportions of atmospheric and rock-derived Sr and Ca in soils and Douglas-fir foliage in forest stands using $^{87}Sr/^{86}Sr$ ratios (1) across a naturally occurring ecosystem N-gradient and (2) overlying two different types of bedrock. Previous work in the OCR found ecosystem N – and not bedrock – to be the primary control on base cation availability in the Oregon Coast Range (Perakis et al., 2006). The limited influence of bedrock on ecosystem Ca availability seen by Perakis et al (2006) contradicts the expected differences in weathering potential of Ca between Ca-rich basaltic rocks and Ca-poor sedimentary rocks; a difference that should be maintained by tectonic uplift and soil rejuvenation in the OCR (Heimsath et al., 2001; Reneau and Dietrich, 1991). Yet, high variability in foliar and exchangeable Ca at low N sites (Perakis et al., 2006) may signal an influence of parent material that has not been fully recognized.

In addition, information on base cation concentrations and pools alone cannot resolve the relative importance of atmospheric versus weathering inputs in shaping long-term Ca supplies and sustainability, especially in managed forests where Ca in biomass is removed. Excess N in terrestrial ecosystems leads to a rapid decline in base cation availability, and in theory could alter base cation sources if rates of mineral weathering are sufficiently slow. Therefore, plant and soil exchangeable pools at low-

N sites should reflect greater Ca inputs from rock-weathering sources, but as N-accumulates and nitrate leaching intensifies base cation sources should shift from rock dominated to atmospheric inputs.

CHAPTER 2 – METHODS

2.1 Overview

We collected foliage, soils in 10-cm increments down to 50-cm depth, and bedrock, and measured soil chemical properties at twenty-four sites dominated by young (22-37 years), monoculture Douglas-fir forests in the Oregon Coast Range. These twenty-four sites were chosen from an initial survey of fifty-four sites of which 39 sites are included in the Swiss Needle Cast Cooperative Growth Impact Study (SNCC-GIS, Maguire et al., 2002), and 15 were sampled while en-route to the SNCC-GIS sites (Appendix A). The goals of the initial survey and subsequent selection criteria of 24 detailed study sites were (1) maximize the range of soil-N concentrations across sites, (2) encompass two distinct bedrock types, and (3) minimize differences in other soil-forming state factors (e.g. precipitation, slope, etc.). These sites do not represent an unbiased sample of OCR forests, and instead are intended to encompass a wide range of soil N biogeochemistry to examine how N shapes patterns and mechanisms of Ca cycling in Douglas-fir forests of the region.

2.2 Study Area

Three major events define the geologic history of the Oregon Coast Range. First, mountain building of the Oregon Coast Range began during the Paleocene Epoch (66 – 56 million years ago) with the accretion of submarine basaltic rocks along the continental margin of western North America (Duncan, 1982; Wells et al., 1984). At this same time, sediments derived from the granitic Idaho Batholith, granitic

Kalamath Mountains, and/or proximal volcanic rocks and ash were accumulating in extensive fore-arc basins and on top of accreted basaltic rocks (Heller et al., 1987). Continued tectonic compression uplifted and exposed sedimentary and accreted basaltic rock units. Secondly, tectonic compression was briefly interrupted by a period of extension (36-32 Ma), producing deep-seated fracturing within existing rock formations and intrusion of gabbroic magma that outcrops irregularly throughout this region (Barnes and Barnes, 1992; Davis, 1995). Lastly, tectonic compression and rock uplift resumed during the late Eocene to early Oligocene, exposing both basaltic and sedimentary formations that are common throughout the Oregon Coast Range today.

Our research sites occur over three Eocene-Tertiary sedimentary rock formations including the Nestucca, Yamhill, and Tyee, and three basaltic rock formations including the Siletz River Volcanics, Tillamook Volcanics, and Diabase of Lee's Falls (**Figure 1**). The Nestucca Formation is described as thin-bedded tuffaceous siltstone and arkosic sandstone (Bukry and Snavely Jr, 1988), with sediments derived from Cascade volcanic arc rocks to the east (Dott Jr, 1966; Heller and Ryberg, 1983). Sedimentary layers interbed with basalt-bearing formations (Snavely and MacLeod, 1974) creating rock units of variable geochemical content. However, volcaniclastic sediments exhibit substantial alteration of primary minerals (to phyllosilicate clays) in modern depositional environments along the Pacific Northwest Coast (Galloway, 1974), suggesting that mudstones contain few remaining primary Ca-bearing minerals of volcanic origin.

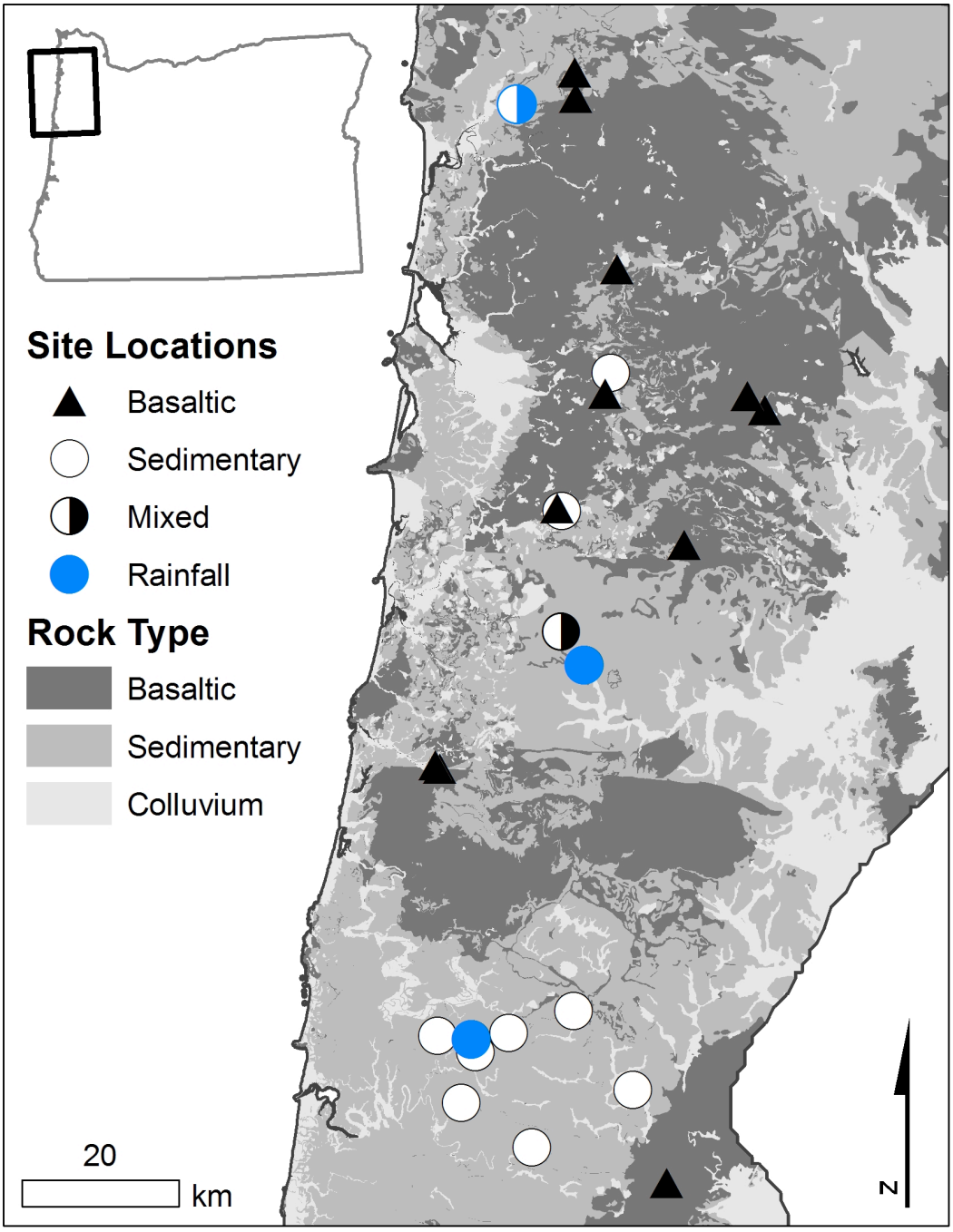

Figure 1. Simplified geologic map, and field sampling locations in the northern Oregon Coast Range, USA. Three sites highlighted in blue (two sedimentary and one mixed lithology site) indicate the locations of our rainfall collectors. Geospatial data from ("Oregon Geologic Data Compilation," 2009).

The Yamhill Formation overlies and interbeds with the Tyee Formation, which are differentiated by the thickness of sandstone lamellae (>6 in. thick for the Tyee Formation), and secondly by the more fissile character of siltstone and mudstone units. Sandstone beds of the Tyee and Yamhill Formations consist of lithic to arkosic micaceous wacke, and arkosic and basaltic wackes, respectively. Dominant minerals include quartz, andesine, and lithic fragments, with trace potassium feldspars, smectite, and calcite (Heller et al., 1985; McWilliams, 1973; Snavely et al., 1964).

The Siletz River Volcanics (SRV) is the oldest rock formation in the Oregon Coast Range and forms the basement rock throughout this region (Wells et al., 2014). The SRV formation consists of thin subaerial alkali basalt flows and breccias that overly substantially thicker submarine theolitic pillow basalts (Snavely et al., 1968). Plagioclase and pyroxene are the dominant minerals in the upper SRV (~40 % each) and locally contain trace amounts of olivine (1-4 %). The composition of plagioclase is highly variable and can be dominated by either Ca-rich anorthite or Na-rich albite (up to 78% and 72% of total plagioclase, respectively). The proportion of opaque groundmass is also highly variable (5 – 58 %) (Snavely et al., 1968). Lower units of the Tillamook Volcanics correlate with SRVs and therefore also consist of layered subaerial (upper) and submarine (middle and lower) basalt flow, breccias, and interbedded sediments (Magill et al., 1981). Lastly, Diabase of Lee's Falls is a late Eocene/early Oligocene intrusive volcanic rock. Plagioclase (50-60%) and pyroxene (10-30%) dominate the mineralogy of ORC intrusive rocks with lesser amounts of

olivine, magnetite, apatite, and zeolites of variable mineral grain size (fine to coarse, Brownfield, 1982).

Contemporary regional climate is temperate and maritime with cool wet winters and warm dry summers. Mean annual precipitation across research sites ranges from 180 to 380 cm yr^{-1} (Table 1) with the majority falling as rain between November and May. Mean annual minimum and maximum temperatures range from 3.97 – 6.02 °C and 13.1 – 16.5 °C. There is no evidence of glaciation in the Oregon Coast Range (Reneau and Dietrich, 1991), though ice fields were present on high peaks during the last glacial maximum (Noller, J, written communication). Native forests are dominated by Douglas-fir (*Pseudotsuga menziesii*) and western hemlock (*Tsuga heterophylla*), but Sitka spruce (*Picea sitchensis*) can be the dominant tree species near the coast. Native forests experienced intense stand replacing fires throughout the Holocene epoch providing a pathway for succession by red alder (Long et al., 2007, 1998). Current land use is a mix of federal and state forestlands of varying histories and management objectives, and private industrial forests focused primarily on Douglas-fir production at 35-50 year rotation intervals (Spies et al., 2002).

2.3 Field Methods

Foliage samples were collected in June 2012 during the initial survey of 54 sites and kept for use in the more detailed study of 24 sites. First-year 'sun' foliage samples were collected from the southwest-most facing branch in the 5th whorl of branches from the treetop of three different trees using a combination of tree climbing

and pole-pruning (3 replicates per site). Replicate foliage samples were combined into a single composite for chemical analyses.

Soil samples were collected in the fall of 2012. The first 10-cm of soil was collected with a 6.8 cm diameter corer, and soil at depth was collected with a 4.7 cm diameter slide hammer in 20 cm (or 30 cm for 70-100 cm depth) increments to maximum depth of 100 cm. Soil within the tip was discarded, and each 20 cm section was split equally by height into 10 cm fractions. Three replicate soil cores were collected per site, pooled into a single composite sample, and then sieved to 2 mm. Both fine (< 2 mm in diameter) and coarse (> 2 mm in diameter) soil fractions were weighed and retained for chemical analyses. Soil texture and color were determined on non-sieved soil sampled by horizon from a soil pit excavated to ~60 cm depth at each site. Soil texture was obtained by hand, and color determined on moist and dry soils using the Munsell color system. In the Oregon Coast Range, soil color is associated with soil age on sedimentary chronosequences (marine and fluvial terrances, Almond et al., 2007; Lindeburg et al., 2013; Sweeney et al., 2012) but has not been previously reported for basaltic soil chronosequences. Hurst's Redness Rating was calculated using Equation 1 (Hurst, 1977) with color values measured on moist soil samples, where RR = Hurst's redness rating, H^* = modified soil hue, V = soil value, and C = chroma.

$$\text{Equation 1:} \quad RR = \frac{H^* \cdot V}{C}$$

Bedrock was collected in April to June of 2013 using a portable drilling assembly (Gabrielli and McDonnell, 2012). At twenty-one sites, drilling occurred directly in the area of foliage and soil collection. For the other three sites we drilled overtop of a nearby outcrop when the depth to bedrock at the site exceeded the maximum depth of our drilling equipment (>11 meters). Our bedrock samples represent the freshest possible samples that we could collect at each site; however, sample recovery per meter drilled was often low (~10% by height). Based on our experience with this equipment and evaluation of exposed bedrock in road cuts near our sites, we believe that low sample recovery reflects drilling through deep friable saprolite and intact rock lenses that exist within the regolith. We report bedrock depth to an accuracy of ± 1 m (Table 1), which is the length of our drill string sections.

Precipitation chemistry was characterized by event based sampling during the late winter to early summer of 2013. Two 1.0 L acid washed plastic bottles were placed in clearings at three locations (sites 7, GV1, 143) spanning the latitudinal range of our research sites (Figure 1, blue symbols) during three different storms: 2/21-26, 4/4-6, and 6/22-27. Bottles were suspended 1 m above the ground surface using a wooden stake, and equipped with a 16 cm diameter polypropylene funnel and screen (mesh size = 2 mm). Samples were acidified to 1% with ultrapure HNO_3, refrigerated, and later evaporated on a hotplate (~100 x concentrated) with five 1 mL additions of ultrapure concentrated nitric acid to dissolve fine particulates.

2.4 Laboratory Methods

Composite foliage and soil samples were dried at 65°C for 24 and 48 hours, respectively, and steel ground to homogenize the sample. Approximately 10 mg of dried and ground foliage and soil were weighed into tin capsules, and C and N concentrations analyzed by Costech ECS 4010 at the USGS Forest and Rangeland Ecosystem Science Center (FRESC, Corvallis, OR). A sub-sample of foliage and soil (0-10 cm) collected during our initial survey of 54 sites was analyzed for ^{15}N using a continuous flow isotope ratio mass spectrometer (PDZ Europa ANCA-GSL elemental analyzer / PDZ Europa 20-20 IRMS) at the U.C. Davis Stable Isotope Facility. An additional sub-fraction of each composite soil sample (24 detailed study sites) was dried at 105°C for at least 48 hours to correct for soil moisture; soil chemistry is reported at 105°C dry soil weight. Soil bulk density was calculated using Equation 2, where D_b = soil bulk density (g/cm^3), M_{soil} is the dry mass of < 2 mm composite soil samples, and V_{total} is the total volume of three replicate soil cores (1089 cm^3 for 0-10 cm depths, and 519 cm^3 for subsurface samples).

Equation 2: $$D_b = \frac{M_{soil}}{V_{soil}}$$

The volume of coarse soil fragments and bedrock samples were determined by displacement with ultra-pure water (MQW). Wet fragments and rock samples were then dried at 105°C for at least 48 hours, weighed, and bulk density calculated using

Equation 2 substituting M_{soil} with M_{cf}. Percentage of coarse fragments (by mass) in each soil section was calculated using Equation 3, where P_{cf} = percentage of coarse fragments, and M_{cf} and M_{soil} are the dry masses of the coarse and fine earth fractions, respectively.

Equation 3: $$P_{cf} = \frac{M_{cf}}{M_{cf} + M_{soil}} \cdot 100\%$$

For major and trace element analyses, 200 mg of dried and steel-ground foliage was dissolved by microwave digestion (Anton Paar Multiwave 3000) in a mixture of ultra-pure concentrated nitric (HNO_3), hydrochloric (HCl), and hydrofluoric (HF) acids (7, 1, and 0.1 mL, respectively). We included a small volume of concentrated HF during the digestion because Douglas-fir foliage contains high amounts of biogenic silica (phytoliths).

Soil 'exchangeable' Na, K, Mg, Ca, and Sr were determined by chemical extraction. Approximately 25 mL of 1.0 N ammonium acetate (NH_4OAc) was added to ~5 g of field moist soil, shaken for 30 minutes, and centrifuged at 2500 rpm for 10 minutes. The supernatant was pipetted into a 60 mL syringe equipped with a 0.45 um filter (Aerodisk PES membrane) and collected in a 60 mL polypropylene bottle. This processes was repeated once, and the supernatants combined into a single sample (Page, 1982). The soil 'residue' remaining after the NH_4OA_C extraction was rinsed with 10 mL ultrapure water, dry-ashed at 500 °C for 12 hours, ground and homogenized, and 200 mg dissolved by microwave digestion with concentrated

ultrapure HNO_3, HCl, and HF (6, 2, and 2 mL, respectively). Indices of weathering including chemical index of alteration (CIA, Nesbitt and Young, 1982), weathering index of Parker (WIP, Parker, 1970), and element losses relative to bedrock (τ, Brimhall and Dietrich, 1987; Chadwick et al., 1990) were calculated from elemental concentrations in soil residues and bulk rock samples (see below for bedrock processing) using Equations 4-6:

Equation 4: $$CIA = \frac{Al_2O_3}{Al_2O_3 + CaO^* + Na_2O + K_2O} \cdot 100\%$$

Equation 5: $$WIP = \left[\frac{2Na_2O}{0.35} + \frac{MgO}{0.90} + \frac{2K_2O}{0.25} + \frac{CaO}{0.70} \right] \cdot 100\%$$

In equations 4 and 5, all oxide concentrations are in percent by mass, and CaO* is corrected for apatite by subtracting 3.33 x P_2O_3 from CaO total. In equation 6, element concentrations are in molar concentrations, where $\tau_{j,w}$ is the relative loss (-) or gain (+) of element *j* from soil with respect to parent rock, $C_{j,w}$ and $C_{j,p}$ are the molar concentrations of element *j* in soil and bedrock, respectively, and $C_{Nb,w}$ and $C_{Nb,p}$ are the molar concentrations of and immobile element such as niobium (Nb) in soil and bedrock, respectively.

Equation 6: $$\tau_{j,w} = \left[\frac{C_{j,w} \cdot C_{Nb,p}}{C_{j,p} \cdot C_{Nb,w}} - 1 \right]$$

$\tau_{j,w}$ values are reported for both the fine earth fraction only and on bulk soil (0-50 cm depth) including coarse soil fragments. When calculating $\tau_{j,w}$ for bulk soil, we assumed that the chemistry of coarse soil fragments measured at 40-50 cm depth was the same for coarse soil fragments throughout the entire profile (0-50 cm depth).

Soil pH was measured in a 2:1 mixture (by mass) of soil and water after incubating for 30 minutes. Exchangeable acidity and aluminum were determined by sequentially extracting a 3 g subsample of field moist soil three times with 30 mL of 1.0 M potassium chloride (KCl). Samples were shaken for 30 minutes, centrifuged at 4000 rpm for 10 minutes, and the supernatant pipetted into a 60 mL syringe equipped with a 0.45 μm filter; filtered extractions were combined in a single bottle. Total acidity was determined by titrating 30 mL of the extractant with 0.01 M NaOH to a phenolphthalein endpoint (persistent light pink color) and calculated using Equation 7, where EA_{total} = total exchangeable acidity (cmol+/g), VA is the volume of titrant added, VB is the volume of titrant added to a blank sample, N_t is the normality of the titrating solution, $V_{s,total}$ is the total extracted volume, M_{sample} is the dry soil mass, and V_s is the volume of titrated extractant.

Equation 7: $$EA_{total} = \frac{(VA - VB) \cdot N_t \cdot V_{s,total} \cdot 100}{M_{sample} \cdot V_s}$$

Acidity from aluminum was determined by adding 5 mL of 0.5 M NaF (Al-complexing agent) to the titrated extractant and back titrating with 0.01 M HCl until the solution turned from fuchsia to clear; exchangeable Al was also calculated using

Equation 8 but by substituting the volumes and concentration of HCl added (as opposed to NaOH) during the back titration (Carter and Gregorich, 2007; Station et al., 1999). Effective cation exchange capacity (ECEC) and base saturation were calculated using equations 8 and 9, where EA_{total} is the total exchangeable acidity (Equation 7), and Na, K, Ca, and Mg are the concentration of these elements (mol g^{-1}) determined by ICP-OES (see below). In equation 9, ECEC is the effective cation exchange capacity (Equation 8) and EA_{total} is the total exchangeable acidity (Equation 7).

Equation 8: $$\mathrm{ECEC} = EA_{total} + \frac{Na + K + 0.5Ca + 0.5Mg}{10}$$

Equation 9: $$BS = \frac{ECEC - EA_{total}}{ECEC} \cdot 100\%$$

Rock samples were crushed using a steel grinder then powdered using an agate ball mill (Retsch PM 100). Approximately 200 mg of powdered 'bulk rock' was microwave digested using the same proportions of HNO_3, HCl, and HF as soil residues. To test for minerals that may preferentially dissolve compared to bulk rock, a separate 200 mg subsample of powdered rock was shaken in 30 mL of 1 M HNO_3 at room temperature for 20 hours, centrifuged, and the supernatant pipetted into a pre-weighed polypropylene bottle (Nezat et al., 2007). This process was repeated once and the supernatants were combined in a single bottle.

All samples were dried and re-suspended in 1% HNO_3 for analysis by ICP-OES at the W. M. Keck Collaboratory for Plasma Spectrometry at Oregon State University. Three U.S. National Institute of Standards and Technology (NIST) plant standard reference materials (SRM1515 apple leaf, SRM1570a spinach leaf, and SRM 1575 pine needle) were used as calibration standards for foliage and exchangeable soil chemistry, and three U.S. Geological Survey (USGS) rock standards (AGV1 andesite, BCR2 basalt, and G2 granite) were used as calibration standards for soil residues, coarse rock fragments, bulk rock digests, and 1 M HNO_3 rock leachates. Separate plant (DFIR1) and soil standards (NIST SRM 2709a) were measured during each OES analysis and were in close agreement with certified values (Appendix B).

For isotopic analysis, 30 ng of Sr from each sample were purified using 1.8 mL of Eichrom AG50W-X8 (H^+ form) cation resin followed by 50 µL of Eichrom Sr-Spec resin. Isotopic measurements were made on a Nu Plasma© multi-collector ICP-MS at the W. M. Keck Collaboratory for Mass Spectrometry at Oregon State University. Masses 83-88 were monitored in static collection mode. Masses 83 and 85 were monitored for Kr (blank only) and Rb (standards and samples) interferences, respectively. Sr-isotopes ratios were measured 40 times per sample and have internal analytical uncertainties < 0.000020. Reported values are corrected to $^{86}Sr/^{88}Sr$ = 0.1194 and Sr standard NBS-987 $^{87}Sr/^{86}Sr$ = 0.710245. This instrument measures an average value of 0.70818 and a 2σ = 0.000045 for in house standard EMD (n=205) over the duration that samples were run; this external reproducibility is the experimental precision reported for our Sr-isotope data.

2.5 Statistical Analyses

All statistical analyses were performed using the program R (R Development Core Team, 2008). We tested for statistical significance using Equation 10 (multiple linear regression, analysis of covariance), where *Nitrogen* is the profile weighted concentration of soil nitrogen from 0-20 cm depth, *Bedrock* is a categorical variable indicating the underlying rock type, and Y_i is a response variable (e.g., exchangeable soil Ca). Basalt was the reference bedrock type in all analyses. Profile weighted averages were calculated using Equation 11, where X is the concentration of the element of interest, y is the total number of 10 cm soil increments, i is the soil increment number, and Db is the soil bulk density. Db_{total} is the sum of all increment bulk densities (increments i through y).

Equation 10: $$Y_i = \beta_0 + \beta_1 nitrogen + \beta_2 rock + \beta_3 rock \cdot nitrogen$$

Equation 11: $$x_{wt} = \frac{\sum_{i-1}^{y} x_i \cdot Db_i}{Db_{total}}$$

To verify that N and not some other site factor structures our gradient of sites, we tested for co-linearity between N and 17 metrics related to soil state factors for each rock type (i.e. basaltic and sedimentary) including mean annual precipitation, mean annual temperature, and distance from the coast (climate factors); slope, soil depth, and abundance of coarse rock fragments (relief factors); within-group bulk rock, 1 M HNO_3 rock leachate, profile weighted soil residue (0-50 cm depth), and

coarse rock fragment (40-50 cm depth) Ca chemistry (parent material factors); and lastly effective cation exchange capacity, chemical index of alteration, weathering index of parker, τ Ca, and Hurst's redness rating (time factors). Although our number of research sites is large compared to similar studies, separating the data by rock type reduces the statistical power of these tests. For this reason, we assumed a relationship to be statistically significant at the $p = 0.01$ level, which for the purposes of this analysis is more conservative than using Bonferroni corrected p-values (statistical significance indicated at $p < 0.004$), because the higher p-value increases the chance of identifying a state-factor variable that is correlated with soil N across sites. Results of this exercise are summarized and discussed in the 'State Factor Analysis' section of the discussion.

CHAPTER 3 – RESULTS

3.1 Soil Carbon and Nitrogen

Surface (0-10 cm depth) mineral soil displayed a wide range of C and N concentrations across sites (Table 2). Surface soil (0-10 cm depth) C concentrations of sedimentary and basaltic sites had a similar range from 2.47 – 15.73 % C and 4.95 – 16.72 % C, respectively. Surface soil N concentrations of sedimentary and basaltic sites also had a similar range from 0.16 – 0.86 % N and 0.21 – 0.97 % N, respectively. These data reflect the study goal of capturing a wide but similar range of soil C and N concentrations over two distinct bedrock types.

Natural abundance nitrogen isotope values ($\delta^{15}N$) in surface soils decreased with increasing soil N concentration (%, 0-10 cm) (Figure 2, $p = 0.028$) and did not differ between rock types ($p = 0.66$, extra sum of squares F-test). A similar but statistically weaker pattern of declining $\delta^{15}N$ values was observed when regressed against the total pool of N in surface (0-10 cm depth, $p = 0.11$). In general, soil $\delta^{15}N$ spanned a greater range of values at low N sites (0.81 to 5.1 ‰) than high N sites (1.4 to 2.6 ‰).

Soil C and N concentrations were greatest at the surface and decreased with increasing soil depth (Table 2). Surface soil N (%, 0-10 cm depth) was a strong predictor of both profile-weighted N concentration and soil N pool size from 0-50 cm soil depth (Figure 3), although variation in N pool size with surface N concentration did differ between rock types ($p = 0.001$, extra sum of squares F-test), primarily due to

slightly higher bulk density (<2 mm) in sedimentary sites. Molar C/N ratios in basaltic soils (0-10 cm depth) ranged from 17.5 to 29.5, and were similar to sedimentary sites, which ranged from 18.0 to 23.8 (Table 2). Molar C/N ratios either decreased or displayed little variation with increasing soil depth at all sites (Table 2).

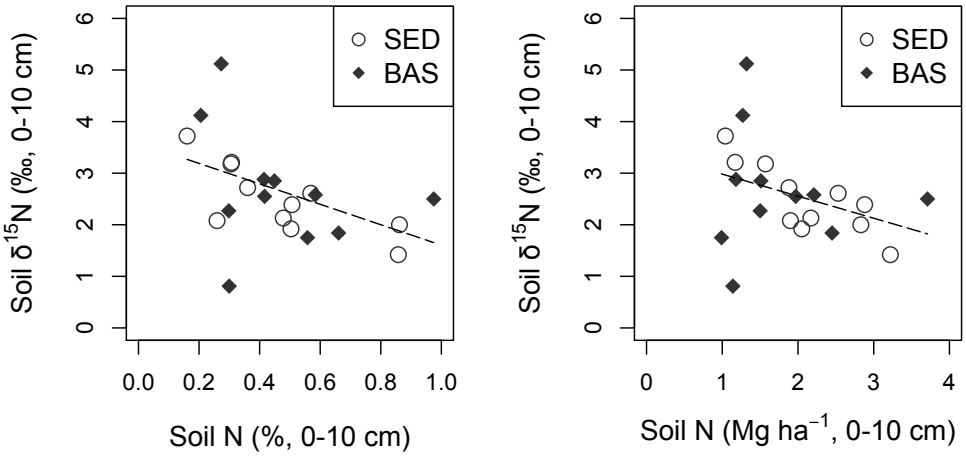

Figure 2. Surface soil (0-10 cm depth) $\delta^{15}N$ versus N concentration (%, left panel) and pool size (Mg/ha, 0-10 cm depth, right panel). Variation in soil $\delta^{15}N$ with N concentration and N pool size (0-10 cm depths) did not differ between rock types ($p = 0.66$ and 0.97, respectively, extra sum of squares F-test). Regression lines include basaltic and sedimentary sites in both left ($y = -1.98x + 3.50$; $R^2 = 0.22$; $p = 0.028$), and right panels ($y = -0.43x + 3.40$; $R^2 = 0.12$; $p = 0.11$).

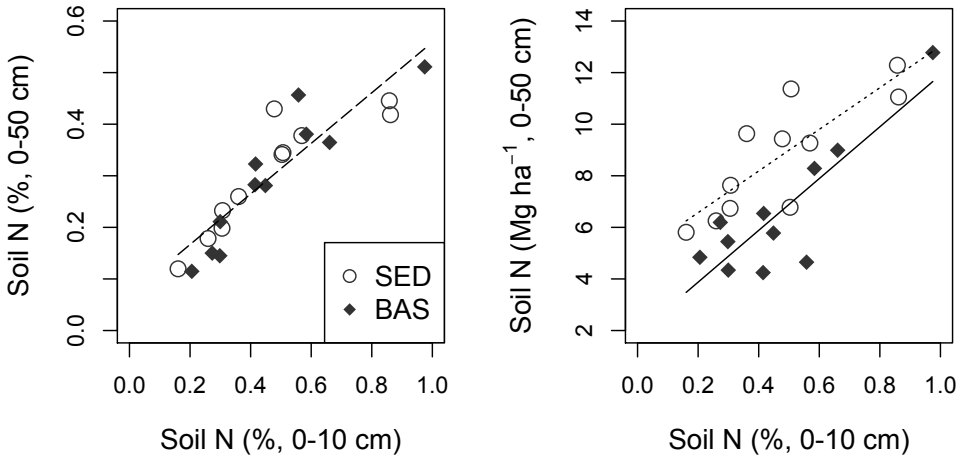

Figure 3. Surface soil N concentration versus profile weighted (0-50 cm depth) N concentration (%, left panel) and pool size (Mg/ha, right panel). Variation in surface N with profile weighted N concentration (0-10 and 0-50 cm depths) did not differ between rock types ($p = 0.92$, extra sum of squares F-test). Left panel regression includes both basaltic and sedimentary sites: $y = 0.49x + 0.069$ ($R^2 = 0.80$; $p < 0.001$). In right panel, basaltic (solid line) and sedimentary regression (dotted line): $y = 10x + 1.9$ ($R^2 = 0.74$; $p = 0.001$), and $y = 8.1x + 5.0$ ($R^2 = 0.64$; $p = 0.002$).

3.2 Soil Color

Soil color is an important tool for distinguishing soil chemical properties including organic matter content (Shields et al., 1968), water saturation frequency (He et al., 2003), and clay mineralogy (Hurst, 1977) among other things. We used soil color as a proxy for soil age because the development of iron (Fe) oxide minerals can cause soils to become increasingly red in color over time (Almond et al., 2007; Lindeburg et al., 2013). Soil color is evaluated based on (1) its color in the visible spectrum or hue, (2) its darkness or value, and (3) the color intensity/reflectiveness or chroma. Despite the large range in soil C and N concentrations (i.e., organic matter

content), field moist soil color values had a narrow range (typically 2 to 3, Table 3). Soil hues also had a narrow range (2.5Y to 10YR, Table 3), while soil chromas had a slightly greater range (1 to 6, Table 3) than color hues and values. Soil hues decreased slightly (became more yellow) with increasing soil depth. In contrast, soil values and chromas increased slightly with depth. The combination of these subtle differences in soil hues, values, and chromas results in a wide range of Redness Ratings (6-50, Table 3). Soil redness did not co-vary with soil N at sedimentary sites ($p = 0.76$), but was positively correlated with soil N at basaltic sites ($p = 0.002$, Figure 4).

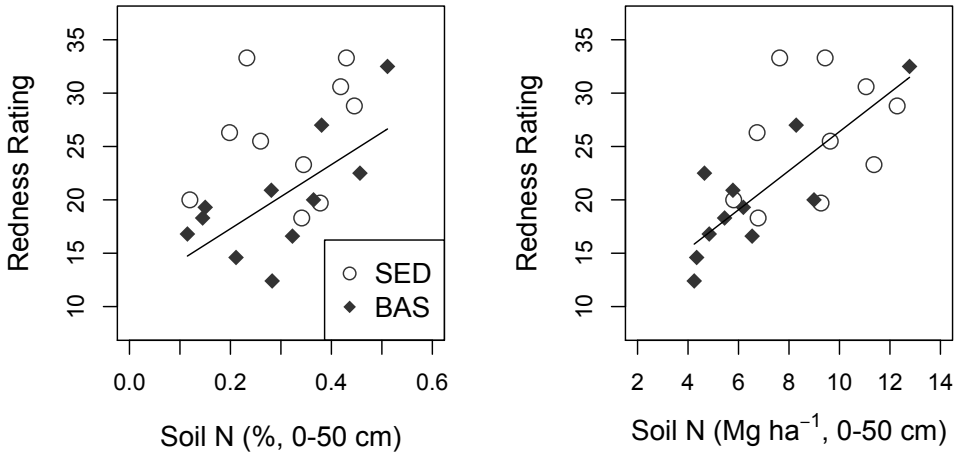

Figure 4. Average soil redness (0-50 cm depth, Hurst's redness rating) versus profile weighted soil N (%, 0-50 cm, left panel) and N pool size (0-50 cm, right panel). Soil redness was significantly related to N on basaltic sites. Regression lines include only basalt sites in left ($y = 30.0x + 11.3$; $R^2 = 0.47$; $p = 0.020$), and right panels ($y = 1.83x + 8.08$; $R^2 = 0.69$; $p = 0.002$).

3.3 Exchangeable Soil Cations

In soils, cations (Al^{3+}, H^{+}, Ca^{2+}, Mg^{2+}, K^{+}, NH_4^{+}, and Na^{+}) that are electrostatically bound to negatively charged clay minerals and organic matter, and in equilibrium with the soil solution phase, are available for plant uptake. Non-nutrient acid cations (Al^{3+}, and H^{+}) bind more strongly to clay minerals and organic matter compared to nutrient base cations (Ca^{2+}, Mg^{2+}, K^{+}), and will displace or exchange with base cations from these negatively charged 'exchange' sites. Our research sites had a large range in soil pH and exchangeable Al (Table 4). Soil pH (0-10 cm depth) decreased (acidity increased, Figure 5) and Al saturation increased (Figure 6) with increasing soil N concentration, and did not differ between rock types.

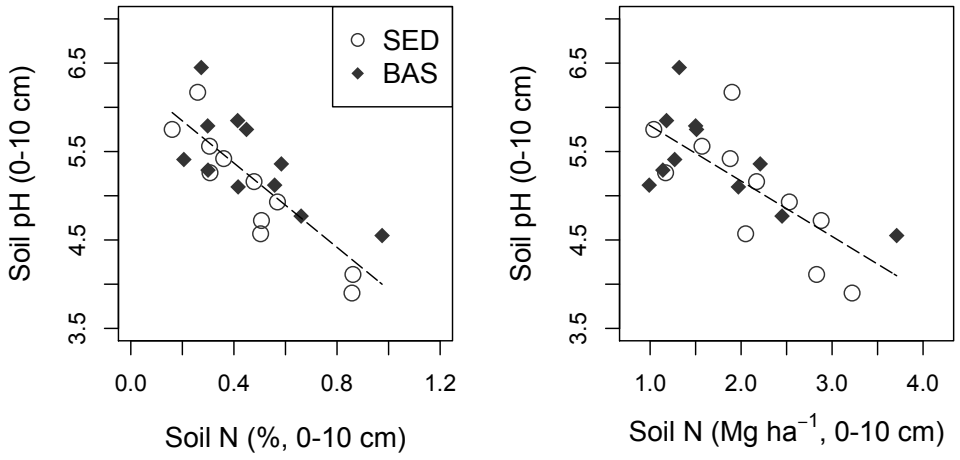

Figure 5. Soil pH (0-10 cm depth) versus soil N concentration (%, 0-10 cm depth, left panel) and N pool size (Mg ha^{-1}, 0-10 cm depth, right panel). Variation in soil pH with soil N concentration and pool size (0-10 cm depths) did not differ between rock types ($p = 0.07$ and 0.63, respectively, extra sum of squares F-test). Regression lines include basaltic and sedimentary sites in left ($y = -2.38x + 6.32$; $R^2 = 0.64$; $p < 0.001$) and right panels ($y = -0.63x + 6.42$; $R^2 = 0.56$; $p < 0.001$).

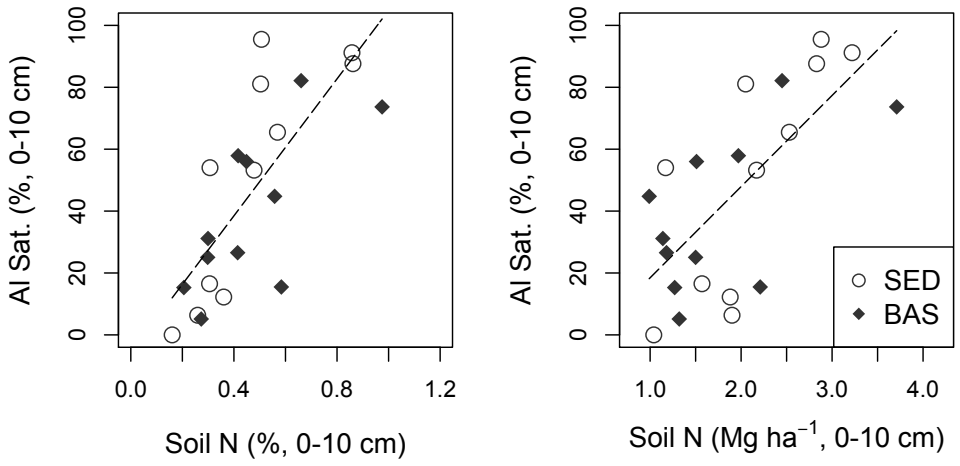

Figure 6. Aluminum saturation (Al Sat., 0-10 cm depth) versus soil N concentration (%, 0-10 cm depth, left panel) and N pool size (Mg ha^{-1}, 0-10 cm depth, right panel). Variation in aluminum saturation with soil N concentration and pool size (0-10 cm depths) did not differ between rock types ($p = 0.38$ and 0.90, respectively, extra sum of squares F-test). Regression lines include basaltic and sedimentary sites in left ($y = 110x – 5.80$; $R^2 = 0.57$; $p < 0.001$) and right panels ($y = 29.5x – 11.0$; $R^2 = 0.52$; $p < 0.001$).

Our research sites had a large range in exchangeable Ca and Sr concentrations, molar Ca/Sr ratios, and $^{87}Sr/^{86}Sr$ ratios (Table 4). Exchangeable Ca in surface soils (0-10 cm depth) ranged from 33.0 to 2860 μg/g and decreased with increasing soil N concentration, although basaltic sites 8 and 60 had among the highest concentrations of exchangeable Ca (>2100 μg/g) despite moderately high concentrations of soil N (~0.6 %) (Figure 7). The pattern of declining exchangeable Ca at high soil N did not differ by rock type ($p = 0.19$), nor did exchangeable Ca overall differ by rock type ($p = 0.27$). Exchangeable Sr concentrations in surface soils ranged from 0.42 – 31.5 μg/g

(Table 4) and exhibited greater variability at low N sites compared to Ca (5 vs. 2-fold). Exchangeable Sr declined with increasing soil N concentration (Figure 8). The declining pattern of exchangeable Sr with increasing soil N did not differ by rock type ($p = 0.36$), but there was some evidence that the mean concentration of exchangeable Sr at basaltic sites was greater than at sedimentary sites ($p = 0.06$).

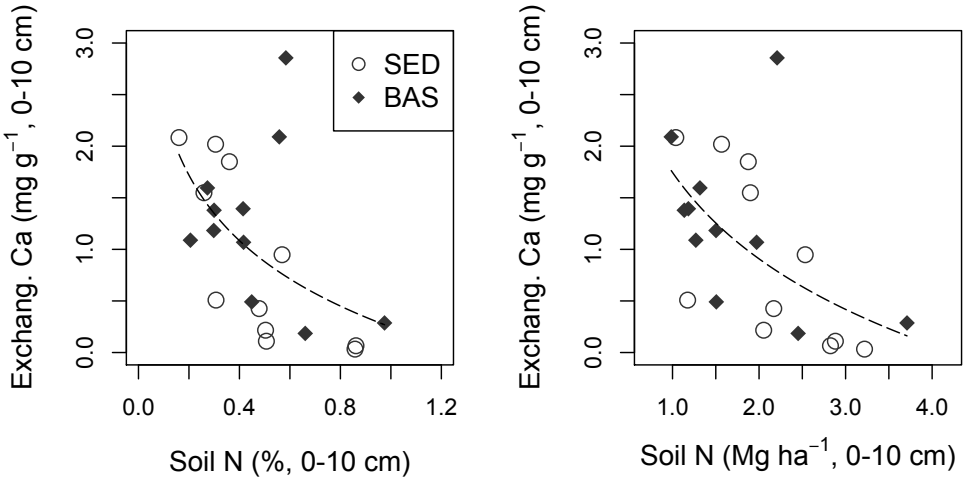

Figure 7. Soil exchangeable Ca (mg g^{-1}, 0-10 cm depth) versus soil N concentration (%, 0-10 cm depth, left panel) and N pool size (Mg ha^{-1}, 0-10 cm depth, right panel). Variation in soil exchangeable Ca with soil N concentration and pool size (0-10 cm depths) did not differ between rock types ($p = 0.39$ and 0.75, respectively, extra sum of squares F-test). Regression lines include basaltic and sedimentary sites in left ($y = -0.92*\ln(x) + 0.25$; $R^2 = 0.28$; $p = 0.009$) and right panels ($y = -1.21*\ln(x) + 1.75$; $R^2 = 0.34$; $p = 0.003$).

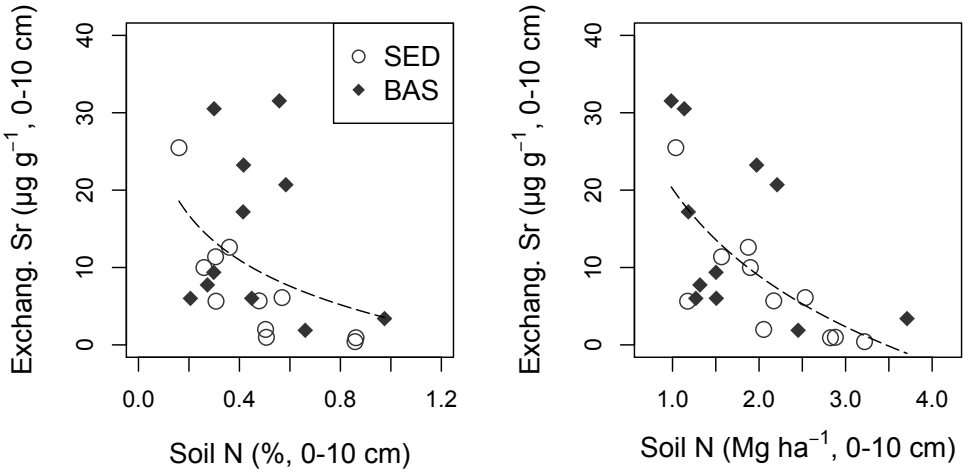

Figure 8. Soil exchangeable Sr (µg g^{-1}, 0-10 cm depth) versus soil N concentration (%, 0-10 cm depth, left panel) and N pool size (Mg ha^{-1}, 0-10 cm depth, right panel). Variation in soil exchangeable Sr with soil N concentration and pool size (0-10 cm depths) did not differ between rock types ($p = 0.15$ and 0.46, respectively, extra sum of squares F-test). Regression lines include basaltic and sedimentary sites in left ($y = -8.34*\ln(x) + 3.33$; $R^2 = 0.16$; $p = 0.052$) and right panels ($y = -16.2*\ln(x) + 20.2$; $R^2 = 0.43$; $p < 0.001$).

Within each site, the concentration of exchangeable Ca was greatest at the surface and decreased with increasing soil depth (Table 4). Exchangeable Sr concentrations followed this same general pattern (Table 4). The range of molar Ca/Sr ratios in surface soils was similar between basaltic and sedimentary sites (95.7 to 450, and 156 to 388, respectively), and generally decreased with increasing soil depth, indicating that Ca was concentrated in surface soils relative to Sr. A Ca/Sr depth trend was unclear at only three sites (Stein, Wow, and WP, Figure 9) where the Ca/Sr ratios in 10-20 cm soil were either greater or less than both the 0-10 cm and 40-50 cm depths

(Table 4). $^{87}Sr/^{86}Sr$ ratios tended to remain constant from 0-10 cm depth to 10-20 cm depth and then decrease slightly from 10-20 to 40-50 cm soil depth (Figure 10), although larger shifts in $^{87}Sr/^{86}Sr$ ratios ($\Delta^{87}Sr/^{86}Sr \sim 0.001$) with depth occurred at two sedimentary rock sites (Steere and Wow).

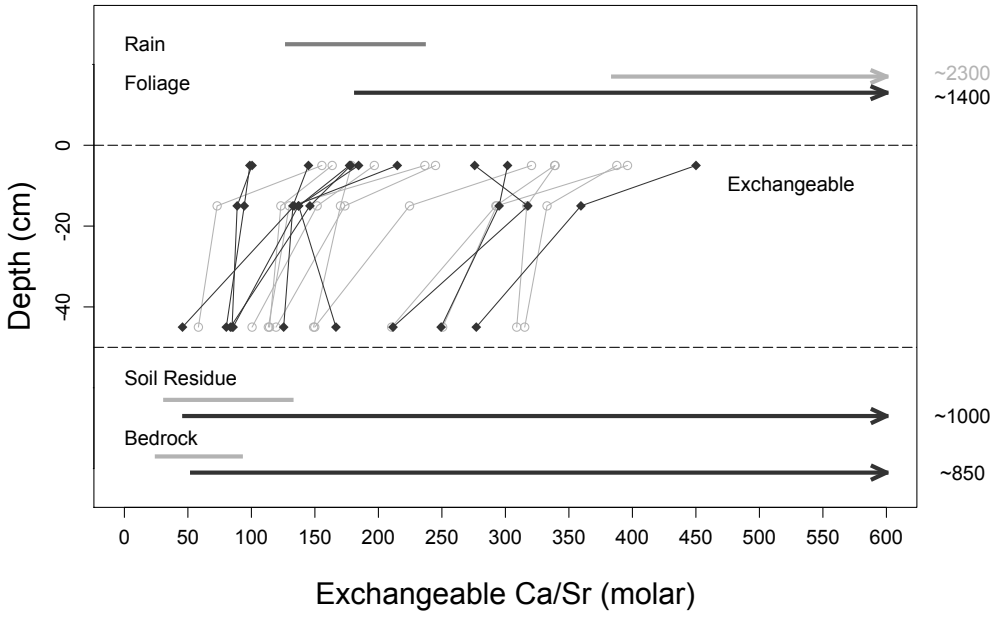

Figure 9. Molar Ca/Sr ratios of the soil exchangeable pool versus soil depth and compared to the range of molar Ca/Sr ratios in other ecosystem pools. Basaltic sites indicated by black diamonds (◆) and sedimentary sites indicated by grey circles (○). Horizontal light grey lines indicate the range of molar Ca/Sr ratios at sedimentary sites, while horizontal black lines indicate basaltic sites. The dark grey line indicates the range of molar Ca/Sr ratios measured in open rainfall. Arrows indicate when the range of molar Ca/Sr ratios is greater than the x-axis with the maximum value displayed outside of the plot area to the right.

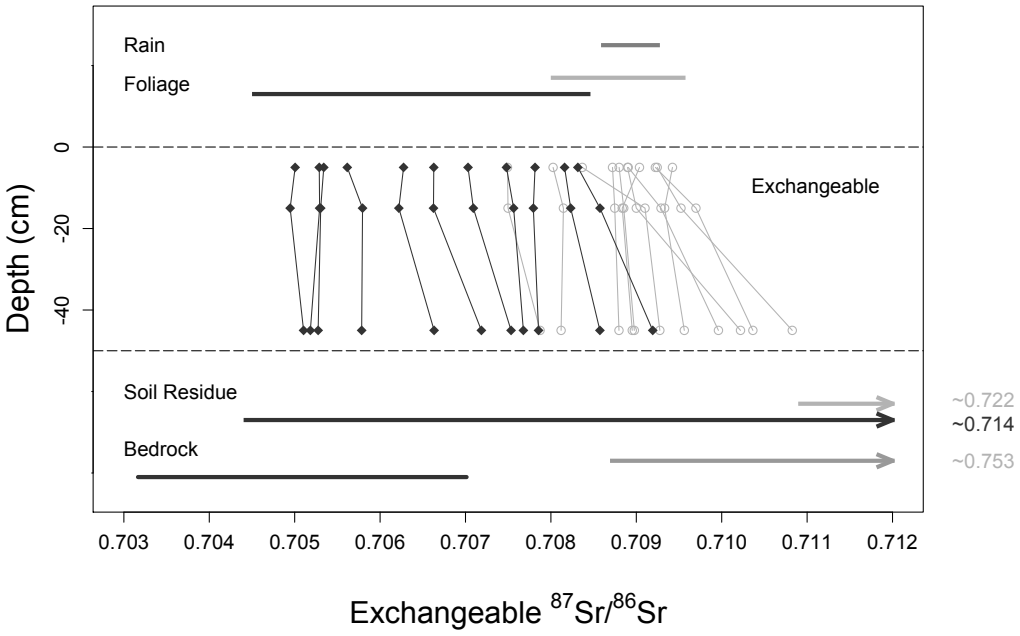

Figure 10. $^{87}Sr/^{86}Sr$ ratios of the soil exchangeable pool versus soil depth and compared to the range of $^{87}Sr/^{86}Sr$ ratios in other ecosystem pools. Basaltic sites indicated by black diamonds (◆) and sedimentary sites indicated by grey circles (○). Horizontal light grey lines indicate the range of $^{87}Sr/^{86}Sr$ ratios at sedimentary sites, while horizontal black lines indicate basaltic sites. The dark grey line indicates the range of $^{87}Sr/^{86}Sr$ ratios measured in open rainfall. Arrows indicate when the range of $^{87}Sr/^{86}Sr$ ratios is greater than the x-axis with the maximum value displayed outside of the plot area to the right.

Effective cation exchange capacity (ECEC) is the total quantity of cations (NH_4OAc extractable Ca, Mg, Na, K, plus KCl extractable H and Al) bound to negatively charged soil functional groups. Base saturation (BS) is the proportion of ECEC occupied by base cations (Ca, Mg, K, Na). Soils across our sites had a wide range of ECEC and BS (Table 4). ECEC of surface soils (0-10 cm depth) ranged from 7.61 to 32.3 cmol(+) kg^{-1} and did not co-vary with soil N concentration or pool size

(p-value = 0.51 and 0.82, Figure 11). ECEC displayed little to no variation with soil depth within sites (Table 4). Base saturation displayed an exceptionally wide range from 4.46 to 96.6 % (0-10 cm depth), but in contrast to ECEC, decreased with increasing soil N at 0-10 cm depths for both rock types (p-value <0.001, Figure 12). BS also decreased with increasing soil depth in both rock types (Table 4).

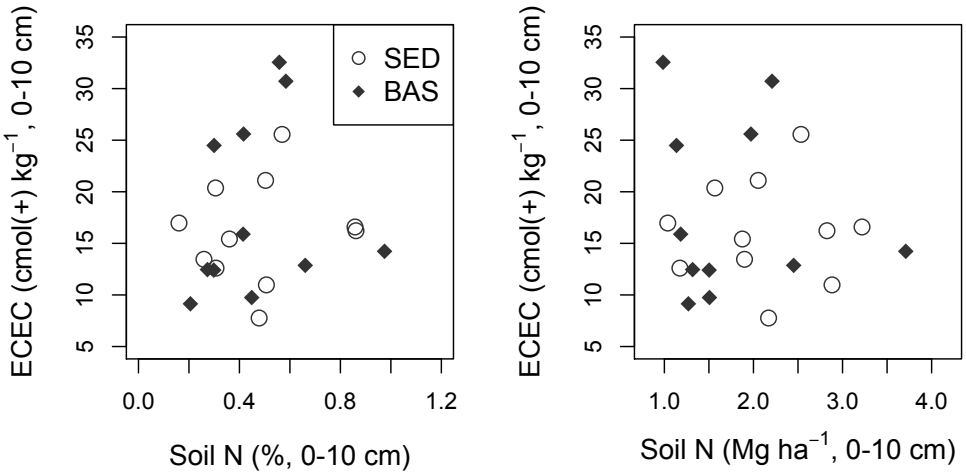

Figure 11. Effective cation exchange capacity (ECEC, 0-10 cm depth) versus surface soil N concentration (%, 0-10 cm depth, left panel) and N pool size (Mg/ha, 0-10 cm depth, right panel). Variation in ECEC did not differ between rock types (p = 0.78), and did not co-vary with soil N concentration or pool size (p = 0.51 and 0.82, respectively).

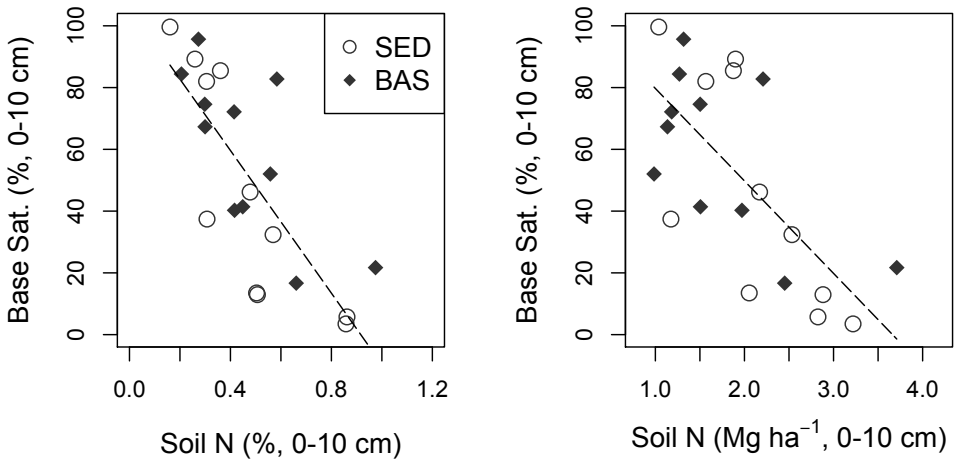

Figure 12. Soil base saturation (Base Sat., 0-10 cm depth) versus surface soil N concentration (%, 0-10 cm depth, left panel) and N pool size (Mg/ha, 0-10 cm depth, right panel). Variation in soil BS with soil N concentration and pool size (0-10 cm depths) did not differ between rock types ($p = 0.31$ and 0.85, respectively, extra sum of squares F-test). Regression lines include basaltic and sedimentary sites in left ($y = -115x + 106$; $R^2 = 0.60$, $p < 0.001$) and right panels ($y = -29.9x + 110$; $R^2 = 0.51$, $p < 0.001$).

3.4 Soil Residue

Soil residues that remain after NH_4OAc extraction contain base cations and other elements in a mixture of primary minerals, secondary minerals, and particulate organic matter, and are considered less available than exchangeable fractions. Calcium concentrations in soil residues from 0-10 cm depth were marginally higher at basaltic sites than sedimentary sites (Table 5). Calcium concentrations in basaltic soil residues from 0-10 cm depth ranged from 1.99 to 8.95 mg/g, excluding sites WP and Hoag that had Ca concentrations > 14.0 mg/g. Calcium concentrations in sedimentary soil residues from 0-10 cm depth ranged from 1.69 to 5.86 mg/g. The range of Sr

concentrations in basaltic soils from 0-10 cm depth was 33.8 to 130 μg/g and was nearly identical to that for soil residues from 0-10 cm depth at sedimentary sites: 35.0 to 188 μg/g. Calcium and Sr concentrations were highest in 0-10 cm soil residues at 17 sites. At the remaining 7 sites, Ca concentrations initially decreased from 0-10 cm to 10-20 cm depth then increased from 10-20 cm to 40-50 cm depth (Table 5). In contrast, Sr concentrations displayed little variation with depth, or increased slightly with increasing soil depth (Table 5).

Ca/Sr ratios in surface soil (0-10 cm depth) residues varied by rock type. Basalt sites had a wide range of Ca/Sr ratios (0-10 cm depth range: 64.6 – 305, Table 5), with a single site (WP) having Ca/Sr ratios greater than 700. Sedimentary soil residues had a narrower range of Ca/Sr ratios (range: 58.7 – 132). Ca/Sr ratios did not display a consistent pattern with depth at basalt sites, but tended to decrease with increasing soil depth at sedimentary sites (Figure 13). Sr-isotope ratios ($^{87}Sr/^{86}Sr$) in soil resides had a large range from 0.7043 – 0.7218 and there was considerable overlap between sites of contrasting rock type (Table 5). Basaltic sites with relatively high $^{87}Sr/^{86}Sr$ ratios (> 0.710) in residues generally displayed increasing $^{87}Sr/^{86}Sr$ with increasing soil depth, while soil residues with low $^{87}Sr/^{86}Sr$ ratios that more closely resembled basaltic rocks displayed little variation or decreased slightly with depth (Figure 14). Sedimentary soil residues did not show a consistent pattern with soil depth.

Tau (τ) values are useful for quantifying the gains or losses of an element during pedogenesis relative to the original concentration of that element in bedrock. A

tau-value of -1 indicates complete elemental loss relative to bedrock, while a value of +1 indicates a 100% gain. Basaltic soil residues had strongly negative $\tau_{Nb}Ca$ values at all soil depths (range = -0.98 to -0.81, 0-10 cm depth) except for WP, which had positive $\tau_{Nb}Ca$ values (Table 6). In contrast, sedimentary soils had a wide range of $\tau_{Nb}Ca$ values including strongly negative and strongly positive values (range = -0.87 to 39.1, 0-10 cm depth). Across all sites $\tau_{Nb}Ca$ values decreased or remained relatively constant with increasing soil depth (Figure 15).

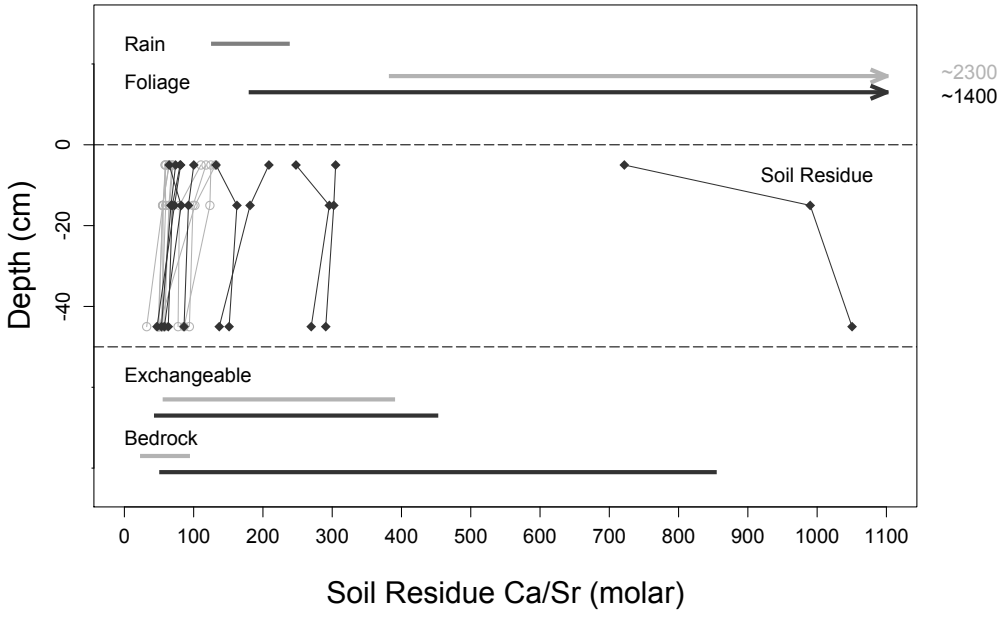

Figure 13. Molar Ca/Sr ratios of residual soil versus soil depth and compared to the range of molar Ca/Sr ratios in other ecosystem pools. Basaltic sites indicated by black diamonds (◆) and sedimentary sites indicated by grey circles (○). Horizontal light grey lines indicate the range of molar Ca/Sr ratios at sedimentary sites, while horizontal black lines indicate basaltic sites. The dark grey line indicates the range of molar Ca/Sr ratios measured in open rainfall. Arrows indicate when the range of molar Ca/Sr ratios is greater than the x-axis with the maximum value displayed outside of the plot area to the right.

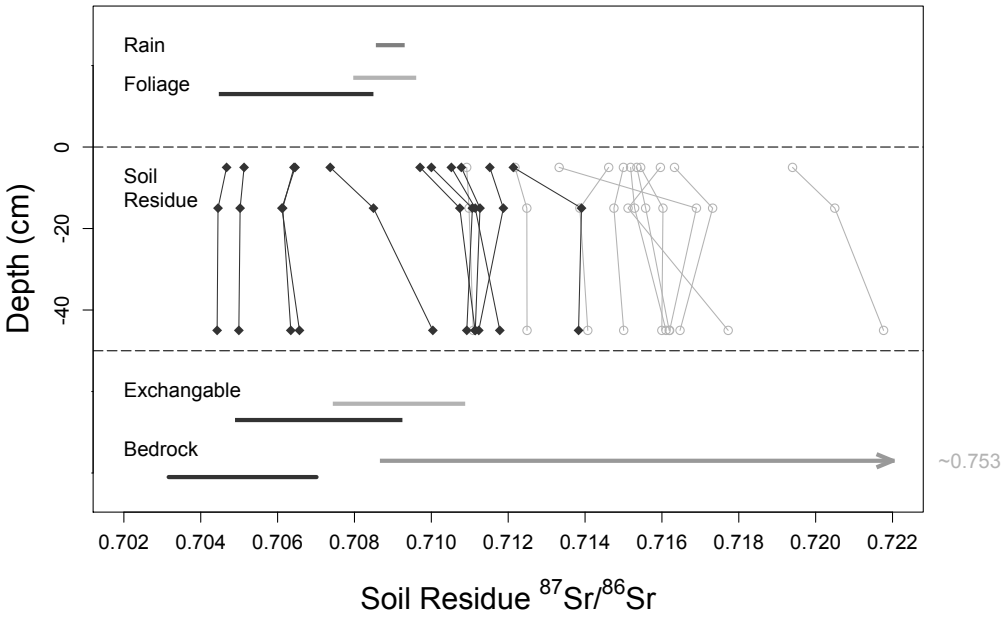

Figure 14. $^{87}Sr/^{86}Sr$ ratios of residual soil versus soil depth and compared to the range of $^{87}Sr/^{86}Sr$ ratios in other ecosystem pools. Basaltic sites indicated by black diamonds (◆) and sedimentary sites indicated by closed grey circles (○). Horizontal light grey lines indicate the range of $^{87}Sr/^{86}Sr$ ratios at sedimentary sites, while horizontal black lines indicate basaltic sites. The dark grey line indicates the range of $^{87}Sr/^{86}Sr$ ratios measured in open rainfall. Arrows indicate when the range of $^{87}Sr/^{86}Sr$ ratios is greater than the x-axis with the maximum value displayed outside of the plot area to the right.

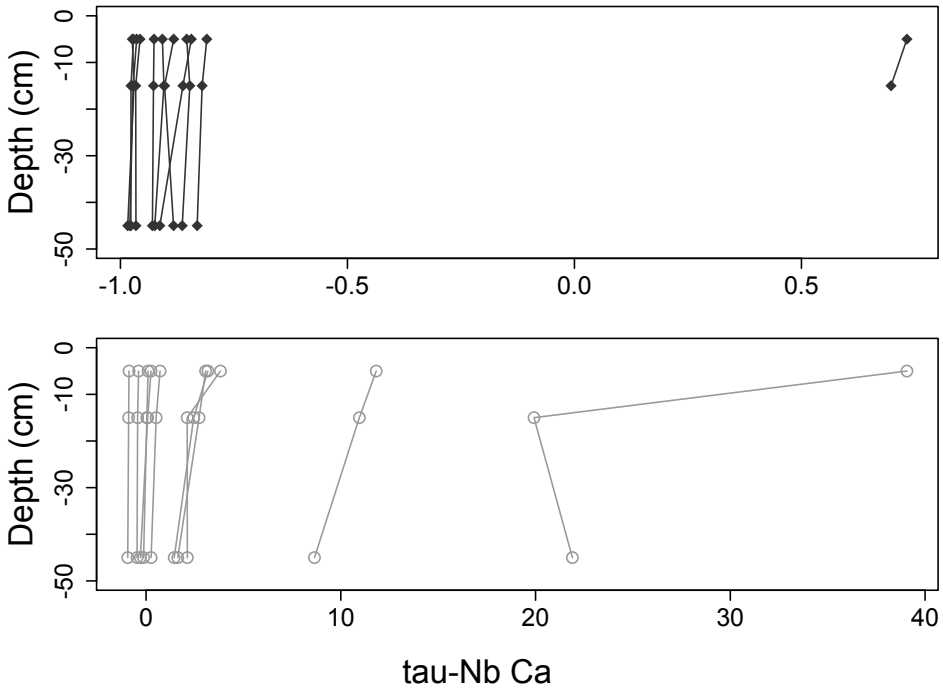

Figure 15. Soil residue τ_{Nb}Ca versus depth. Upper panel shows basaltic sites (◆) and lower panel shows sedimentary sites (○).

3.5 Coarse Soil Fragments

The coarse soil fragment content (i.e., particles > 2 mm in diameter) of bulk soils varied substantially across our research sites (Table 7). Coarse soil fragment content ranged from 1.65 to 28.0 % by mass (profile average, 0-50 cm depth) at sedimentary sites, and 5.38 to 55.1 % by mass at basaltic sites. Coarse soil fragments also had a large range in Ca concentration, ranging from 0.42 to 6.24 mg/g at sedimentary sites and 2.6 to 62.6 mg/g at basaltic sites (40-50 cm depth, Table 7). Calcium in soil residues increased with increasing Ca in coarse soil fragments and did not differ between rock types (Figure 16). Strontium in soil residues (40-50 cm depth) also increased with increasing Sr in coarse soil fragments but did differ slightly between rock types ($p = 0.07$, extra sum of squares F-test, Figure 17).

Coarse soil fragment molar Ca/Sr ratios ranged from 31.5 to 194 at sedimentary rock sites (40-50 cm depth, Table 7). Molar Ca/Sr ratios had a larger range at basaltic sites, ranging from 61.5 to 883 (40-50 cm depth, Table 7). In general, molar Ca/Sr ratios in coarse soil fragments increased with increasing Ca/Sr ratios in bulk rocks (Figure 18). Similarly, molar Ca/Sr ratios in soil residues increased with increasing Ca/Sr ratios in coarse soil fragments (Figure 18). We measured $^{87}Sr/^{86}Sr$ ratios in coarse soil fragments at 6 sites where bulk rock samples were not recovered directly at the site. Of these sites 5 were basaltic sites, and coarse soil fragments had a narrow range of $^{87}Sr/^{86}Sr$ ratios that were slightly greater than bulk rock samples collected at nearby locations (Figure 19). In contrast, at one sedimentary site the $^{87}Sr/^{86}Sr$ ratio of coarse soil fragments was much greater than bulk rock collected

nearby (Figure 19). Strontium isotope ratios in soil residues varied in their similarity to coarse soil fragments. At two basalt sites and the single sedimentary site, $^{87}Sr/^{86}Sr$ ratios were similar between soil residues and coarse soil fragments; however, $^{87}Sr/^{86}Sr$ ratios in soil residues were much greater than coarse soil fragments in the remaining three basaltic sites (Figure 19).

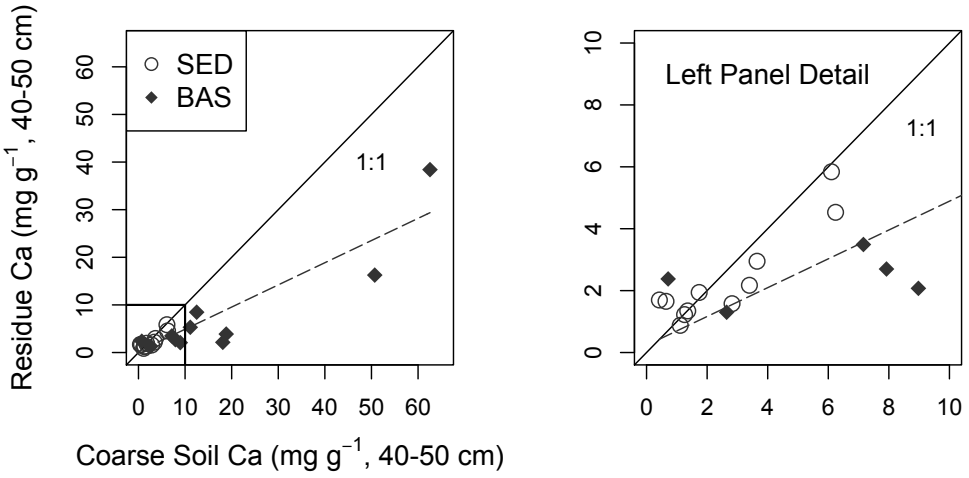

Figure 16. Coarse rock fragment versus fine earth soil residue Ca concentration (mg/g, 40-50 cm depth). Black box (left panel) indicates detail shown in right panel. Variation in Ca concentrations between soil residue and coarse fragments did not differ between rock types ($p = 0.16$, extra sum of squares F-test). Solid black line indicates 1:1 relationship. Left and right panel regression (dashed line) includes basaltic and sedimentary sites: $y = 0.466x + 0.233$ ($R^2 = 0.86$; $p < 0.001$).

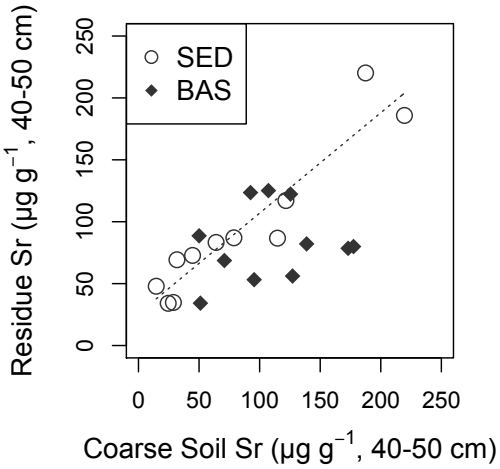

Figure 17. Coarse rock fragment versus fine earth soil residue Sr concentration (µg/g, 40-50 cm depth). Solid black line indicates 1:1 relationship. Variation in soil residue with coarse fragment Sr concentration differed between rock types ($p = 0.07$, extra sum of squares F-test) and varied systematically only for sedimentary sites. Sedimentary regression (dotted line): $y = 0.811x + 25.8$ ($R^2 = 0.88$; $p < 0.001$)

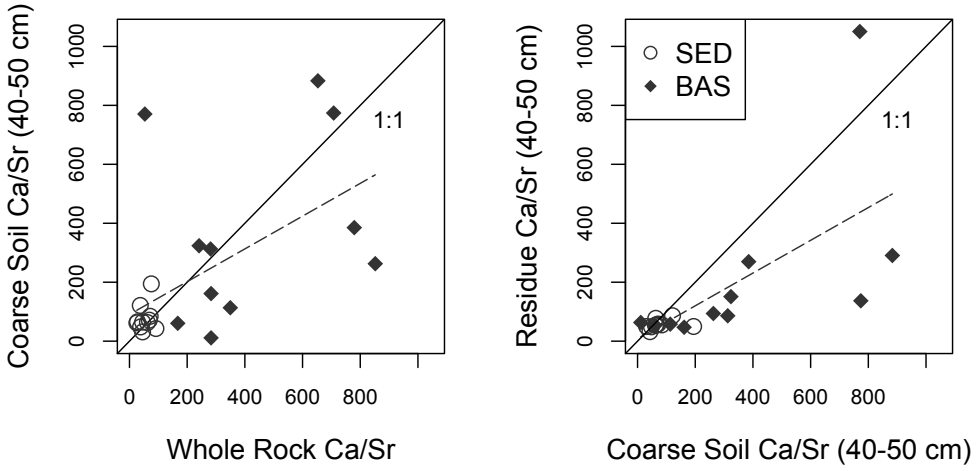

Figure 18. Comparison of molar Ca/Sr ratios in coarse soil fragments (40-50 cm depth) to bulk rocks and soil residues (40-50 cm depth) (left and right panels, respectively). Solid lines (both panels) indicate a 1:1 relationship. Variation in bulk rock with coarse soil fragment Ca/Sr ratios did not differ between rock types (p-value = 0.20, extra sum of squares F-test), nor did they differ with coarse soil fragments and

soil residues (p-value = 0.88). Regression lines (dashed) include basaltic and sedimentary sites in left ($y = 0.556x + 90.7$; $R^2 = 0.32$; $p = 0.006$) and right panels ($y = 0.556x + 8.86$; $R^2 = 0.45$; $p < 0.001$).

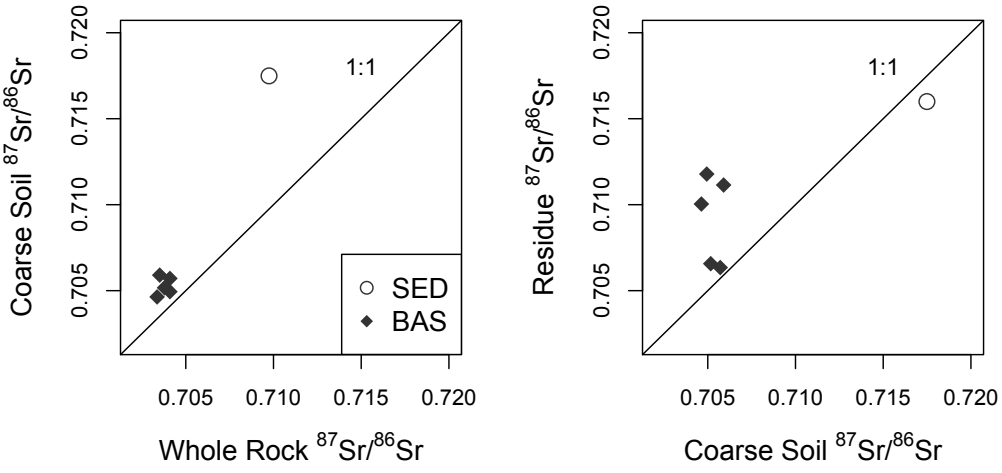

Figure 19. Comparison of $^{87}Sr/^{86}Sr$ ratios in coarse soil fragments (40-50 cm depth) to bulk rocks and fine earth soil residues (40-50 cm depth). Solid black line indicates 1:1 relationship.

3.6 Douglas-fir Foliage

Douglas-fir foliage had a wide range of Ca and Sr concentrations (Table 8). Foliar Ca concentrations ranged from 12.3 to 27.0 mg g^{-1}, decreased with increasing soil N concentrations, and did not differ between rock types along the soil N-gradient (Figure 20). Foliar Sr concentrations ranged from 1.26 to 22.2 μg g^{-1}, displayed high variability at low-N sites, but were always low at high-N sites (Figure 21). Foliar Ca increased with increasing Sr concentrations (Figure 22). Molar Ca/Sr ratios ranged from 194 to 2340 (Table 8) and were not related to soil N for either rock type (Figure 23).

Douglas-fir foliage had a narrow range of $^{87}Sr/^{86}Sr$ ratios at sedimentary sites, and a broad range of $^{87}Sr/^{86}Sr$ ratios at basaltic sites (Table 8). Across all sites, foliar $^{87}Sr/^{86}Sr$ ratios were the same as mass-weighted soil exchangeable $^{87}Sr/^{86}Sr$ ratios ($p = 0.99$; 0-10, 10-20, and 40-50 cm soil depths; Figure 24). Molar Ca/Sr ratios of foliage increased with increasing mass-weighted soil exchangeable Ca/Sr ratios, but Ca/Sr ratios of foliage were greater than soil exchangeable Ca/Sr ratios by a factor of 1.3 to 21 (Figure 24).

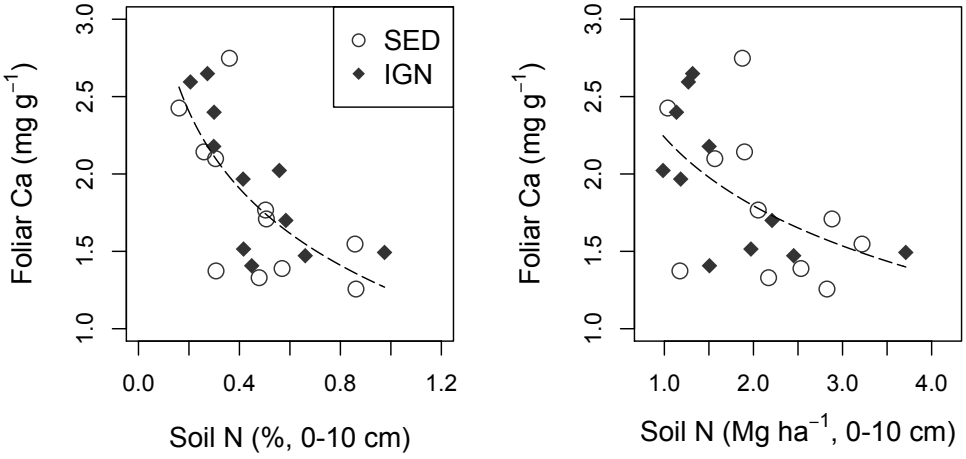

Figure 20. Foliar Ca (mg g^{-1}) versus soil N concentration (%, 0-10 cm depth, left panel) and N pool size (Mg ha^{-1}, 0-10 cm depth, right panel). Variation in foliar Ca with soil N concentration and pool size (0-10 cm depths) did not differ between rock types ($p = 0.59$ and 0.93, respectively, extra sum of squares F-test). Regression lines (dashed) include basaltic and sedimentary sites in left ($y = -0.717\ln(x) + 1.25$; $R^2 = 0.48$; $p < 0.001$) and right panels ($y = -0.64\ln(x) + 2.24$; $R^2 = 0.27$, $p = 0.009$).

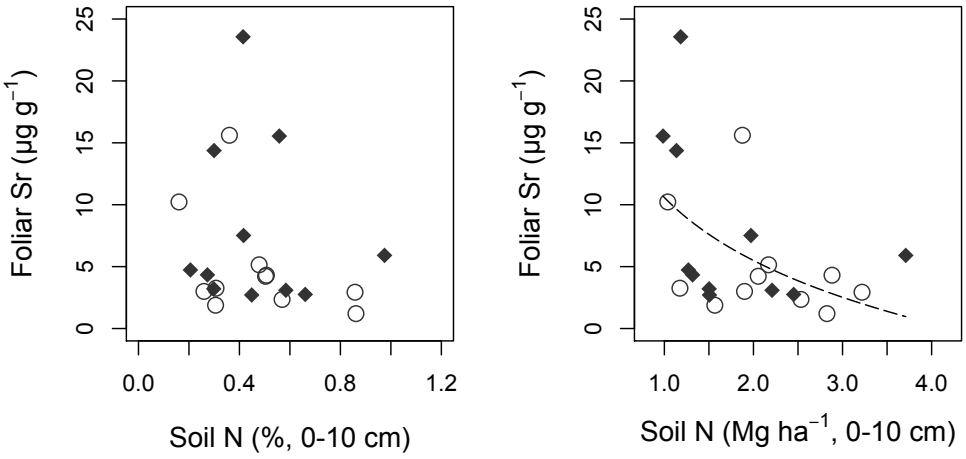

Figure 21. Foliar Sr (µg g^{-1}) versus soil N concentration (%, 0-10 cm depth, left panel) and N pool size (Mg ha^{-1}, 0-10 cm depth, right panel). Variation in foliar Sr with soil N concentration and pool size (0-10 cm depths) did not differ between rock types (p = 0.34 and 0.66, respectively, extra sum of squares F-test). Right panel regression includes basaltic and sedimentary sites: y = -7.33x + 10.6 (R^2 = 0.25; p = 0.013).

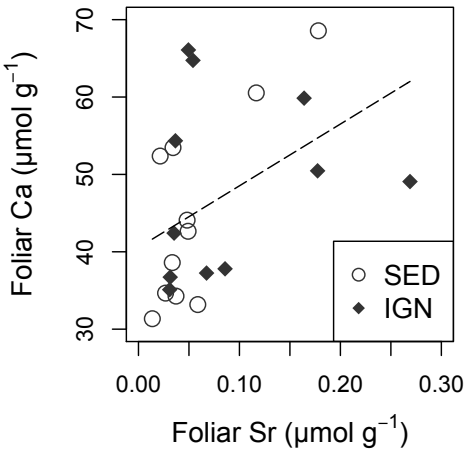

Figure 22. Foliar Sr versus foliar Ca concentration (µmol g^{-1}). Variation in foliar Ca with Sr did not differ between rock types (p = 0.89, extra sum of squares F-test). Regression includes basaltic and sedimentary sites: y = 79.8x + 40.5 (R^2 = 0.19; p = 0.032).

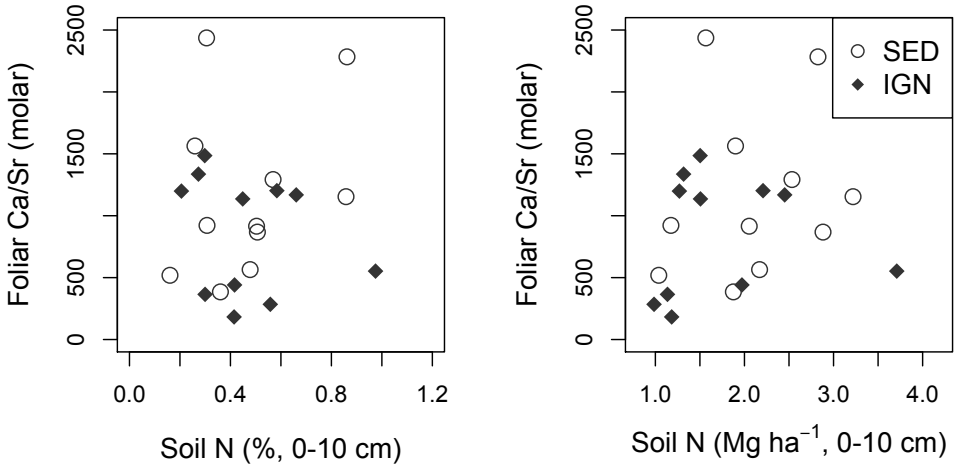

Figure 23. Foliar Ca/Sr (molar) versus soil N concentration (%, 0-10 cm depth, left panel) and N pool size (Mg/ha, 0-10 cm depth, right panel). Variation in foliar Ca/Sr with soil N concentration and pool size (0-10 cm depths) did not differ between rock types (p = 0.30 and 0.39, respectively, extra sum of squares F-test).

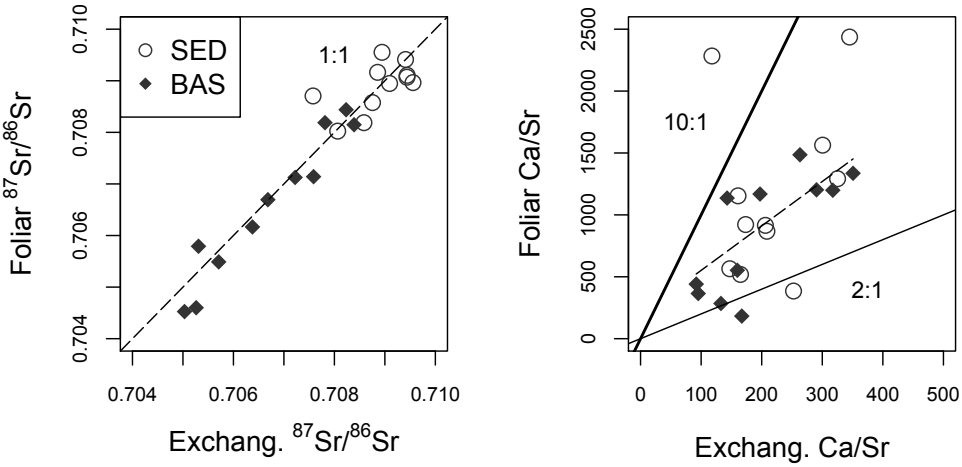

Figure 24. Foliar $^{87}Sr/^{86}Sr$ and Ca/Sr ratios versus mass weighted soil exchangeable $^{87}Sr/^{86}Sr$ and Ca/Sr (0-10, 10-20, and 40-50 cm depths). Exchangeable $^{87}Sr/^{86}Sr$ was weighted by the exchangeable Sr pool size, and Ca/Sr was weighted by soil mass. Variation in foliar $^{87}Sr/^{86}Sr$ with exchangeable $^{87}Sr/^{86}Sr$ did not differ between rock types (p = 0.30, respectively, extra sum of squares F-test), and the slope of foliar $^{87}Sr/^{86}Sr$ with exchangeable $^{87}Sr/^{86}Sr$ did not differ from 1 (p = 0.97, extra sum of

squares F-test). On right panel, thick and thin solid black lines indicate a 10:1 and 2:1 relationship, respectively. Right panel regression includes sedimentary and basalt sites but excludes the two sites with foliar Ca/Sr ratios > 2000: $y = 3.59x + 193$ ($R^2 = 0.37$, p-value = 0.002).

3.7 Bedrock

Calcium concentration of basaltic rocks averaged 70.5 mg g^{-1} (range: 42.5 to 84.8 mg g^{-1} Ca) and was nearly 20-times greater than the sedimentary rock average of 4.26 mg g^{-1} Ca (range: 0.176 to 16.6 mg g^{-1} Ca) (Table 9). Strontium concentrations were also higher in basaltic rocks compared to sedimentary rocks, ranging from 181 to 1743 μg g^{-1} and 6.19 to 379 μg g^{-1}, respectively. In sedimentary rocks, Sr increased with increasing Na and Ca concentrations (Figure 25).

Basaltic rocks had an extremely narrow range of $^{87}Sr/^{86}Sr$ ratios (0.7032 – 0.7041). In contrast, sedimentary rocks had a wide range of $^{87}Sr/^{86}Sr$ ratios (0.7087 – 0.7526) that increased with increasing K/Sr ratios along a mixing line (Figure 26). Ca/Sr ratios are routinely plotted against $^{87}Sr/^{86}Sr$ ratios in the geochemical literature to evaluate end-member mixing patterns. We deviated from this convention by comparing molar Sr/Ca ratios of rock leaches to Sr/Ca ratios in bulk rocks, which allows us to evaluate the leverage that rock leaches versus whole rocks would have in our mixing calculations. Leachable Sr/Ca ratios varied for both sedimentary and basaltic rocks (Table 10), but generally increased with whole rock Sr/Ca ratios (Figure 27). Leachable $^{87}Sr/^{86}Sr$ of basaltic rocks plotted near the 1:1 line with whole rock $^{87}Sr/^{86}Sr$, while sedimentary rock leaches were less radiogenic in ^{87}Sr compared to

whole rocks (Figure 27). The rock leach from several sedimentary sites had molar Ca/P ratios close to that expected for apatite (1.67), while the Ca/P ratio of basaltic rock leaches was always greater than apatite stoichiometry (Figure 28).

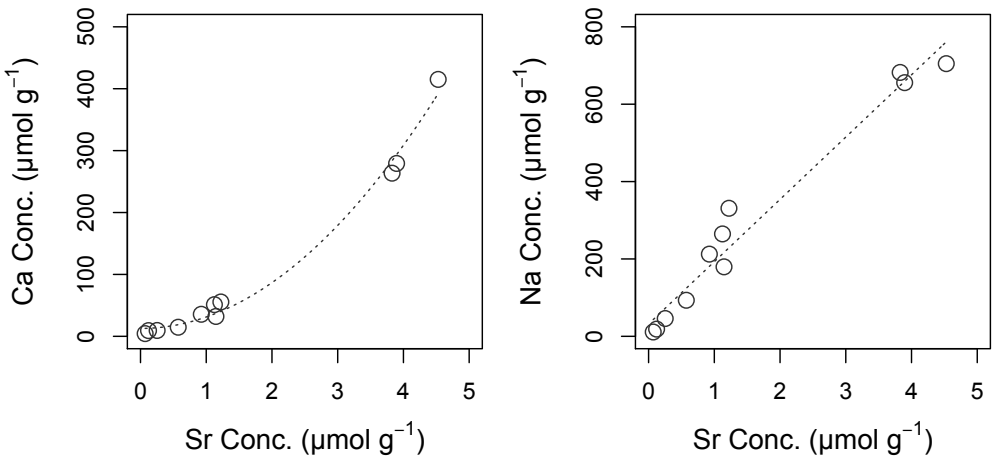

Figure 25. Molar Sr versus Ca (left panel) and Na concentrations (right panel) in sedimentary rocks. Left panel regression: $y = 18.5x^2 + 12.7$ ($R^2 = 0.99$, p-value < 0.001). Right panel regression: $y = 161x + 31.9$ ($R^2 = 0.97$, p-value < 0.001).

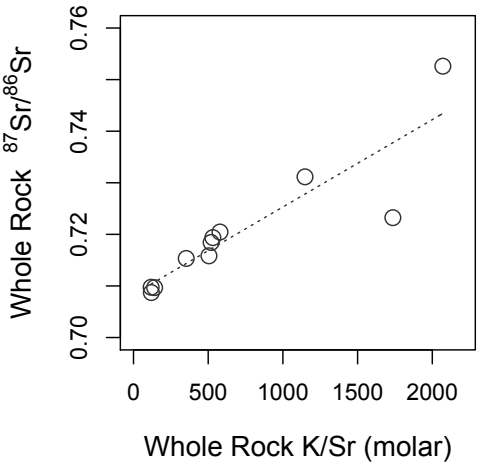

Figure 26. Molar K/Sr versus $^{87}Sr/^{86}Sr$ ratios in sedimentary rocks. Regression: $y = 1.69*10^{-5}x + 0.708$ ($R^2 = 0.79$, p-value = < 0.001).

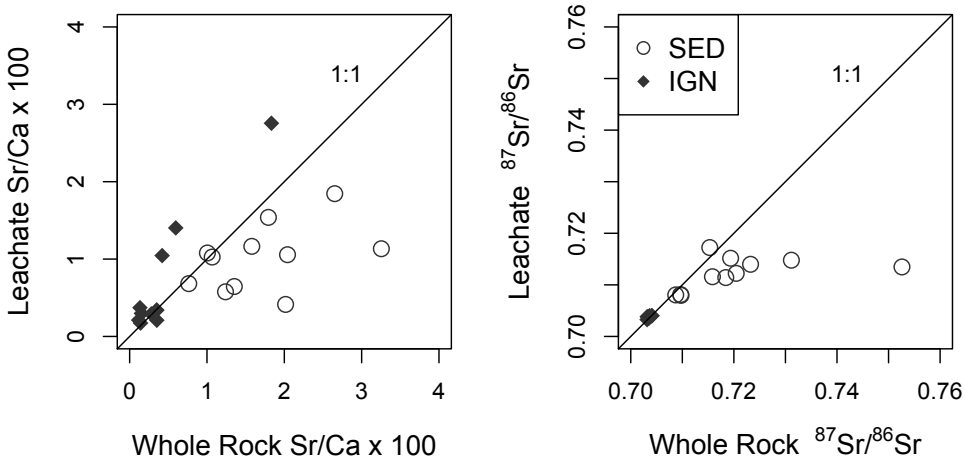

Figure 27. Comparison of molar Sr/Ca (left panel) and $^{87}Sr/^{86}Sr$ (right panel) ratios in whole rocks versus 1 M HNO_3 rock leachates. In left and right panels, the line indicates a 1:1 relationship.

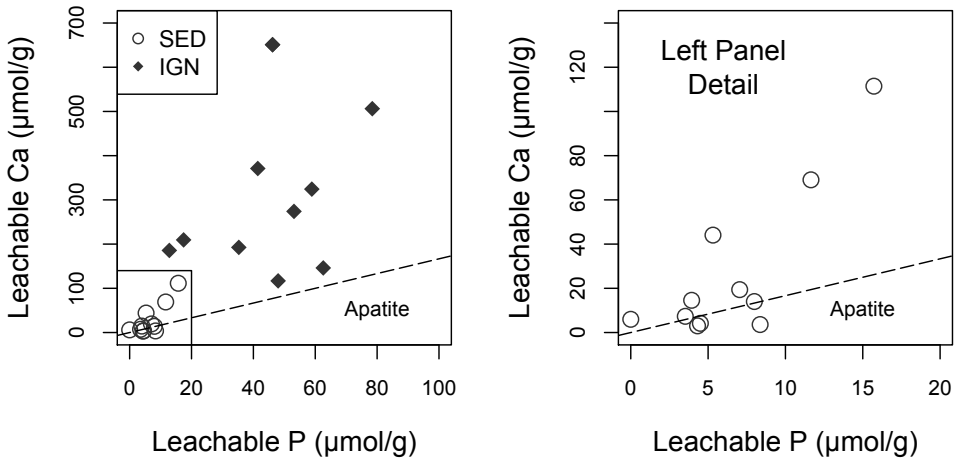

Figure 28. Molar P versus Ca concentration in 1 M HNO_3 rock leachates. Black box (left panel) indicates detail shown in right panel. In both panels, the line indicates Ca:P stoichiometry of apatite (molar Ca/P = 1.67).

3.8 Open Wet-Deposition

A long-term (1997-2006) weekly record of precipitation chemistry (Ca, Na, K, Mg, etc.) in the Oregon Coast Range (NADP, 2014) indicates strong baseline inputs of marine aerosols in wet deposition resembling seawater stoichiometry (Figure 29). For this reason, rainfall should have an Sr-isotope signature close to modern seawater ($^{87}Sr/^{86}Sr$ = 0.70917 and Ca/Sr ~ 115, Dia et al., 1992). To confirm that the Sr-isotope signature of wet deposition was similar to seawater, precipitation chemistry was characterized by event-based sampling at three locations during the late winter to early summer of 2013.

Base cation (K, Na, Mg, and Ca) and Sr concentrations, Ca/Sr ratios, and Sr-isotopes measured in open wet-deposition are presented in Table 11. Concentrations of all elements were similar between sites for each storm that we sampled (low spatial variability), but declined from winter to summer (high temporal variability) (Table 11). Molar Mg/Na ratios, which are conservative from seawater to rainfall, consistently fell close to seawater (Figure 29). Molar Ca/Na ratios, which are less conservative from seawater to rainfall, were elevated by ~10% compared to seawater and well within the range of 10 years of weekly wet deposition values from a nearby NADP site (Alsea Station, OR02, discontinued in 2006, data in Figure 29).

Ca/Sr ratios in precipitation were slightly higher than seawater (Figure 30). No long-term precipitation data for Sr were available from the Oregon Coast Range. Similarly, we found a very small range in $^{87}Sr/^{86}Sr$ ratios in open wet-deposition (0.7086 to 0.7093), with a calculated flux-weighted average for precipitation (0.70916) that was nearly identical to seawater (0.70917, Table 11). Sr-isotope ($^{87}Sr/^{86}Sr$) ratios increased with increasing molar Na/Sr ratios and decreased from late winter to early summer (Figure 31). Although we did not sample the three wettest months (i.e., November, December and January), the long-term median Ca/Na ratios in NADP data indicate that precipitation in these wettest months is more similar to seawater than the months we sampled (Figure 32), suggesting that seawater is the dominant source of Sr in wet deposition across our sites.

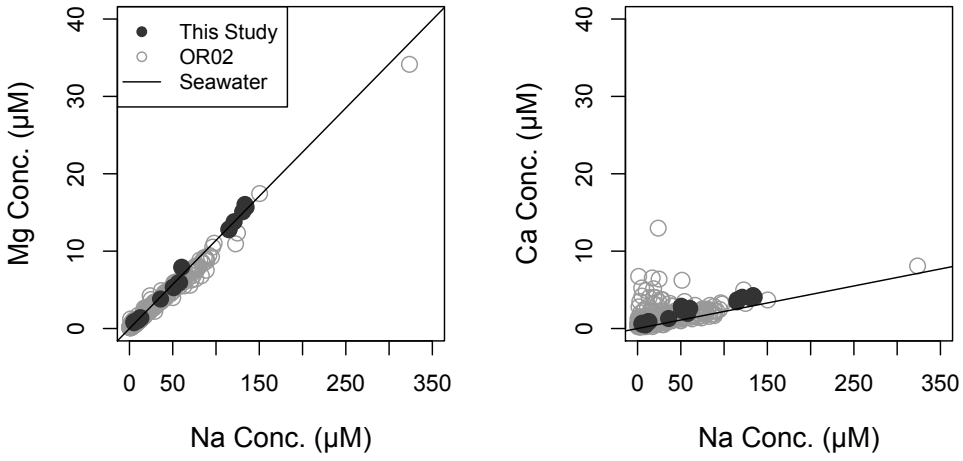

Figure 29. Molar Na versus Mg (left panel) and Ca concentrations (right panel) in open rainfall samples. In left and right panels, solid black line indicates the molar stoichiometry of Mg/Na and Ca/Na in seawater, respectively.

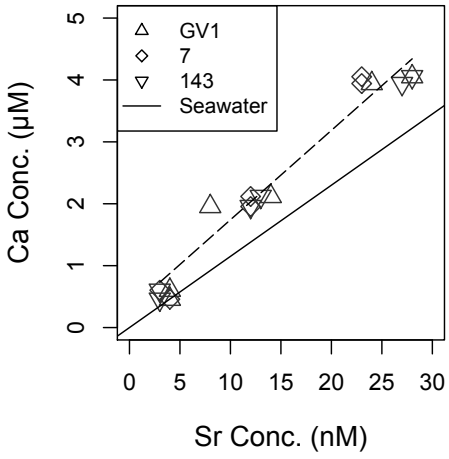

Figure 30. Molar Sr versus Ca concentration in open rainfall. Solid black line indicates the molar stoichiometry of Ca/Sr in seawater (115), but note the difference in units between x and y axis which result in a Ca/Sr ratio of 0.115. Dashed line regression: y 0.144x + 0.297 ($R^2 = 0.96$, p-value < 0.001).

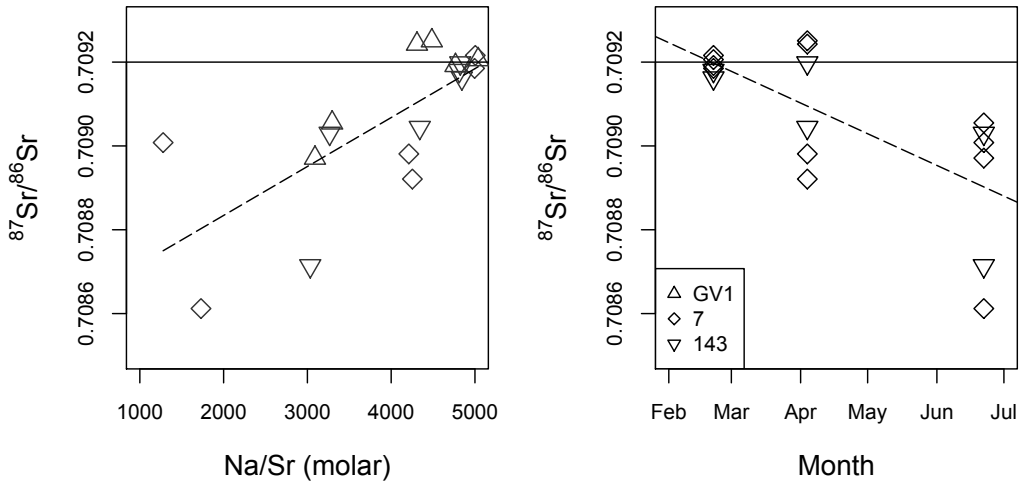

Figure 31. Strontium isotope ratios ($^{87}Sr/^{86}Sr$) in open rainfall versus molar Na/Sr ratios (left panel) and sampling date (right panel). In both left and right panels, horizontal solid black line indicates the $^{87}Sr/^{86}Sr$ ratio of seawater. Left panel regression: $y = 1.17*10^{-7}x + 0.7086$ ($R^2 = 0.54$, p-value < 0.001). Right panel regression: $y = -2.44*10^{-6}x + 0.748$ ($R^2 = 0.49$, p-value = 0.001).

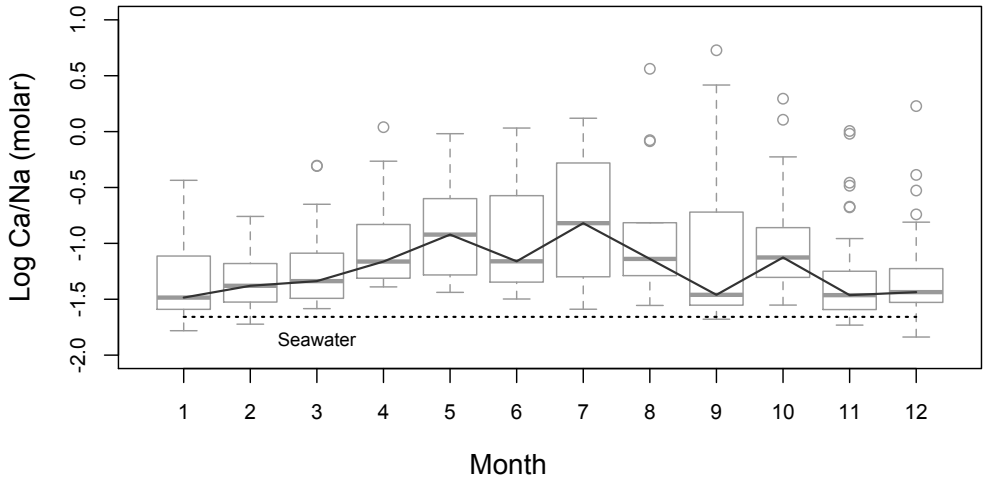

Figure 32. Boxplot of molar Ca/Na ratios in weekly open wet-deposition samples from NADP site OR02 (1997 to 2006) grouped by month. Horizontal black dotted line indicates the molar stoichiometry of Ca/Na in seawater. Black line connects median monthly Ca/Na ratios.

CHAPTER 4 – DISCUSSION

Nitrogen availability is a dominant factor shaping the size and distribution of base cation pools in forest ecosystems of the Pacific Northwest. However, the relative importance of atmospheric versus geologic inputs as long-term sources of base cations to these forests remains unclear, and cannot be inferred from traditional nutrient pool data alone. Likewise, it is possible that other state factors of soil formation and ecosystem development co-vary with N availability across sites and may also influence pools and sources of base cations. In particular, the mineralogy and base cation content of parent rocks is fundamental to the supply of Ca to ecosystems via weathering, raising the possibility that base cation pools and sources across a gradient of N availability vary by rock type. To resolve these questions, we (1) use $^{87}Sr/^{86}Sr$ signatures to differentiate atmospheric vs geologic sources of base cations across a wide gradient of soil N, (2) examine variation in soil N against a suite of 17 site properties related to the five major state-factors of soil and ecosystem development, and (3) evaluate the relative importance of geology versus ecosystem N-status in controlling long-term base cation sources in Oregon Coast Range (OCR) forests.

4.1 Ecosystem Inputs of Strontium and Calcium

Inputs of Sr and Ca to forests can originate from a variety of sources, including precipitation, local or far travelled dust, and chemical dissolution of primary and secondary minerals in soils and rocks. Although end-member mixing models with a single source tracer are most robust when only two end-members are considered, it is

possible to use other detailed sampling and chemical budgeting to constrain the magnitude of any particular source, or eliminate it as a possibility altogether. To quantify the number and Sr isotope signature of Ca sources in coastal Oregon forests, we measured $^{87}Sr/^{86}Sr$ ratios and Sr and Ca concentrations in open wet-deposition, non-exchangeable soil pools that include primary and secondary minerals, coarse rock fragments in soils, and whole and acid-leachable bedrock. In cases where it was not possible to directly measure each potential source (e.g. long-traveled dust deposition), we relied on published literature to obtain isotopic values and estimate Ca and Sr fluxes.

The Ca content of bedrock is a fundamental factor governing Ca supply to ecosystems (Page and Mitchell, 2008). Across our research sites, the mean Ca content of basaltic rocks was 20-times higher than sedimentary rocks (Table 8). Yet, the stark differences in whole-rock Ca contents and $^{87}Sr/^{86}Sr$ ratios between basaltic and sedimentary rocks are not surprising given their different conditions of formation. The basaltic rocks we drilled yielded samples of fresh unweathered bedrock of relatively young geologic age. Consequently, our basaltic rock samples exhibited minimal geochemical and isotopic variation among sites, as expected for other basaltic rocks in the OCR (Parker et al., 2010; Snavely et al., 1968). In contrast, sedimentary rocks of the OCR have a more complex history, being composed of mineral grains that have been subjected to weathering over long timescales (age of sediments ~100 Ma, VanLaningham et al., 2008) and physical abrasion during sediment transport over 100's of km prior to deposition and lithification (Heller et al., 1985). It has long been

recognized that Ca-bearing silicate minerals are among the least stable silicate minerals at low-temperature and pressure (Goldich, 1938), which increases the likelihood of Ca loss from parent minerals prior to their incorporation in sedimentary rocks. Therefore, the abundance of Ca is low in sedimentary rocks of the OCR and may limit Ca supply from rock sources, while high Ca in basaltic rocks may supply ample Ca to these ecosystems.

The differences in chemistry between basaltic and sedimentary rocks were accentuated by their responses to treatment with 1 M HNO_3. This low-molarity acid chemical treatment characterizes mineral phases that are more susceptible to weathering in granitic rocks and soils including calcite and apatite, and thus most likely to supply Ca to plants in weakly developed soils (Blum et al., 2002; Hamburg et al., 2003; Nezat et al., 2007). Basaltic rocks, which are composed of a suite of fine-grained minerals and volcanic glass, are expected to dissolve congruently with respect to calcium (Eggleton et al., 1987). Accordingly, OCR basaltic rocks displayed strong similarity between whole rock and rock-leachable $^{87}Sr/^{86}Sr$ despite modest differences in Ca/Sr ratios (Figure 16). In contrast to the basaltic sites, we observed relatively large differences in the chemical and isotopic composition of whole versus rock leaches of sedimentary rocks, suggesting that sedimentary rocks of the OCR undergo differential weathering of Sr-bearing minerals. Therefore, at basaltic sites it makes no difference whether whole rock or acid-leachable chemistry is used as the rock end-member for Sr-isotope partitioning, but this choice of end-members does matter at sedimentary sites.

Strontium isotope ratios of our sedimentary rock leachates are similar to previously reported $^{87}Sr/^{86}Sr$ ratios for feldspar minerals of the Tyee Formation ($^{87}Sr/^{86}Sr$ = 0.7109 – 0.7142), and our high, whole rock $^{87}Sr/^{86}Sr$ ratios reflect the disproportionate influence of K-rich sheet silicates on Sr-isotopes as previously reported for micas of the Tyee Formation ($^{87}Sr/^{86}Sr$ = 0.7446 – 0.7917, Heller et al., 1985). Granitic rocks, from which sedimentary rocks of the Oregon Coast Range are derived, frequently exhibit preferential weathering of plagioclase minerals relative to K-rich sheet silicates, and this difference in weathering susceptibility is reflected in Sr isotope signatures of vegetation (Blum et al., 2008, 2002) and stream waters (Bullen and Kendall, 1998; Clow et al., 1997). Low $^{87}Sr/^{86}Sr$ ratios in rock leachates at three of our sites ($^{87}Sr/^{86}Sr$ ~ 0.708, Devitt, 43, and 143) reflect contributions from calcite ($^{87}Sr/^{86}Sr$ = 0.7078, Peterman et al., 1970), which is among the most easily weathered Ca-bearing minerals and reported to be the cementing agent of this rock type (Anderson et al., 2002). Yet, calcite only appears to be available to plants at site 43 (foliar $^{87}Sr/^{86}Sr$ = 0.7080), and the lack of a calcite Sr-isotope signature in other sedimentary rock leaches suggests that calcite weathering takes place beyond the reach of our sampling equipment (11 m) and is thus likely to bypass upland vegetation.

Like calcite, apatite [$Ca_5(PO_4)_3(OH,F,Cl)$] is an easily weathered often trace-abundance but Ca-rich mineral that can disproportionately affect Ca and P nutrient budgets in base-poor soils (Blum et al., 2002). Apatite can occur as an inclusion in more resistant minerals (e.g. K-feldspar), and in this way is physically protected from rapid weathering (White and Brantley, 1995). Sedimentary rock leachates from our

sites have a wide range of molar Ca/P ratios (0.5 – 10.3) that encompass the theoretical Ca/P ratio expected from apatite weathering (Ca/P = 1.67) (Figure 17). However, given the relatively fine grain size of lithified Tyee sediments (Chan, 1985), it seems unlikely that apatite would be preserved in near-surface soils in quantities sufficient to influence Ca budgets in these forests. To our current knowledge, Sr-isotope ratios of apatite have not been previously reported for OCR sedimentary rocks or the Idaho Batholith, making it difficult to unequivocally evaluate apatite as a Ca source in our sites.

Soil residues that remain after extraction of exchangeable base cations include a mixture of crystalline primary and secondary minerals, as well as organic matter. Only primary minerals represent a new source of Ca and Sr to ecosystems, whereas secondary minerals and organic matter contain internally recycled Ca and Sr. Decreasing Ca/Sr ratios (Table 5) and τCa values (Table 6) with increasing soil depth across our field sites mirrors depth related changes in the soil exchangeable pool and do not reflect Ca depletion expected through weathering processes (Blum et al., 2008; Vitousek and Chadwick, 2013). τCa estimates the mass loss of Ca from bedrock, after accounting for changes in soil volume using the concentration of an immobile element (Nb) in rock and soil as a reference point. Thus, patterns of Ca/Sr and τCa at our sedimentary sites likely reflect biological uplift and recycling of Ca, signals which are particularly sensitive due to the low intrinsic Ca concentrations of these sedimentary rocks (Table 9). In contrast, high Ca concentrations in basaltic rocks make τCa less sensitive to biological uplift, and instead indicate that basaltic soils are highly depleted

in Ca, having lost an average of 95% of their original Ca contents (Table 6). Similar mass losses of Ca have been reported in 20,000 year-old basaltic soils of Hawaii receiving 2500 mm rainfall yr^{-1} (Vitousek et al., 1997). Thus, soil residues appear to contain appreciable amounts of biologically recycled Sr and Ca that may be either atmospheric or rock-weathering in origin, and do not provide a reliable signature for rock-weathering inputs alone.

Soil residues overlying basaltic parent materials (whole rock $^{87}Sr/^{86}Sr$ ~ 0.7036) at 6 sites contained unusually high $^{87}Sr/^{86}Sr$ ratios (>0.710, Table 4). While the source of these high $^{87}Sr/^{86}Sr$ ratios is not definitively clear, it most likely represents a legacy of sedimentary (granitic) overburden that weathered away to expose the underling basaltic rocks (Figure 33). Accumulation of long-travelled dust from the China Plateau ($^{87}Sr/^{86}Sr$ range > 0.714, Nakai et al., 1993), extra-local Missoula flood sediments from the neighboring Willamette Valley (ultimately derived from a mixture of granitic and basaltic rocks), and/or coastal plain sediments could also cause basaltic soil residues to be more radiogenic (i.e., have high $^{87}Sr/^{86}Sr$ ratios). Our estimate of Asian dust deposition (~2.06 Mg Ca ha^{-1}, see Appendix C for calculation) during the last glacial maximum is only slightly less than the total Ca pool size of soil residues to 100 cm depth across these 6 sites, and we know of no estimates for regional dust deposition of Missoula flood or coastal plain sediments to OCR forests during the last glacial maximum. Presumably, dust from any one of these

Figure 33. Basalt quarry with overlying sedimentary rocks in the Oregon Coast Range. Exposed sedimentary (white line) and basaltic (black line) rock units are outlined in the lower panel. Quarry is located near the southwestern most extent of our sampling sites in the Tyee Formation (LAT/LONG = 44.623, -123.809).

sources would be broadly distributed. Yet, given the broad spatial distribution of basaltic sites with unusually high $^{87}Sr/^{86}Sr$ ratios, their close proximity to basaltic sites with low $^{87}Sr/^{86}Sr$ ratios, and the lack of a coherent $^{87}Sr/^{86}Sr$ signature across all of our sites, it seems unlikely that our unusually high $^{87}Sr/^{86}Sr$ ratios at basaltic sites are due to dust deposition. An analysis of rare earth element patterns or an additional isotope system (e.g., Pb or Nd) in soil residues, coarse soil fragments, and whole rock samples could be used to better constrain the potential source of high $^{87}Sr/^{86}Sr$ ratios in some basaltic site residues (Prytulak et al., 2006), even though these residues do not appear to contribute appreciably to the available pool of exchangeable or foliar Sr.

Neither incongruent weathering of basaltic rocks nor deposition of Cascadia volcanic ash can explain the high $^{87}Sr/^{86}Sr$ ratios of residues at some basaltic sites. Rather, these processes would result in soil residues with $^{87}Sr/^{86}Sr$ ratios that are less than or equal to our bulk basaltic rocks (Dunn and Sen, 1994; $^{87}Sr/^{86}Sr$ of Mazama ash ~ 0.7036 Goles and Lambert, 1990; Irving, 1978). In addition, although volcanism is pervasive in the recent geologic history of the Pacific Northwest, prevailing westerly winds limited ash deposition in OCR forests with only 1-2 cm of Mazama ash deposited in lake sediments spanning our sampling sites (~7000 years B.P., Long et al., 2007). This relatively thin layer of ash contains approximately as much Ca (~260 kg ha^{-1}, Appendix D) as the total aboveground biomass in typical, young Douglas-fir forests of this region (98.9 – 184 kg/ha, Perakis et al., 2013), far less Ca than the approximate sea-salt flux over the past 10,000 years (15.5 Mg ha^{-1}), and would have both weathered rapidly (within 5-years, Dahlgren et al., 1999) and mostly leached out

of the system leaving little influence on modern vegetation. Therefore, volcanic ash is a negligible source of Sr and Ca to OCR forests over long timescales.

Rainwater originating from the ocean can be an important source of base cations to forests ecosystems in coastal (Chadwick et al., 1999) and distal (several hundred km inland, Bain and Bacon, 1994) areas. A long-term (1997-2006) weekly record of precipitation chemistry (Ca, Na, K, Mg, etc.) in the OCR (NADP, Site OR02, Alsea Guard Ranger Station) indicates strong baseline inputs of marine aerosols in OCR wet deposition, but shows some Ca and K enrichment compared to Ca/Na and K/Na ratios expected in seawater (Figure 2). This precipitation station was located in an OCR river valley, and Ca and K enrichment could possibly result from nearby agricultural activity (i.e., dust). For these reasons, wet-deposition in the OCR is expected to have a $^{87}Sr/^{86}Sr$ signature close to seawater ($^{87}Sr/^{86}Sr = 0.70917$, Dia et al., 1992) but may contain some variability due to regional dust sources. The small variation in Ca/Sr (140 – 250) and $^{87}Sr/^{86}Sr$ ratios (0.7086-0.7092) over time in our wet-deposition samples suggests that small amounts of dust or biologic material were incorporated into precipitation during drier months. However, flux-weighted $^{87}Sr/^{86}Sr$ measured in open wet-deposition was nearly identical to seawater ($^{87}Sr/^{86}Sr = 0.70916$ versus 0.70917), confirming that atmospheric fluxes of Sr and Ca to coastal Oregon forests are dominated by marine aerosols, and lack a regionally significant secondary atmospheric source.

Our analysis of Sr-isotopes in open rainfall, rocks, and soils indicates that inputs of Sr and Ca to OCR forests are dominated by two sources: ocean aerosols in

rainwater ($^{87}Sr/^{86}Sr$ ~ 0.7092) and weathering of bedrock ($^{87}Sr/^{86}Sr$ of bedrock varies by site and ranges from 0.7032 – 0.7526). This simple two-component isotope system allows us to directly partition Sr and Ca contained in plants and exchangeable soil pools into atmospheric versus rock-derived components (Equations 12-13) using Sr-isotope and Sr/Ca ratios measured in our rainwater samples and 1 M HNO_3 rock leachates. The choice of whole rock vs. rock leachate $^{87}Sr/^{86}Sr$ (and Sr/Ca) as the weathering end-member has little effect on our mixing calculations at basaltic sites (Figure 27), so we used rock leachate values at all sites, which has the benefit of capturing the signature of differential weathering at our sedimentary sites. At sites Devitt and 143 (both sedimentary sites), we used the profile weighted soil residue as our rock weathering end-member. A carbonate signature dominates whole rock and rock leachate $^{87}Sr/^{86}Sr$ values at these sites, but carbonate sources are not reflected in foliage or exchangeable soil pools ($^{87}Sr/^{86}Sr$ of whole rocks and rock leachates < $^{87}Sr/^{86}Sr$ rainwater < $^{87}Sr/^{86}Sr$ foliage and exchangeable soil pools), suggesting that Ca from carbonate weathering is not accessible to surface vegetation.

To account for slight variability in the chemistry and isotopic composition of rainfall, we elected to use the full range of $^{87}Sr/^{86}Sr$ and Sr/Ca ratios as a way to incorporate uncertainty into the mixing model. Specifically, precipitation minimum and maximum $^{87}Sr/^{86}Sr$ values (0.7086 and 0.7093) were paired with the minimum and maximum Sr/Ca ratios (0.004 and 0.007), respectively, and therefore represent the overall maximum amount of uncertainty.

We calculated the mass fraction of atmospheric Sr in foliage with Equation 12:

Equation 12: $$f_{atm,Sr} = \frac{\left(\frac{^{87}Sr}{^{86}Sr}\right)_{mix} - \left(\frac{^{87}Sr}{^{86}Sr}\right)_{rock}}{\left(\frac{^{87}Sr}{^{86}Sr}\right)_{atm} - \left(\frac{^{87}Sr}{^{86}Sr}\right)_{rock}}$$

where $(^{87}Sr/^{86}Sr)_{mix}$ is the Sr-isotope ratio measured in foliage, $(^{87}Sr/^{86}Sr)_{rock}$ is the Sr-isotope ratio of the 1 M HNO_3 rock leachate (or in two cases 40-50 cm soil residue), and $(^{87}Sr/^{86}Sr)_{atm}$ is the Sr-isotope ratio measured in rainfall. Equation 12 can be modified using the molar Sr/Ca ratios of each end-member to obtain the mass fraction of atmospheric Ca (Equation 13):

Equation 13:

$$f_{atm,Ca} = \frac{\left[\left(\frac{^{87}Sr}{^{86}Sr}\right)_{mix} - \left(\frac{^{87}Sr}{^{86}Sr}\right)_{rock}\right] \cdot \left(\frac{Sr}{Ca}\right)_{rock}}{\left[\left(\frac{^{87}Sr}{^{86}Sr}\right)_{mix} - \left(\frac{^{87}Sr}{^{86}Sr}\right)_{rock}\right] \cdot \left(\frac{Sr}{Ca}\right)_{rock} - \left[\left(\frac{^{87}Sr}{^{86}Sr}\right)_{atm} - \left(\frac{^{87}Sr}{^{86}Sr}\right)_{mix}\right] \cdot \left(\frac{Sr}{Ca}\right)_{atm}}$$

It is well appreciated that plants discriminate Ca from Sr, which restricts the use of Ca/Sr ratios as a tracer for long-term Ca sources (Dasch et al., 2006). Discrimination of Ca over Sr is reflected in the large difference between Ca/Sr ratios in foliage versus exchangeable soil pools within our sites (Figure 24), and previous work in OCR Douglas-fir forests identified that Ca discrimination over Sr occurs at the whole plant scale (Dauer 2012). This suggests that the large range of Ca/Sr ratios in foliage between our sites is likely due to differences in Ca-cycling in these forests rather than processes internal to the plant. Nevertheless, our calculations are based on

$^{87}Sr/^{86}Sr$ ratios in foliage and not Ca/Sr in foliage. Biological processes do not discriminate between Sr-isotopes (i.e., ^{86}Sr versus ^{87}Sr), and therefore $^{87}Sr/^{86}Sr$ ratios preserve the long-term signature of Sr and Ca sources despite variation in Ca-Sr discrimination.

Our end-member mixing models based on $^{87}Sr/^{86}Sr$ ratios indicate that forests at sedimentary sites rely almost exclusively on atmospheric sources of Ca and Sr, whereas basaltic sites display greater weathering contributions to base cation pools. At 10 of 11 sedimentary rock sites, atmospheric Sr and Ca had a narrow range from 80 to 122 % and 87 to 125 %, respectively (Table 12). Values greater than 100% occurred when foliar $^{87}Sr/^{86}Sr$ values fell just below our high atmospheric end-member value ($^{87}Sr/^{86}Sr = 0.70925$), or in a single case (site Trask) where foliar $^{87}Sr/^{86}Sr$ fell just below our low atmospheric end-member value ($^{87}Sr/^{86}Sr = 0.70861$). This latter deviation may reflect the redistribution of biologic material from nearby basaltic sites that are more prevalent near this site, or local dust input from gravel logging roads that rely extensively on local basalt. In contrast, percent atmospheric Sr and Ca in foliage from basaltic sites was lower than sedimentary rock sites (p-value < 0.001 for both Sr and Ca), ranging from (11 – 96% and 10 – 84%, respectively). Percent atmospheric Sr and Ca in foliage at our two mixed lithology sites more closely resembled the range of basaltic sites (51 to 82%, and 49 to 83%, respectively), reflecting the greater Ca content and ease of weathering of basaltic rocks compared to sedimentary rocks. These results demonstrate that lithology is an influential factor shaping base cation sources across our research sites.

4.2 State Factor Analysis of Research Sites

Our soil nitrogen gradient ranges from low-N sites that are characteristic of N-limited temperate forests to high-N sites that are among the highest reported worldwide (Post et al., 1985). In coastal regions of the Pacific Northwest, high N-availability results primarily from red alder (Cole et al., 1990; Tarrant, 1969), a widespread, symbiotic N-fixing tree species that typically colonizes areas following landslide, wildfire, or logging disturbance. Nitrogen availability is a dominant factor shaping base cation pools in PNW forests, yet the long-term effect of high N availability on base cation sources remains unknown. Prior work in many of the young conifer forests that we examined has shown that N variation across sites is minimally confounded with other state factors (Perakis et al., 2011, 2006). Nevertheless, to verify that soil N is the primary factor that forms a gradient across our sites and not some other factor that happens to co-vary with N, we evaluated variation in climate, topography, parent material, and time with soil N across sites (Jenny, 1941).

Our stable isotope soil $\delta^{15}N$ data confirms the idea biological N fixation by red alder is the dominant factor shaping N balances of coastal Oregon forests (Perakis et al. 2011). Nitrogen fixation by pure stands of red alder in the Oregon Coast Range average 100-200 kg N ha^{-1} yr^{-1} (Binkley et al., 1994), which is considerably higher than N inputs from regional wet-deposition (< 1 kg N ha^{-1} yr^{-1}, NADP OR02), asymbiotic N-fixation in the forest floor (< 1 kg N ha^{-1} yr^{-1}, Heath et al., 1988) and woody detritus (< 1 kg N ha^{-1} yr^{-1}, Hicks, 2000), and symbiotic N fixation by canopy

cyanolichens (3 to 4 kg N ha^{-1} yr^{-1}, Denison, 1979). Biologically fixed nitrogen enters ecosystems at an isotopic value similar to atmospheric N_2 gas (0‰), and as N accumulates, most studies show that soil $\delta^{15}N$ either remains near-zero (Menge et al., 2011; Pérez et al., 2014), or increases due to fractionating N loss (Brenner et al., 2001). In contrast to these patterns, we observed a decline in soil $\delta^{15}N$ as soil N increased across our sites (Figure 2), reflecting N balances dominated not by fractionating N loss, but instead by large N inputs from symbiotic N-fixing red alder. Increased erosional loss of N can also lower soil $\delta^{15}N$ towards the signature of inputs (Hilton et al., 2013), but erosional loss is inconsistent with our observation of low soil $\delta^{15}N$ associated with high N accumulation. Nitrogen that accumulates under red alder can persist in soil for millennia, leaving a legacy of high N availability that influences biogeochemical cycling even after red alder is replaced by non-fixers (Perakis and Sinkhorn, 2011).

Variation in climate can present a significant challenge to interpreting the effects of organisms (and hence our N-gradient) on Ca sources, because climate influences the distribution of organisms, rates of organic matter turnover, N-cycling, and mineral weathering (Schlesinger and Bernhardt, 2013). Although precipitation and temperature did vary somewhat among our sites (Table 1), this variation was low compared to broader regional climatic factors that shape soil carbon stocks (Homann et al., 1995) and rock-weathering rates (Dixon et al., 2009; Rasmussen et al., 2011; Stewart et al., 2001). Neither MAP nor MAT was significantly correlated with soil N across our sites (Table 13), suggesting that climate does not structure our gradient of

sites. Soil nitrogen did increase significantly with proximity to the coast across our sites (Table 13), as observed previously, and likely reflecting greater N fixation by red alder near the coast due to lower plant moisture stress associated with summer coastal fog and humidity (Perakis and Sinkhorn, 2011).

On low-relief stable landforms, climate can be a dominant factor regulating the availability of rock-derived nutrients due to effects on primary mineral weathering. In contrast, landslides and erosional processes rejuvenate soils in areas with active tectonic uplift and/or steep terrain by exposing fresh rock surfaces (Porder et al., 2005; Vitousek et al., 2003), but these processes may also limit N accumulation (Takyu et al., 2002). Slope was highly variable across our research sites (Table 1), but did not co-vary with soil N (Table 13). Relatively thick regolith (high depth to rock) across our research sites (Table 1) and elsewhere in the Coast Ranges of Oregon and Washington (Carpenter et al., 2014) may suggest that rejuvenation of fresh rock surfaces may be limited at many of our field sites. On the other hand we observed abundant (> 15% by mass) coarse rock fragments at 15 of our field sites (Table 6) which are typically representative of younger, less intensely weathered soils (Chadwick et al., 2003). However, neither depth to bedrock nor the abundance of coarse rock fragments varied significantly with soil N (Table 13), suggesting that relief is not a confounding factor with soil N across our research sites.

The mineralogy and nutrient content of soil parent materials (i.e. bedrock) influences weathering inputs of base cations to ecosystems (Anderson, 1988). Mean Ca concentration varied 20-fold between basaltic and sedimentary rocks and is the

basis for our geologic contrast across sites (Table 9). Within each rock group, research sites occur over 3-different rock formations (Table 1), yet variation in whole-rock and rock leachable Ca concentrations was smaller within than between rock groups (Tables 9 and 10). Within-group rock chemistry did not correlate with soil N (Table 13), suggesting that within-group rock chemistry is not a confounding factor with soil N across our field sites.

Bedrock itself is often overlooked as a potential N source to ecosystems, but some sedimentary and metamorphic rocks can be important sources of nitrogen in forests (Holloway and Dahlgren, 1999; Morford et al., 2011). Indeed, metamorphic bedrock in some areas of southern Oregon has been shown to contribute appreciable N to forests, and one feature of such sites is an increase in the N concentration of fine-earth soil fractions at depth (Scott Morford, personal communication). However, soil N concentrations did not increase with increasing soil depth at our sites (Table 2), suggesting that rocks are not a significant source of N at our sites.

Although we do not have independent estimates of soil age at our sites, we use systematic changes in soil chemical properties associated with weathering and soil development to evaluate soil age in a relative sense among our sites. Effective cation exchange capacity (ECEC) and soil redness (RR) are related to neoformation of aluminosilate and sesquioxide secondary minerals (Hurst, 1977; McBride, 1994). In particular, soil redness was linked to soil age across a fluvial chronosequence in sedimentary parent material in the OCR (Lindeburg et al., 2013) and, based on this relationship, our sedimentary sites have a suggested age range of < 3.5 to 140 ky

(Figure 34). In contrast, soil redness was not related to soil age across a basaltic soil chronosequence in Hawaii (Table 3; chronosequence established by Chadwick et al., 1999 but soil color data from NCSS Soil Characterization Database) and, therefore, we cannot use soil color as an index of time at our basaltic sites. We found no correlation between ECEC and soil N across our research sites, and no correlation between soil color and N for sedimentary sites (Table 13), both of which suggest that soil development is not directly confounded with soil N across our sites.

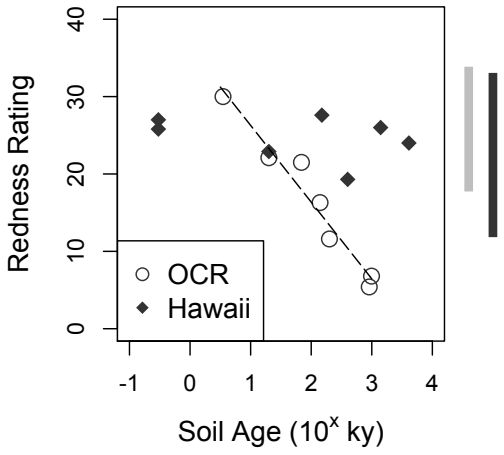

Figure 34. Average soil redness rating (0-50 cm depth, Hurst's redness rating) versus soil age for a fluvial chronosequence on sedimentary rocks in the Oregon Coast Range and a volcanic island-arc chronosequence on basaltic rocks in Hawaii. Light grey and black line segments to the right of the plot area indicate the range of soil redness for our sedimentary and basaltic soils, respectively. Chronosequence data from Lindeburg et al., 2013 (OCR) and "NCSS Soil Characterization Database" (Hawaii; pedon IDs 94HI001017, 94HI001018, 94HI001019, 94HI001020, 94HI007001, 96HI009001, and 97HI009003). Regression for OCR chronosequence (black dashed line):
$y = -9.92*\log(x) + 36.2$ ($R^2 = 0.95$, p-value = < 0.001)

Element mass losses are an alternative method for evaluating the cumulative effects of time on soil development and nutrient availability. The chemical index of

alteration (CIA), weathering index of Parker (WIP), and immobile element ratios (τ-Ca) are common indices of soil weathering. The CIA scale ranges from 0 to 100% and is positively related to the degree of chemical weathering, such that low CIA values indicate limited base cation loss and high CIA values indicate substantial base cation loss. In contrast, WIP (which also has a scale from 0 – 100%) is inversely related to the degree of chemical weathering, such that low WIP values indicate substantial base cation loss and high WIP values indicate low base cation loss. In regions with similar rainfall to the Oregon Coast Range, base cation depletion from basaltic soils on stable geomorphic landscape positions occurs within 20 ka of soil development (Chadwick et al., 1999), which is within the estimated range of soil ages at our field sites and similar to the maximum time required for soil N to achieve steady-state in OCR soils (Perakis et al., 2011). Neither CIA, WIP, or $\tau_{Nb}Ca$ were significantly correlated with soil N across our research sites (Table 13) suggesting that Ca-sources are disconnected from the weathering status of soils across our research sites. Therefore, we found no evidence that time, as interpreted through soil chemical properties, is a confounding factor with soil N across our research sites.

Overall, our state factor analysis of 17 metrics related to climate, relief, parent material, and time support our hypothesis that N is the main driver of chemical variation across our sites.

4.3 Interactions between Nitrogen and Bedrock Control Ecosystem Ca Sources

Our analysis of $^{87}Sr/^{86}Sr$ ratios in precipitation, bedrock, soils, and plants indicates that Ca sources in OCR forests depend on an interactive-effect between ecosystem N status and lithology. Specifically, we found that forests overlying Ca-poor sedimentary rocks depend almost exclusively on atmospheric deposition of ocean aerosols to meet Ca demands, independent of soil N status (Figure 35). In contrast, forests overlying Ca-rich basaltic rocks consistently displayed greater reliance on bedrock sources of Sr and Ca. Yet, reliance on bedrock supply of Sr and Ca on basaltic sites systematically decreased from > 80 to ~ 20% across a 5-fold increase in soil N concentration (Figure 35). While rock weathering is an important source of Ca and Sr to ecosystems, Ca and Sr release from minimally altered rocks (where weathering fluxes are greatest) may occur deeper than plant roots and bypass upland ecosystems. Even in our highly weathered soil residues, sizeable Ca and Sr pools exist relative to biotic uptake, but Ca and Sr released from these highly weathered soil residues is low relative to fresh bedrock, and $^{87}Sr/^{86}Sr$ ratios suggest that at most sites this pool of nutrients is not being used by plants. In addition, $^{87}Sr/^{86}Sr$ ratios in plants that reflect strong rock-weathering sources (i.e., low N basaltic sites) may reflect Ca that was acquired by plants long ago and the isotopic signature retained due to highly efficient recycling of nutrients through litter-fall. However, because nutrient cycling is not perfectly efficient, atmospheric Ca may replace rock-derived Ca in plants over time especially if roots more easily acquire Ca in rainwater than from minerals. These

results highlight that soil parent material exerts the strongest control on Ca sources at low-N sites. However, long-term increases in N availability reduce the importance of geology as a factor shaping base cation sources, and instead cause ecosystems to converge towards atmospheric reliance on base cation sources at high-N sites.

Our finding that Ca-rich basaltic rocks displayed more rock derived Sr and Ca to forests than Ca-poor sedimentary rocks is consistent with previous studies that, collectively, span a wide variety of bedrock types. In general, a review of the literature suggests that forests growing on top of base-poor parent materials rely more strongly on atmospheric than rock weathering sources of base cations. For example, atmospheric inputs dominate Ca sources in spruce forests on granitic rocks in New Mexico (~75% Sr only; Gosz and Moore, 1989), temperate beech forests receiving high N-deposition on base-poor shale in Belgium (~78% Drouet et al., 2005), and coastal temperate Chilean rainforests growing on low-N soils derived from Precambian mica-schist (>90%, Kennedy et al., 2002). The exceptionally high dominance of atmospheric Ca sources across our sedimentary sites (>90%) points to the fact that base-poor bedrock combined with intense weathering conditions may predispose forests to limited Ca supply from weathering, even at low N sites.

Further investigation indicates that ecosystems growing on Ca-rich bedrock exhibit greater variability in base cation sources than ecosystems on base-poor bedrock. Weathering of Ca-rich bedrock can dominate ecosystem Ca sources on young soils in warm, moist climates (Chadwick et al., 1999; Kennedy et al., 1998; Stewart et al., 2001), on old but dry landscapes (Reynolds et al., 2012), and even in

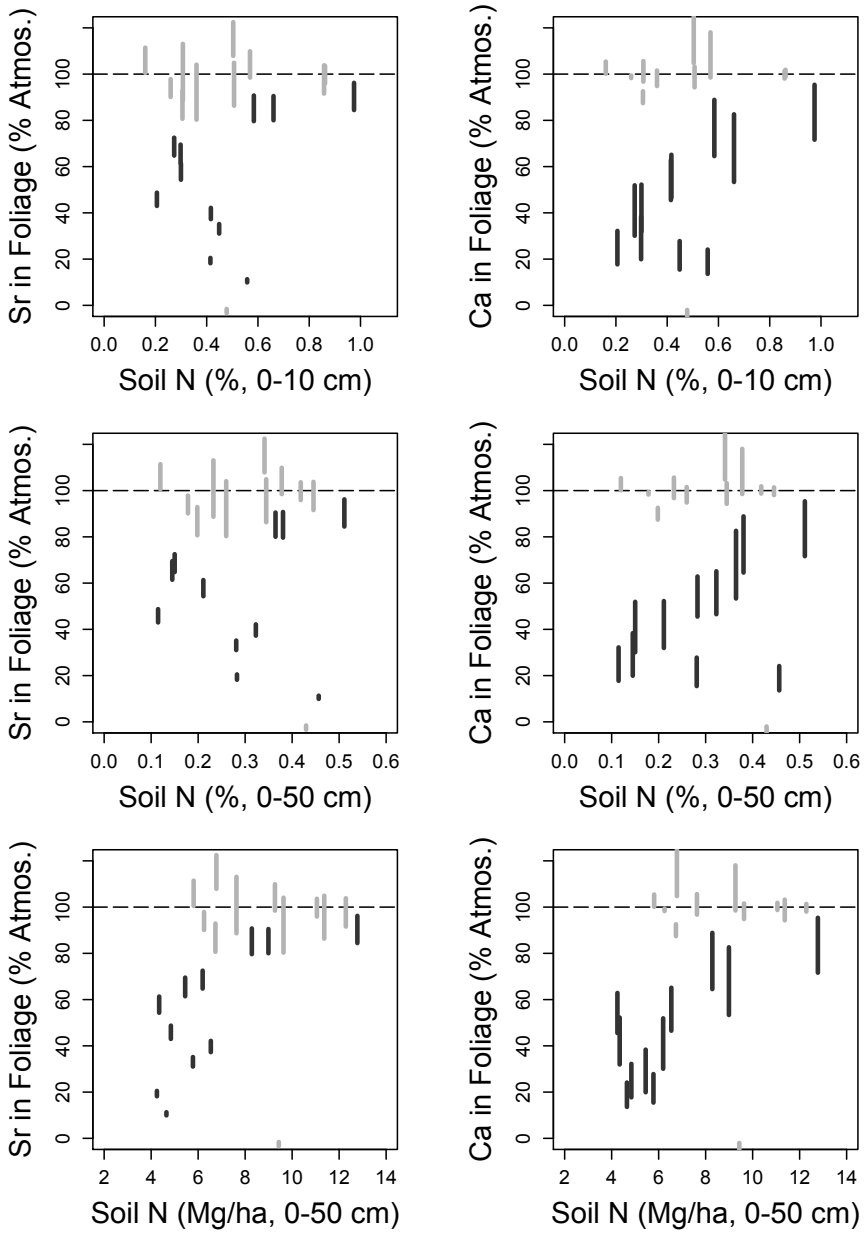

Figure 35. Soil N conc. (top and center panels) or pool size (bottom panels) versus percent atmospheric Sr (left panels) and Ca (right panels) in tree foliage. Line segments represent the range of atmospheric Sr and Ca contained in foliage based on variation in Sr/Ca and $^{87}Sr/^{86}Sr$ ratios in the atmospheric end-member. The dashed black line indicates 100% atmospheric Sr and Ca.

ecosystems with highly weathered soils where the source of fresh rock is not obvious (Bern et al., 2005; Pett-Ridge et al., 2009). In contrast, atmospheric deposition can dominate Ca sources in older, more highly weathered basaltic soils (Kennedy et al., 1998; Stewart et al., 2001) , or in dry regions receiving high dust fluxes (Reynolds et al., 2012). Base cation sources have been shown to shift from rock (basaltic) to atmospheric dominated following dramatic declines (thresholds) in rock weathering rates (Chadwick et al., 1999; Stewart et al., 2001), and although our research sites fall within the climate range where weathering rates are expected to drop off precipitously (~200 cm yr^{-1}) neither climate nor a threshold in weathering (as interpreted through indices of weathering status) appear to facilitate the transition in base cation sources at our basaltic sites (Table 13). Instead, base cation sources across our basaltic sites are increasingly dominated by atmospheric inputs (from ~20 % to over 80%) as soil N increases. Because soil N accumulation at our sites is driven primarily by large pulsed N inputs from symbiotic N fixation, these findings illustrate a novel biotic effect on long-term sources of base cations that occurs via changes in the N cycle.

Our $^{87}Sr/^{86}Sr$ evaluation also illustrates a profound disconnect between Ca sources and both exchangeable Ca pools and base saturation, which are often used as indicators of soil fertility (Johnston and Crossley Jr., 2002; Schoenholtz et al., 2000). Our sites had an exceptionally large range in soil base saturation (3.5 to 100%, 0-10 cm depth, Table 4) driven by changes in exchangeable soil Ca pools that decreased with increasing soil N yet did not differ between rock types (Figure 7). Atmospheric inputs should not differ between rock types, and if Sr and Ca cycles are near steady-

state, then the greater influence of rock Sr and Ca in plants and soils at basaltic sites must reflect greater weathering inputs and/or a greater retention of weathering inputs in basaltic soils. Therefore, despite equal levels of soil fertility at low N sedimentary and basaltic sites based on exchangeable Ca pools and base saturation, the net input of Ca to these ecosystems is much larger in basaltic systems. That long-term base cation sources and the magnitude of base cation inputs do not necessarily correlate with the size of exchangeable Ca pools or the percent base saturation points to caution when using static pool or concentration metrics of soil fertility to infer sustainable nutrient supply.

Our soils have a range of moderately acidic pH, between 3.9 and 6.5 (Table 2), despite the narrow climate and age range that these sites cover, and similarity in soil type (Table 1). This range of pH suggests that the acid buffering capacity of these soils remains high, most likely due to base cation exchange at low N sites and the hydrolytic release of Al^{3+} from soil colloid surfaces at high N sites (Bloom et al., 1979). Our large range of soil base saturation (Table 4 and Figure 12) values from 3.48 to 99.6 % is particularly surprising given the relatively limited variation in soil state factors (Table 1). Our range of values is comparable to an extremely wide precipitation gradient (0.16 to >3.5 m yr^{-1} MAP) in basaltic soils of Hawaii (Vitousek and Chadwick, 2013). Similarly, our range in base saturation is much larger than the 26 to 69% range observed across a basaltic soil elevation gradient (250 to 2500 m elevation, and 0.78 to 1.3 m yr^{-1} MAP) in northern California with a much larger range in mean annual soil temperature (5 to 17 ° C) (Rasmussen et al 2010). Overall, these

patterns illustrate the powerful nature of nitrate leaching under contemporary stands of red alder (Cole et al., 1990; Homann et al., 1992; Van Miegroet and Cole, 1985) and across an N gradient in this same region (Perakis and Sinkhorn, 2011; Perakis et al., 2006) that causes soil acidification and stimulates Ca loss through ion exchange (by H^+ and Al^{+3}) and counter-ion (nitrate) leaching.

The coupled processes associated with high N under alder (i.e., nitrate leaching, soil acidification, base cation depletion, and Al release) are similar to anthropogenic N-deposition (Adams et al., 2007; Johnson et al., 1992; Lawrence et al., 1997, 1995), raising the possibility that N richness in general may shape ecosystem base cation sources. Short-term (decadal scale) inputs of anthropogenic N-deposition can increase the importance of atmospheric base cation sources in forest ecosystems (Drouet et al., 2005a, 2005b), and for the first time our work demonstrates that high N-availability over long timescales causes persistent dependence on atmospheric base cation sources in forest ecosystems (Figure 21). The influence of N-availability over other state factors in shaping base cation sources at our sites is particularly important given that increased N cycling can impact ecosystems over much shorter timescales when compared to timescales of pedogenic development (Peltzer et al., 2010).

Though our results emphasize how changes in N can influence the Ca cycle, it is clear more broadly that couplings between N and Ca can be reciprocal rather than unidirectional. In northeastern US forests, Ca availability influences forest successional pathways and, consequently, N-cycling processes by (1) reducing the vigor of mature trees and seedlings with high quality litter (i.e., sugar maple, *Acer*

saccharum, and American basswood, *Tilia americana*) and (2) leading to dominance by American beech (*Fagus grandifolia*), which is more tolerant of Ca-poor sites and has low litter quality (Mitchell, 2011; Page and Mitchell, 2008). In addition, calcium fertilization can increase foliar Ca concentrations, crown health, and tree growth (Juice et al., 2006; Mainwaring et al., 2014) as well as suppress N-cycling and therefore nitrate-production rates (Groffman and Fisk, 2011). Nitrogen thus appears to be the more dominant element in coupled N-Ca cycles because N accumulation and nitrate loss lead to soil acidification and a greater than 10-fold depletion in exchangeable soil Ca pools (Perakis et al., 2006). Therefore, variation in N can drive nutrient limitation by both N and Ca, but variation in Ca availability and sources has only a minimal effect on long-term N and Ca limitation.

Prior work identified that forest harvest on sites with naturally low Ca may further deplete Ca from forest soils in the Oregon Coast Range (Perakis et al., 2006). Our work confirms and critically refines that idea by distinguishing between the controls on base cation pools versus $^{87}Sr/^{86}Sr$ ratios that reflect long-term base cation sources. Our results indicate that N saturation associated with high N sites cause losses of available base cations and increases reliance on atmospheric base cation sources, regardless of the base cation content of underlying parent materials. Thus, at high N sites, atmospheric inputs determine the long-term rate of Ca supply and the sustainability of Ca removals by biomass harvest. In contrast, the sustainability of Ca supply at low N sites appears to rely more on weathering inputs, especially for basaltic sites. Our results suggest overall that Ca depletion may still be a significant concern on

low-Ca sedimentary rocks in the OCR, particularly because both foliar and soil exchangeable Sr display a persistent atmospheric signature, with no clear evidence of an additional soil Ca source that has gone unmeasured. At low N sites in general, our results caution against using size of the exchangeable base cation pool or base saturation as a metric of soil fertility to interpret sustainable Ca supply. It remains unclear, however, whether successive biomass removal or planting of different tree species could increase the contribution of weathering sources of base cations on high N sites on Ca-rich basaltic rocks.

CHAPTER 5 – CONCLUSIONS

Oregon Coast Range (OCR) forests are an ideal system for evaluating the interactive effects between biotic and abiotic factors that control long-term base cation sources. First, these ecosystems are minimally influenced by anthropogenic N-deposition; yet contain a unique symbiotic N-fixing tree species (red alder) that causes large and persistent changes in ecosystem N status. Soil N across our research sites encompasses a biogeochemical threshold in N cycling that impacts other biogeochemical cycles, especially Ca. At high N sites (N-saturated), nitrate leaching causes a net production of acidity (H^+) that releases soluble aluminum, displaces base cations from soil exchange sites and, coupled with counter ion leaching, leads to ecosystem level declines in Ca availability.

Secondly, underlying bedrock across the OCR varies from Ca-poor sedimentary to Ca-rich basaltic rocks. Mineralogy and base cation content of parent rocks are fundamental to the supply of Ca to ecosystems via weathering. Therefore, the combination of contrasting bedrock types with a naturally occurring gradient in N availability allows for a unique opportunity to investigate the relative importance of geologic versus biological controls on base cation sources. Finally, we found that base cation inputs to OCR forests are dominated by two sources – rock weathering and atmospheric deposition of ocean aerosols in rainwater – that have unique $^{87}Sr/^{86}Sr$ signatures. This simple two-component isotope system allows us to directly partition Sr and Ca contained in plants and exchangeable soil pools into atmospheric versus rock-derived components using $^{87}Sr/^{86}Sr$ and Sr/Ca ratios. Collectively, these

conditions allow for an unparalleled investigation of the interactions between ecosystem N and bedrock on long-term base cation sources.

Using Sr-isotopes ($^{87}Sr/^{86}Sr$), we identified a novel biological effect of N fixation inputs that interacts with rock type to control base cation sources in OCR forests. At sedimentary sites, atmospheric deposition (ocean aerosols in rainwater) supplied nearly 100% of Ca contained in plants and exchangeable soil pools independent of soil N status. In contrast, at basaltic sites the proportion of atmospheric Ca systematically increased from ~20% to over 80% with increasing soil N availability. Therefore, rock type appears to control key baseline inputs of Ca to ecosystems via weathering. Yet, in forest ecosystems across rock types, intense nitrate leaching conditions at high N sites reduce the importance of geology in shaping base cation supply, with new base cation inputs potentially limited by atmospheric fluxes. Overall, the influence of N-availability over other state factors in shaping base cation sources at our sites is particularly important given that increased N cycling can impact ecosystems over much shorter timescales when compared to timescales of pedogenic development (Peltzer et al., 2010).

Finally, this work provides insight to the long-term consequences of nitrogen deposition and forest harvest, which may also deplete Ca pools in forest ecosystems. Short-term (decadal scale) pulses of anthropogenic N-deposition can increase the importance of atmospheric base cation sources in forest ecosystems (Drouet et al., 2005a, 2005b). Our work demonstrates that high N-availability over long timescales exceeds soil parent materials in regulating Ca sources and causes persistent

dependence on atmospheric Ca in forest ecosystems. At our highest N sites, soil Ca pools are depleted, and Ca in aboveground biomass is approximately equal to the 200-year flux of atmospheric Ca inputs. Whole tree-harvest has the potential to further deplete ecosystem Ca at the highest N sites, but the ability of forests to recover from Ca depletion may depend strongly on parent material and *in-situ* rates of mineral weathering.

BIBLIOGRAPHY

Aber, J.D., Nadelhoffer, K.J., Steudler, P., Melillo, J.M., 1989. Nitrogen saturation in northern forest ecosystems. BioScience 39, 378–286.

Åberg, G., 1995. The use of natural strontium isotopes as tracers in environmental studies, in: Biogeochemical Monitoring in Small Catchments. Springer, pp. 309–322.

Adams, M.B., Kochenderfer, J.N., Edwards, P.J., 2007. The Fernow watershed acidification study: ecosystem acidification, nitrogen saturation and base cation leaching. Water, Air, & Soil Pollution: Focus 7, 267–273.

Almond, P., Roering, J., Hales, T.C., 2007. Using soil residence time to delineate spatial and temporal patterns of transient landscape response. J. Geophys. Res. 112, F03S17. doi:10.1029/2006JF000568

Anderson, D.W., 1988. The effect of parent material and soil development on nutrient cycling in temperate ecosystems. Biogeochemistry 5, 71–97.

Anderson, S.P., Dietrich, W.E., Brimhall, G.H., 2002. Weathering profiles, mass-balance analysis, and rates of solute loss: Linkages between weathering and erosion in a small, steep catchment. Geological Society of America Bulletin 114, 1143–1158.

Antoine, M.E., 2004. An Ecophysiological Approach to Quantifying Nitrogen Fixation by Lobaria oregana. The Bryologist 107, 82–87. doi:10.1639/0007-2745(2004)107[82:AEATQN]2.0.CO;2

Bain, D.C., Bacon, J.R., 1994. Strontium isotopes as indicators of mineral weathering in catchments. Catena 22, 201–214.

Barnes, M.A., Barnes, C.G., 1992. Petrology of Late Eocene basaltic lavas at Cascade Head, Oregon Coast Range. Journal of Volcanology and Geothermal Research, Special Issue in Honour of Alexander R. McBirney 52, 157–170. doi:10.1016/0377-0273(92)90138-4

Bern, C.R., Townsend, A.R., Farmer, G.L., 2005. Unexpected dominance of parent-material strontium in a tropical forest on highly weathered soils. Ecology 86, 626–632.

Berner, E.K., Berner, R.A., 2012. Global environment: water, air, and geochemical cycles. Princeton University Press.

Binkley, D., Cromack Jr, K., Baker, D.D., 1994. Nitrogen fixation by red alder: biology, rates, and controls. The biology and management of red alder. Oregon State University Press, Corvallis 57–72.

Bloom, P.R., McBride, M.B., Weaver, R.M., 1979. Aluminum Organic Matter in Acid Soils: Buffering and Solution Aluminum Activity1. Soil Science Society of America Journal 43, 488. doi:10.2136/sssaj1979.03615995004300030012x

Blum, J.D., Dasch, A.A., Hamburg, S.P., Yanai, R.D., Arthur, M.A., 2008. Use of foliar Ca/Sr discrimination and 87Sr/86Sr ratios to determine soil Ca sources to sugar maple foliage in a northern hardwood forest. Biogeochemistry 87, 287–296.

Blum, J.D., Erel, Y., 1995. A silicate weathering mechanism linking increases in marine 87Sr/86Sr with global glaciation.
Blum, J.D., Klaue, A., Nezat, C.A., Driscoll, C.T., Johnson, C.E., Siccama, T.G., Eagar, C., Fahey, T.J., Likens, G.E., 2002. Mycorrhizal weathering of apatite as an important calcium source in base-poor forest ecosystems. Nature 417, 729–731.
Bonneville, S., Smits, M.M., Brown, A., Harrington, J., Leake, J.R., Brydson, R., Benning, L.G., 2009. Plant-driven fungal weathering: Early stages of mineral alteration at the nanometer scale. Geology 37, 615–618. doi:10.1130/G25699A.1
Brady, N.C., Weil, R.R., 2010. Elements of the nature and properties of soils. Pearson Prentice Hall.
Brenner, D.L., Amundson, R., Baisden, W.T., Kendall, C., Harden, J., 2001. Soil N and< sup> 15</sup> N variation with time in a California annual grassland ecosystem. Geochimica et Cosmochimica acta 65, 4171–4186.
Brimhall, G.H., Dietrich, W.E., 1987. Constitutive mass balance relations between chemical composition, volume, density, porosity, and strain in metasomatic hydrochemical systems: results on weathering and pedogenesis. Geochimica et Cosmochimica Acta 51, 567–587.
Brownfield, M., 1982. Geologic map of the Grande Ronde quadrange, Polk and Yamhill Counties. Oregon Department of Geology and Mineral Industries, Geologic Map Series 23.
Bruggman, P.E., Bacon, C.R., Mee, J.S., Pribblel, S.T., Siems, D.F., 1993. Chemical analyses of pre-Mazama silicic volcanic rocks, inclusions, and glass separates, Crater Lake, Oregon. US Department of the Interior, US Geological Survey.
Bukry, D., Snavely Jr, P.D., 1988. Coccolith zonation for Paleogene strata in the Oregon Coast Range.
Bullen, T.D., Kendall, C., 1998. Tracing of weathering reactions and water flowpaths: a multi-isotope approach. Isotope tracers in catchment hydrology 611–646.
Capo, R.C., Stewart, B.W., Chadwick, O.A., 1998. Strontium isotopes as tracers of ecosystem processes: theory and methods. Geoderma 82, 197–225.
Carpenter, D.N., Bockheim, J.G., Reich, P.F., 2014. Soils of temperate rainforests of the North American Pacific Coast. Geoderma 230, 250–264.
Carter, M.R., Gregorich, E.G., 2007. Soil Sampling and Methods of Analysis, Second Edition. CRC Press.
Chadwick, O.A., Brimhall, G.H., Hendricks, D.M., 1990. From a black to a gray box—a mass balance interpretation of pedogenesis. Geomorphology 3, 369–390.
Chadwick, O.A., Derry, L.A., Vitousek, P.M., Huebert, B.J., Hedin, L.O., 1999. Changing sources of nutrients during four million years of ecosystem development. Nature 397, 491–497.

Chadwick, O.A., Gavenda, R.T., Kelly, E.F., Ziegler, K., Olson, C.G., Elliott, W.C., Hendricks, D.M., 2003. The impact of climate on the biogeochemical functioning of volcanic soils. Chemical Geology 202, 195–223.
Chan, M.A., 1985. Correlations of Diagenesis with Sedimentary Facies in Eocene Sandstones, Western Oregon. Journal of Sedimentary Research 55.
Clow, D.W., Mast, M.A., Bullen, T.D., Turk, J.T., 1997. Strontium 87/strontium 86 as a tracer of mineral weathering reactions and calcium sources in an alpine/subalpine watershed, Loch Vale, Colorado. Water Resources Research 33, 1335–1351.
Cole, D.W., Compton, J., Van Miegroet, H., Homann, P., 1990. Changes in soil properties and site productivity caused by red alder. Water, Air, and Soil Pollution 54, 231–246.
Colman, S.M., 1981. Rock-weathering rates as functions of time. Quaternary Research 15, 250–264.
Cross, A., Perakis, S.S., 2011. Complementary models of tree species–soil relationships in old-growth temperate forests. Ecosystems 14, 248–260.
Dahlgren, R.A., Ugolini, F.C., Casey, W.H., 1999. Field weathering rates of Mt. St. Helens tephra. Geochimica et Cosmochimica Acta 63, 587–598.
Dasch, A.A., Blum, J.D., Eagar, C., Fahey, T.J., Driscoll, C.T., Siccama, T.G., 2006. The relative uptake of Ca and Sr into tree foliage using a whole-watershed calcium addition. Biogeochemistry 80, 21–41.
Davis, A.S., 1995. Petrology of late Eocene lavas erupted in the forearc of central Oregon. US Department of the Interior, US Geological Survey.
Denison, W.C., 1979. Lobaria oregana, a nitrogen-fixing lichen in old-growth Douglas fir forests. Symbiotic nitrogen fixation in the management of temperate forests 266–275.
Dia, A.N., Cohen, A.S., O'Nions, R.K., Shackleton, N.J., 1992. Seawater Sr isotope variation over the past 300 kyr and influence of global climate cycles. Nature 356, 786–788.
Dixon, J.L., Heimsath, A.M., Amundson, R., 2009. The critical role of climate and saprolite weathering in landscape evolution. Earth Surface Processes and Landforms 34, 1507–1521.
Dott Jr, R.H., 1966. Eocene deltaic sedimentation at Coos Bay, Oregon. The Journal of Geology 373–420.
Drouet, T., Herbauts, J., Demaiffe, D., 2005a. Long-term records of strontium isotopic composition in tree rings suggest changes in forest calcium sources in the early 20th century. Global change biology 11, 1926–1940.
Drouet, T., Herbauts, J., Gruber, W., Demaiffe, D., 2005b. Strontium isotope composition as a tracer of calcium sources in two forest ecosystems in Belgium. Geoderma 126, 203–223. doi:10.1016/j.geoderma.2004.09.010
Duncan, R.A., 1982. A captured island chain in the Coast Range of Oregon and Washington. Journal of Geophysical Research: Solid Earth (1978–2012) 87, 10827–10837.

Dunn, T., Sen, C., 1994. Mineral/matrix partition coefficients for orthopyroxene, plagioclase, and olivine in basaltic to andesitic systems: A combined analytical and experimental study. Geochimica et Cosmochimica Acta 58, 717–733. doi:10.1016/0016-7037(94)90501-0

Eggleton, R.A., Foudoulis, C., Varkevisser, D., 1987. Weathering of basalt: Changes in rock chemistry and mineralogy. Clays Clay Miner 35, 161–169.

Epstein, E., Bloom, A.J., 2005. Mineral nutrition of plants: principles and perspectives. Sinauer Associates. Inc. Sunderland, Mass.

Essington, M.E., 2004. Soil and water chemistry: An integrative approach. CRC press.

Federer, C.A., Hornbeck, J.W., Tritton, L.M., Martin, C.W., Pierce, R.S., Smith, C.T., 1989. Long-term depletion of calcium and other nutrients in eastern US forests. Environmental Management 13, 593–601.

Gabrielli, C.P., McDonnell, J.J., 2012. An inexpensive and portable drill rig for bedrock groundwater studies in headwater catchments. Hydrological Processes 26, 622–632. doi:10.1002/hyp.8212

Galloway, W.E., 1974. Deposition and Diagenetic Alteration of Sandstone in Northeast Pacific Arc-Related Basins: Implications for Graywacke Genesis. Geological Society of America Bulletin 85, 379–390. doi:10.1130/0016-7606(1974)85<379:DADAOS>2.0.CO;2

Goldich, S.S., 1938. A study in rock-weathering. The Journal of Geology 17–58.

Goles, G.G., Lambert, R.S.J., 1990. A strontium isotopic study of Newberry volcano, central Oregon: Structural and thermal implications. Journal of Volcanology and Geothermal Research 43, 159–174. doi:10.1016/0377-0273(90)90050-P

Gosz, J.R., Brookins, D.G., Moore, D.I., 1983. Using strontium isotope ratios to estimate inputs to ecosystems. BioScience 33, 23–30.

Gosz, J.R., Moore, D.I., 1989. Strontium isotope studies of atmospheric inputs to forested watersheds in New Mexico. Biogeochemistry 8, 115–134.

Graustein, W.C., 1989. 87Sr/86Sr ratios measure the sources and flow of strontium in terrestrial ecosystems, in: Stable Isotopes in Ecological Research. Springer, pp. 491–512.

Green, M.B., Bailey, A.S., Bailey, S.W., Battles, J.J., Campbell, J.L., Driscoll, C.T., Fahey, T.J., Lepine, L.C., Likens, G.E., Ollinger, S.V., 2013. Decreased water flowing from a forest amended with calcium silicate. Proceedings of the National Academy of Sciences 110, 5999–6003.

Groffman, P.M., Fisk, M.C., 2011. Calcium constrains plant control over forest ecosystem nitrogen cycling. Ecology 92, 2035–2042.

Hamburg, S.P., Yanai, R.D., Arthur, M.A., Blum, J.D., Siccama, T.G., 2003. Biotic control of calcium cycling in northern hardwood forests: acid rain and aging forests. Ecosystems 6, 399–406.

He, X., Vepraskas, M.J., Lindbo, D.L., Skaggs, R.W., 2003. A method to predict soil saturation frequency and duration from soil color. Soil Science Society of America Journal 67, 961–969.

Heath, B., Sollins, P., Perry, D.A., Cromack Jr, K., 1988. Asymbiotic nitrogen fixation in litter from Pacific Northwest forests. Canadian Journal of Forest Research 18, 68–74.

Hedin, L.O., Granat, L., Likens, G.E., Buishand, T.A., Galloway, J.N., Butler, T.J., Rodhe, H., 1994. Steep declines in atmospheric base cations in regions of Europe and North America.

Heimsath, A.M., Dietrich, W.E., Nishiizumi, K., Finkel, R.C., 2001. Stochastic processes of soil production and transport: Erosion rates, topographic variation and cosmogenic nuclides in the Oregon Coast Range. Earth Surface Processes and Landforms 26, 531–552.

Heller, P.L., Peterman, Z.E., O'NEIL, J.R., Shafiqullah, M., 1985. Isotopic provenance of sandstones from the Eocene Tyee Formation, Oregon Coast Range. Geological Society of America Bulletin 96, 770–780.

Heller, P.L., Ryberg, P.T., 1983. Sedimentary record of subduction to forearc transition in the rotated Eocene basin of western Oregon. Geology 11, 380–383. doi:10.1130/0091-7613(1983)11<380:SROSTF>2.0.CO;2

Heller, P.L., Tabor, R.W., Suczek, C.A., 1987. Paleogeographic evolution of the United States Pacific Northwest during Paleogene time. Canadian Journal of Earth Sciences 24, 1652–1667.

Hicks, W.T., 2000. Modeling nitrogen fixation in dead wood (Thesis).

Hilton, R.G., Galy, A., West, A.J., Hovius, N., Roberts, G.G., 2013. Geomorphic control on the δ15N of mountain forests. Biogeosciences 10, 1693–1705.

Hinsinger, P., Plassard, C., Tang, C., Jaillard, B., 2003. Origins of root-mediated pH changes in the rhizosphere and their responses to environmental constraints: a review. Plant and soil 248, 43–59.

Holloway, J.M., Dahlgren, R.A., 1999. Geologic nitrogen in terrestrial biogeochemical cycling. Geology 27, 567–570.

Homann, P.S., Miegroet, H. van, Cole, D.W., Wolfe, G.V., 1992. Cation distribution, cycling, and removal from mineral soil in Douglas-fir and red alder forests. Biogeochemistry 16, 121–150. doi:10.1007/BF00002828

Homann, P.S., Sollins, P., Chappell, H.N., Stangenberger, A.G., 1995. Soil Organic Carbon in a Mountainous, Forested Region: Relation to Site Characteristics. Soil Science Society of America Journal 59, 1468. doi:10.2136/sssaj1995.03615995005900050037x

Huntington, T.G., Hooper, R.P., Johnson, C.E., Aulenbach, B.T., Cappellato, R., Blum, A.E., 2000. Calcium depletion in a southeastern United States forest ecosystem. Soil Science Society of America Journal 64, 1845–1858.

Hurst, V.J., 1977. Visual estimation of iron in saprolite. Geological Society of America Bulletin 88, 174–176.

Huxman, T.E., Wilcox, B.P., Breshears, D.D., Scott, R.L., Snyder, K.A., Small, E.E., Hultine, K., Pockman, W.T., Jackson, R.B., 2005. Ecohydrological Implications of Woody Plant Encroachment. Ecology 86, 308–319.

Hyman, M.E., Johnson, C.E., Bailey, S.W., Hornbeck, J.W., April, R.H., 1998. Chemical weathering and cation loss in a base-poor watershed. Geological Society of America Bulletin 110, 85–95.
Irving, A.J., 1978. A review of experimental studies of crystal/liquid trace element partitioning. Geochimica et Cosmochimica Acta, Experimental trace element geochemistry 42, 743–770. doi:10.1016/0016-7037(78)90091-1
Jahn, B., Gallet, S., Han, J., 2001. Geochemistry of the Xining, Xifeng and Jixian sections, Loess Plateau of China: eolian dust provenance and paleosol evolution during the last 140 ka. Chemical Geology 178, 71–94.
Jenny, H., 1941. Factors of soil formation: a system of quantitative pedology. Courier Dover Publications.
Johnson, D.W., Lindberg, S.E., others, 1992. Atmospheric deposition and forest nutrient cycling. A synthesis of the Integrated Forest Study. Springer-Verlag.
Johnston, J.M., Crossley Jr., D.A., 2002. Forest ecosystem recovery in the southeast US: soil ecology as an essential component of ecosystem management. Forest Ecology and Management, Forest Ecology in the next Millennium : Putting the long view into Practice 155, 187–203. doi:10.1016/S0378-1127(01)00558-8
Juice, S.M., Fahey, T.J., Siccama, T.G., Driscoll, C.T., Denny, E.G., Eagar, C., Cleavitt, N.L., Minocha, R., Richardson, A.D., 2006. Response of sugar maple to calcium addition to northern hardwood forest. Ecology 87, 1267–1280.
Kennedy, M.J., Chadwick, O.A., Vitousek, P.M., Derry, L.A., Hendricks, D.M., 1998. Changing sources of base cations during ecosystem development, Hawaiian Islands. Geology 26, 1015–1018.
Kennedy, M.J., Hedin, L.O., Derry, L.A., 2002. Decoupling of unpolluted temperate forests from rock nutrient sources revealed by natural 87Sr/86Sr and 84Sr tracer addition. PNAS 99, 9639–9644. doi:10.1073/pnas.152045499
Landeweert, R., Hoffland, E., Finlay, R.D., Kuyper, T.W., van Breemen, N., 2001. Linking plants to rocks: ectomycorrhizal fungi mobilize nutrients from minerals. Trends in Ecology & Evolution 16, 248–254.
Langan, S.J., Hodson, M.E., Bain, D.C., Skeffington, R.A., Wilson, M.J., 1995. A preliminary review of weathering rates in relation to their method of calculation for acid sensitive soil parent materials. Water Air Soil Pollut 85, 1075–1081. doi:10.1007/BF00477124
Laurance, W.F., Fearnside, P.M., Laurance, S.G., Delamonica, P., Lovejoy, T.E., Rankin-de Merona, J.M., Chambers, J.Q., Gascon, C., 1999. Relationship between soils and Amazon forest biomass: a landscape-scale study. Forest Ecology and Management 118, 127–138. doi:10.1016/S0378-1127(98)00494-0
Lawrence, G.B., David, M.B., Bailey, S.W., Shortle, W.C., 1997. Assessment of soil calcium status in red spruce forests in the northeastern United States. Biogeochemistry 38, 19–39. doi:10.1023/A:1005790130253
Lawrence, G.B., David, M.B., Shortle, W.C., others, 1995. A new mechanism for calcium loss in forest-floor soils. Nature 378, 162–165.

Likens, G.E., Driscoll, C.T., Buso, D.C., 1996. Long-term effects of acid rain: response and recovery of a forest ecosystem. Science-AAAS-Weekly Paper Edition 272, 244–245.
Lindeburg, K.S., Almond, P., Roering, J.J., Chadwick, O.A., 2013. Pathways of soil genesis in the Coast Range of Oregon, USA. Plant and soil 367, 57–75.
Long, C.J., Whitlock, C., Bartlein, P.J., 2007. Holocene vegetation and fire history of the Coast Range, western Oregon, USA. The Holocene 17, 917–926.
Long, C.J., Whitlock, C., Bartlein, P.J., Millspaugh, S.H., 1998. A 9000-year fire history from the Oregon Coast Range, based on a high-resolution charcoal study. Canadian Journal of Forest Research 28, 774–787.
Magill, J., Cox, A., Duncan, R., 1981. Tillamook volcanic series: Further evidence for tectonic rotation of the Oregon Coast Range. Journal of Geophysical Research: Solid Earth (1978–2012) 86, 2953–2970.
Maguire, D.A., Kanaskie, A., Voelker, W., Johnson, R., Johnson, G., 2002. Growth of young Douglas-fir plantations across a gradient in Swiss needle cast severity. Western Journal of Applied Forestry 17, 86–95.
Mahowald, N., Kohfeld, K., Hansson, M., Balkanski, Y., Harrison, S.P., Prentice, I.C., Schulz, M., Rodhe, H., 1999. Dust sources and deposition during the last glacial maximum and current climate: A comparison of model results with paleodata from ice cores and marine sediments. Journal of Geophysical Research: Atmospheres 104, 15895–15916. doi:10.1029/1999JD900084
Mainwaring, D.B., Maguire, D.A., Perakis, S.S., 2014. Three-year growth response of young Douglas-fir to nitrogen, calcium, phosphorus, and blended fertilizers in Oregon and Washington. Forest Ecology and Management 327, 178–188. doi:10.1016/j.foreco.2014.05.005
Marcus, Y., Kertes, A.S., 1969. Ion exchange and solvent extraction of metal complexes.
Matoh, T., Kobayashi, M., 1998. Boron and calcium, essential inorganic constituents of pectic polysaccharides in higher plant cell walls. Journal of Plant research 111, 179–190.
McBride, M.B., 1994. Environmental chemistry of soils. Oxford university press.
McWilliams, R.G., 1973. Stratigraphic and biostratigraphic relationships of the Tyee and Yamhill Formations in central-western Oregon. Oregon Department of Geology and Mineral Industries, The Ore Bin 35, 169–186.
Menge, D.N., Troy Baisden, W., Richardson, S.J., Peltzer, D.A., Barbour, M.M., 2011. Declining foliar and litter δ15N diverge from soil, epiphyte and input δ15N along a 120 000 yr temperate rainforest chronosequence. New Phytologist 190, 941–952.
Mitchell, M.J., 2011. Nitrate dynamics of forested watersheds: spatial and temporal patterns in North America, Europe and Japan. Journal of Forest Research 16, 333–340.
Morford, S.L., Houlton, B.Z., Dahlgren, R.A., 2011. Increased forest ecosystem carbon and nitrogen storage from nitrogen rich bedrock. Nature 477, 78–81.

NADP, 2014. National Atmospheric Deposition Program (NRSP-3). NADP Program Office, Illinois State Water Survey, 2204 Griffith Dr., Champaign, IL 61820. [WWW Document]. URL http://nadp.isws.illinois.edu/nadpdata/weeklyRequest.asp?site=OR02

Nakai, S., Halliday, A.N., Rea, D.K., 1993. Provenance of dust in the Pacific Ocean. Earth and Planetary Science Letters 119, 143–157.

National Cooperative Soil Survey [WWW Document], n.d. National Cooperative Soil Characterization Database. URL http://ncsslabdatamart.sc.egov.usda.gov

Nesbitt, H.W., Young, G.M., 1982. Early Proterozoic climates and plate motions inferred from major element chemistry of lutites. Nature 299, 715–717.

Nesbitt, H.W., Young, G.M., 1984. Prediction of some weathering trends of plutonic and volcanic rocks based on thermodynamic and kinetic considerations. Geochimica et Cosmochimica Acta 48, 1523–1534.

Nezat, C.A., Blum, J.D., Yanai, R.D., Hamburg, S.P., 2007. A sequential extraction to determine the distribution of apatite in granitoid soil mineral pools with application to weathering at the Hubbard Brook Experimental Forest, NH, USA. Applied Geochemistry 22, 2406–2421.

NRCS, U., 2009. Web soil survey. URL http://www. websoilsurvey. ncsc. usda. gov/app/[verified October 29, 2009].

Oregon Geologic Data Compilation, 2009.

Page, A.L., 1982. Methods of soil analysis. Part 2. Chemical and microbiological properties. American Society of Agronomy, Soil Science Society of America.

Page, B.D., Mitchell, M.J., 2008. Influences of a calcium gradient on soil inorganic nitrogen in the Adirondack Mountains, New York. Ecological Applications 18, 1604–1614.

Parker, A., 1970. An index of weathering for silicate rocks. Geological Magazine 107, 501–504.

Parker, D.F., Hodges, F.N., Perry, A., Mitchener, M.E., Barnes, M.A., Ren, M., 2010. Geochemistry and petrology of late Eocene Cascade Head and Yachats Basalt and alkalic intrusions of the central Oregon Coast Range, USA. Journal of Volcanology and Geothermal Research 198, 311–324.

Peltzer, D.A., Wardle, D.A., Allison, V.J., Baisden, W.T., Bardgett, R.D., Chadwick, O.A., Condron, L.M., Parfitt, R.L., Porder, S., Richardson, S.J., others, 2010. Understanding ecosystem retrogression. Ecological Monographs 80, 509–529.

Perakis, S.S., Maguire, D.A., Bullen, T.D., Cromack, K., Waring, R.H., Boyle, J.R., 2006. Coupled nitrogen and calcium cycles in forests of the Oregon Coast Range. Ecosystems 9, 63–74.

Perakis, S.S., Sinkhorn, E.R., 2011. Biogeochemistry of a temperate forest nitrogen gradient. Ecology 92, 1481–1491. doi:10.1890/10-1642.1

Perakis, S.S., Sinkhorn, E.R., Catricala, C.E., Bullen, T.D., Fitzpatrick, J.A., Hynicka, J.D., Cromack, K., 2013. Forest calcium depletion and biotic retention along a soil nitrogen gradient. Ecological Applications 23, 1947–1961. doi:10.1890/12-2204.1

Perakis, S.S., Sinkhorn, E.R., Compton, J.E., 2011. δ15N constraints on long-term nitrogen balances in temperate forests. Oecologia 167, 793–807. doi:10.1007/s00442-011-2016-y

Pérez, C.A., Aravena, J.C., Silva, W.A., Enríquez, J.M., Fariña, J.M., Armesto, J.J., 2014. Ecosystem development in short-term postglacial chronosequences: N and P limitation in glacier forelands from Santa Inés Island, Magellan Strait. Austral Ecology 39, 288–303. doi:10.1111/aec.12078

Peterman, Z.E., Hedge, C.E., Tourtelot, H.A., 1970. Isotopic composition of strontium in sea water throughout Phanerozoic time. Geochimica et Cosmochimica Acta 34, 105–120. doi:10.1016/0016-7037(70)90154-7

Pett-Ridge, J.C., Derry, L.A., Barrows, J.K., 2009. Ca/Sr and< sup> 87</sup> Sr/< sup> 86</sup> Sr ratios as tracers of Ca and Sr cycling in the Rio Icacos watershed, Luquillo Mountains, Puerto Rico. Chemical Geology 267, 32–45.

Porder, S., Paytan, A., Vitousek, P.M., 2005. Erosion and landscape development affect plant nutrient status in the Hawaiian Islands. Oecologia 142, 440–449.

Post, W.M., Pastor, J., Zinke, P.J., Stangenberger, A.G., 1985. Global patterns of soil nitrogen storage. Nature 317, 613–616. doi:10.1038/317613a0

Prytulak, J., Vervoort, J.D., Plank, T., Yu, C., 2006. Astoria Fan sediments, DSDP site 174, Cascadia Basin: Hf–Nd–Pb constraints on provenance and outburst flooding. Chemical geology 233, 276–292.

R Development Core Team, 2008. R: A language and environment for statistical computing. R Foundation for Statistical Computing, Vienna, Austria.

Rasmussen, C., Brantley, S., Richter, D. deB., Blum, A., Dixon, J., White, A.F., 2011. Strong climate and tectonic control on plagioclase weathering in granitic terrain. Earth and Planetary Science Letters 301, 521–530. doi:10.1016/j.epsl.2010.11.037

Reich, P.B., Oleksyn, J., Modrzynski, J., Mrozinski, P., Hobbie, S.E., Eissenstat, D.M., Chorover, J., Chadwick, O.A., Hale, C.M., Tjoelker, M.G., 2005. Linking litter calcium, earthworms and soil properties: a common garden test with 14 tree species. Ecology Letters 8, 811–818.

Reneau, S.L., Dietrich, W.E., 1991. Erosion rates in the southern Oregon Coast Range: Evidence for an equilibrium between hillslope erosion and sediment yield. Earth Surface Processes and Landforms 16, 307–322.

Reuss, J.O., Johnson, D.W., others, 1986. Acid depostion and acidification of soils and waters. Springer-Verlag.

Reynolds, A.C., Quade, J., Betancourt, J.L., 2012. Strontium isotopes and nutrient sourcing in a semi-arid woodland. Geoderma 189, 574–584.

Riebe, C.S., Kirchner, J.W., Granger, D.E., Finkel, R.C., 2001. Strong tectonic and weak climatic control of long-term chemical weathering rates. Geology 29, 511–514.

Sarna-Wojcicki, A.M., Shipley, S., Jr, W., B, R., Dzurisin, D., Wood, S.H., 1981. Areal Distribution, Thickness, Mass, Volume, and Grain Size of Air-Fall Ash from the Six Major Eruptions of 1980 1250, 577–600.

Schlesinger, W.H., Bernhardt, E.S., 2013. Biogeochemistry: an analysis of global change. Academic press.
Schoenholtz, S.H., Miegroet, H.V., Burger, J.A., 2000. A review of chemical and physical properties as indicators of forest soil quality: challenges and opportunities. Forest ecology and management 138, 335–356.
Shields, J.A., Paul, E.A., St. Arnaud, R.J., Head, W.K., 1968. Spectrophotometry measurement of soil color and its relationship to moisture and organic matter. Canadian Journal of Soil Science 48, 271–280.
Short, H.L., Dietz, D.R., Remmenga, E.E., 1966. Selected Nutrients in Mule Deer Browse Plants. Ecology 47, 222–229. doi:10.2307/1933768
Snavely, P.D., MacLeod, N.S., Wagner, H.C., 1968. Tholeiitic and alkalic basalts of the Eocene Siletz River Volcanics, Oregon Coast Range. Am J Sci 266, 454–481. doi:10.2475/ajs.266.6.454
Snavely, P.D., Wagner, H.C., MacLeod, N.S., 1964. Rhythmic-bedded eugeosynclinal deposits of the Tyee formation, Oregon coast range. Kans. Geol. Surv. Bull 169, 461–480.
Spies, T.A., Hibbs, D.E., Ohmann, J.L., Reeves, G.H., Pabst, R.J., Swanson, F.J., Whitlock, C., Jones, J.A., Wemple, B.C., Parendes, L.A., 2002. The ecological basis of forest ecosystem management in the Oregon Coast Range. SD Hobbs, JP Hayes, RL Johnson, GH Reeves, TA Spies, JC Tappeiner, II, and GE Wells, editors. Forest and stream management in the Oregon Coast Range. Oregon State University Press, Corvallis, Oregon, USA 31–67.
Station, M.S.U.G.P.R.P. of C. and S.S.W.K.K.B., Ecology, U. of G.D.C.C.R.P. of E.I. of, Davis, A.C.S.B.P. of S.E. in the D. of L., and Water Resources University of California, University, P.S.P. of F.E. and S. in the F.S.D.O.S., 1999. Standard Soil Methods for Long-Term Ecological Research. Oxford University Press.
Stewart, B.W., Capo, R.C., Chadwick, O.A., 2001. Effects of rainfall on weathering rate, base cation provenance, and Sr isotope composition of Hawaiian soils. Geochimica et Cosmochimica Acta 65, 1087–1099. doi:10.1016/S0016-7037(00)00614-1
Svensson, A., Biscaye, P.E., Grousset, F.E., 2000. Characterization of late glacial continental dust in the Greenland Ice Core Project ice core. Journal of Geophysical Research: Atmospheres (1984–2012) 105, 4637–4656.
Sweeney, K.E., Roering, J.J., Almond, P., Reckling, T., 2012. How steady are steady-state landscapes? Using visible–near-infrared soil spectroscopy to quantify erosional variability. Geology 40, 807–810.
Takyu, M., Aiba, S.-I., Kitayama, K., 2002. Effects of topography on tropical lower montane forests under different geological conditions on Mount Kinabalu, Borneo. Plant Ecology 159, 35–49. doi:10.1023/A:1015512400074
Tarrant, R.F., 1969. Nitrogen enrichment of two forest ecosystems by red alder. Pacific Northwest Forest and Range Experiment Station, US Department of Agriculture.

Van Breemen, N., Finlay, R., Lundström, U., Jongmans, A.G., Giesler, R., Olsson, M., 2000. Mycorrhizal weathering: A true case of mineral plant nutrition? Biogeochemistry 49, 53–67.

Van Miegroet, H., Cole, D.W., 1985. Acidification sources in red alder and Douglas fir soils-importance of nitrification. Soil Science Society of America Journal 49, 1274–1279.

VanLaningham, S., Duncan, R.A., Pisias, N.G., Graham, D.W., 2008. Tracking fluvial response to climate change in the Pacific Northwest: a combined provenance approach using Ar and Nd isotopic systems on fine-grained sediments. Quaternary Science Reviews 27, 497–517.

Vitousek, P., Chadwick, O., Matson, P., Allison, S., Derry, L., Kettley, L., Luers, A., Mecking, E., Monastra, V., Porder, S., 2003. Erosion and the rejuvenation of weathering-derived nutrient supply in an old tropical landscape. Ecosystems 6, 762–772.

Vitousek, P.M., Chadwick, O.A., 2013. Pedogenic thresholds and soil process domains in basalt-derived soils. Ecosystems 16, 1379–1395.

Vitousek, P.M., Chadwick, O.A., Crews, T.E., Fownes, J.H., Hendricks, D.M., Herbert, D., 1997. Soil and Ecosystem Development Across the Hawaiian Islands. GSA Today 7.

Walker, J.C., Hays, P.B., Kasting, J.F., 1981. A negative feedback mechanism for the long-term stabilization of Earth's surface temperature. Journal of Geophysical Research: Oceans (1978–2012) 86, 9776–9782.

Wang, T., Hamann, A., Spittlehouse, D., 2009. ClimateWNA. University of British Columbia, Department of Forest Sciences, Centre for Forest Conservation Genetics, Vancouver, BC http://www. genetics. forestry. ubc. ca/cfcg/ClimateWNA_web/(Accessed May 2012).

Wells, R., Bukry, D., Friedman, R., Pyle, D., Duncan, R., Haeussler, P., Wooden, J., 2014. Geologic history of Siletzia, a large igneous province in the Oregon and Washington Coast Range: Correlation to the geomagnetic polarity time scale and implications for a long-lived Yellowstone hotspot. Geosphere 10, 692–719.

Wells, R.E., Engebretson, D.C., Snavely, P.D., Coe, R.S., 1984. Cenozoic plate motions and the volcano-tectonic evolution of western Oregon and Washington. Tectonics 3, 275–294. doi:10.1029/TC003i002p00275

White, A.F., Brantley, S.L., 1995. Chemical weathering rates of silicate minerals: an overview. Chemical Weathering Rates of Silicate Minerals 31, 1–22.

White, A.F., Brantley, S.L., 2003. The effect of time on the weathering of silicate minerals: why do weathering rates differ in the laboratory and field? Chemical Geology 202, 479–506.

Table 1. Site characteristics of our twenty-four detailed sampling sites in 2012

Site	Latitude	Longitude	Elevation	Distance from the Coast	MAP[1]	MAT[1]	Slope	Depth to Bedrock	Soil Series[2]	Soil Taxa[2]	Rock Formation[3]
Sedimentary			(m)	(km)	(mm)	(°C)	(degrees)	(m)			
Lake	44.5698	-123.6933	298	30.10	1838	10.9	33	4-7	Preaher-Bohannon-Slickrock	Andic Humudept	Tyee
Devitt	44.6413	-123.5348	230	41.87	1837	10.7	13	9-10	Digger-Bohannon	Andic Humudept	Tyee
Steere	44.7287	-123.6359	374	33.27	2642	10.3	14	5-6	Astoria silt loams	Andic Humudept	Tyee
7	45.1261	-123.6439	286	26.66	2217	10.5	14	3-7	Astoria silt loams	Andic Humudept	Nestucca
56	44.6997	-123.7386	333	25.22	2038	10.2	32	7-8	Bohannon-Preacher	Andic Humudept	Tyee
43	44.6927	-123.8531	117	16.15	2037	10.9	15	5-6	Preacher-Bohannon	Andic Humudept	Nestucca
Trask	45.4620	-123.6222	303	26.77	2712	10.0	16	roadcut, 3-6	Hemcross-Klistan	Alic Hapludand	Yamhill
HC1	44.6760	-123.7908	126	21.15	1959	10.9	9.1	3-5	Preacher-Bohannon	Andic Humudept	Tyee
108B	45.3015	-123.6920	232	21.27	2740	10.9	43	6-8	Ginsberg medial loams	Andic Humudept	Tyee
Wow	44.6173	-123.8092	95	20.28	2050	11.7	32	1-5	Preacher-Bohannon	Andic Humudept	Tyee
143	44.6890	-123.7977	224	20.53	2014	10.5	25	>10	Preacher-Bohannon	Andic Humudept	Tyee
Basaltic											
NFT	45.4274	-123.3684	517	46.38	2160	9.20	6	1-5	Hembre silt loam	Andic Humudept	Lee's Falls
Jensen	44.5362	-123.4743	371	48.00	1927	10.6	17	>10	Honeygrove-Shivigny	Typic Palehumult	Siletz RV
Stein	45.4426	-123.3982	537	43.82	2275	9.20	14	8-9	Hembre silt loam	Andic Humudept	Lee's Falls
19	45.4380	-123.6300	241	25.65	2804	10.5	29	outcrop, 3-5	Necanicum-Ascar-Klootchie	Typic Fulvudand	Tillamook
WP	45.5817	-123.6201	592	25.67	3832	9.10	30	1-3	Klistan-Harslow-Hemcross	Alic Hapludand	Tillamook
14B	45.3041	-123.6993	189	20.68	2737	11.1	17	5-7	Ginsberg medial loams	Alic Hapludand	Tillamook
Hoag	45.2691	-123.4908	761	37.24	2559	8.90	14	3-5	Murtip-Caterl-Laderly	Alic Hapludand	Lee's Falls
60	45.8050	-123.7038	204	20.22	3137	10.1	27	outcrop, 5-7	Necanicum-Ascar complex	Typic Fulvudand	Tillamook
8	44.9995	-123.8698	265	11.20	2503	10.2	20	>11	Klootchie-Neotsu silt loams	Typic Fulvudand	Siletz RV
RR1	45.7756	-123.7003	517	20.22	3171	8.70	23	outcrop, 1-3	Skipanon gravelly silt loam	Andic Humudept	Tillamook
BC1	45.0030	-123.8776	173	10.54	2476	10.7	23	>11	Klootchie-Neotsu silt loams	Typic Fulvudand	Siletz RV
Mixed											
54	45.1628	-123.6834	277	22.74	3227	10.6	17	6-7	Astoria silt loam	Andic Humudept	Tyee
GV1	45.7657	-123.7961	246	12.53	2866	9.90	10	roadcut, 7-9	Templeton medial silt loam	Andic Humudept	Smuggler Cove

1 - Mean annual precipitaiton (MAP) and mean annual temperature (MAT) estimated as 30 year means from PRISM model, according to Wang et al., 2009
2 - NRCS, 2009
3 – "Oregon Geologic Data Compilation," 2009

Table 2. Soil C and N concentrations and C/N ratios of < 2 mm in diameter soil fraction for sedimentary sites.

Site	Depth	pH	C	N	C/N	Site	Depth	pH	C	N	C/N
	cm		%		molar		cm		%		molar
Lake	0-10	5.75	2.47	0.16	18.0	Trask	0-10	4.57	9.84	0.50	22.8
	10-20	5.38	1.84	0.13	16.2		10-20	4.75	5.89	0.36	19.3
	20-30	5.22	1.68	0.12	16.4		20-30	4.84	4.67	0.28	19.1
	30-40	6.07	1.47	0.11	15.3		30-40	5.04	5.02	0.31	18.9
	40-50	6.05	1.34	0.09	17.0		40-50	5.03	4.14	0.26	18.6
Devitt	0-10	6.17	4.70	0.26	21.1	HC1	0-10	4.72	8.42	0.51	19.4
	10-20	6.03	3.75	0.22	20.1		10-20	4.62	7.00	0.45	18.0
	20-30	6.23	3.35	0.18	21.9		20-30	4.81	5.16	0.35	17.2
	30-40	6.19	2.04	0.13	18.7		30-40	5.20	3.88	0.27	16.6
	40-50	5.56	1.17	0.09	15.4		40-50	5.48	2.82	0.19	17.3
Steere	0-10	5.26	5.90	0.31	22.4	108B	0-10	4.93	8.84	0.57	18.1
	10-20	5.08	4.98	0.29	19.9		10-20	4.86	7.18	0.45	18.5
	20-30	5.12	3.85	0.24	18.9		20-30	5.20	6.20	0.37	19.6
	30-40	5.07	3.75	0.24	18.5		30-40	5.25	5.06	0.29	20.2
	40-50	5.14	2.61	0.16	18.7		40-50	5.36	4.12	0.24	20.4
7	0-10	5.56	6.23	0.31	23.8	Wow	0-10	4.11	13.87	0.86	18.8
	10-20	5.24	4.85	0.25	22.6		10-20	4.33	8.93	0.52	19.9
	20-30	6.17	3.37	0.19	20.9		20-30	4.61	6.59	0.40	19.4
	30-40	5.26	2.81	0.16	20.0		30-40	5.38	5.69	0.33	20.0
	40-50	6.05	2.08	0.13	18.0		40-50	5.13	3.85	0.23	19.9
56	0-10	5.42	5.75	0.36	18.6	143	0-10	3.90	15.73	0.86	21.4
	10-20	5.18	5.73	0.37	18.2		10-20	4.28	8.88	0.46	22.7
	20-30	5.12	4.67	0.31	17.5		20-30	4.57	6.97	0.40	20.5
	30-40	5.26	4.05	0.28	16.9		30-40	4.54	6.67	0.38	20.6
	40-50	5.08	3.63	0.25	17.1		40-50	4.55	5.41	0.31	20.2
43	0-10	5.16	8.53	0.48	20.8						
	10-20	5.13	7.72	0.42	21.6						
	20-30	5.24	8.03	0.48	19.5						
	30-40	4.86	7.64	0.44	20.5						
	40-50	5.33	5.95	0.35	20.0						

Table 2 continued. Soil Ca and N concentrations and C/N ratios of < 2 mm in diameter soil fraction for basaltic sites.

Site	Depth	pH	C	N	C/N	Site	Depth	pH	C	N	C/N
	cm		%		molar		cm		%		molar
NFT	0-10	5.41	4.95	0.21	28.0	Hoag	0-10	5.75	11.3	0.45	29.5
	10-20	6.12	3.08	0.13	27.1		10-20	5.11	8.93	0.35	29.9
	20-30	5.93	2.00	0.10	22.3		20-30	5.64	6.97	0.27	29.7
	30-40	5.61	1.59	0.09	21.1		30-40	5.91	4.70	0.23	24.3
	40-50	5.87	1.38	0.08	21.0		40-50	5.84	3.79	0.19	23.7
Jensen	0-10	6.45	6.74	0.27	28.8	60	0-10	5.12	11.4	0.56	23.8
	10-20	6.30	4.05	0.17	27.0		10-20	5.26	6.71	0.41	18.9
	20-30	6.40	2.89	0.15	23.0		20-30	5.19	6.97	0.45	18.2
	30-40	6.43	2.66	0.13	23.7		30-40	5.51	7.76	0.46	19.6
	40-50	6.01	1.91	0.10	22.6		40-50	5.59	6.59	0.42	18.2
Stein	0-10	5.79	7.12	0.30	27.8	8	0-10	5.36	10.8	0.58	21.5
	10-20	5.68	4.36	0.19	26.8		10-20	5.35	7.61	0.45	19.6
	20-30	6.04	3.32	0.16	23.9		20-30	5.41	6.88	0.39	20.4
	30-40	6.15	1.73	0.09	23.4		30-40	5.23	5.62	0.33	19.9
	40-50	5.65	1.38	0.07	21.7		40-50	5.55	4.32	0.26	19.7
19	0-10	5.29	6.07	0.30	23.6	RR1	0-10	4.77	15.1	0.66	26.7
	10-20	5.20	4.94	0.23	24.6		10-20	4.75	9.30	0.43	25.5
	20-30	5.63	4.27	0.20	24.9		20-30	4.97	7.93	0.37	25.1
	30-40	5.41	4.19	0.20	24.1		30-40	5.40	6.32	0.28	26.5
	40-50	5.95	2.68	0.14	22.8		40-50	5.44	4.57	0.23	23.6
WP	0-10	5.85	9.90	0.41	27.9	BC1	0-10	4.55	16.7	0.97	20.0
	10-20	5.80	7.91	0.33	27.8		10-20	5.17	9.69	0.51	22.1
	20-30	5.54	7.35	0.32	26.7		20-30	5.32	8.40	0.46	21.4
	30-40	6.08	5.74	0.24	27.4		30-40	5.43	7.70	0.44	20.4
	40-50	5.64	3.43	0.15	25.9		40-50	5.33	6.17	0.33	21.8
14B	0-10	5.10	6.26	0.42	17.5						
	10-20	5.10	4.71	0.35	15.9						
	20-30	5.17	4.48	0.32	16.4						
	30-40	5.44	3.81	0.26	17.0						
	40-50	5.32	3.76	0.26	17.1						

Table 2 continued. Soil C and N concentrations and C/N ratios of < 2 mm in diameter soil fraction for mixed lithology sites.

Site	Depth	pH	C	N	C/N
	cm		%		molar
54	0-10	5.14	13.9	0.55	29.5
	10-20	4.93	6.47	0.34	21.9
	20-30	5.41	4.60	0.27	19.7
	30-40	5.59	4.17	0.24	20.3
	40-50	5.53	2.63	0.16	19.0
GV1	0-10	4.3	11.0	0.63	20.5
	10-20	4.58	8.70	0.47	21.5
	20-30	4.65	7.09	0.37	22.3
	30-40	4.92	7.96	0.39	24.0
	40-50	4.93	6.00	0.31	22.4

Table 3. Soil pedon descriptions, colors, and textures for sedimentary sites

Site	Depth cm	Horizon	Boundary	Color (dry)	Color (moist)	Redness Rating	Texture
Lake	0-1	Oi	AW				
	1-4	A	AS	10 YR 5/2	10 YR 2/2	20	clay loam
	4-44+	AB	---	10 YR 5/2	10 YR 2/2	20	silty clay loam
Devitt	0-1	Oi	AS				
	1-5	A	CS				sandy clay loam
	5-15	AB	CW				loam
	15-50+	B	---				clay loam
Steere	0-1	Oi	AS				
	1-4	A	AI	10 YR 4/3	10 YR 2/2	20	loamy sand
	4-25	AB	GS	10 YR 3/2	10 YR 2.5/1	50	loamy sand
	25-60+	B	---	10 YR 4.5/3.5	10 YR 3/2	30	sandy loam
7	0-2	Oi	AS				
	2-6	A	AI	10 YR 4/3	7.5 YR 3/2	26	clay loam
	6-51+	Bt	---	10 YR 3/4	7.5 YR 3/2	26	clay loam
56	0-5	Oi	AS				
	5-15	A	AS	10YR 5/2	10YR 2.5/2	25	loam
	15-50+	Bt	---	2.5Y 5/3	2.5Y 3.5/3	26	clay loam
43	0-1	Oi	CA				
	1-11	A	CG	10 YR 3/2	10 YR 2/1	40	sandy loam
	11-41	AB	AW	10 YR 3/2	10 YR 2/1	40	sandy loam
	41-68+	B	---	10 YR 5/2	10 YR 2/2	20	sandy loam

Table 3 continued. Soil pedon descriptions, colors, and textures for sedimentary sites

Site	Depth cm	Horizon	Boundary	Color (dry)	Color (moist)	Redness Rating	Texture
Trask	0-1	Oi	AW				
	1-4	A	CS	10 YR 4/3	10 YR 2/2	20	sandy loam
	4-38	B	AI	10 YR 5/3	10 YR 3/4	15	silty clay loam
	38-58+	B	---	10 YR 6/4	10 YR 4/4	20	silty clay loam
HC1	0-2	Oi	AS				
	2-4	A	CG	10 YR 4/3	10 YR 2/2	20	sandy loam
	4-45	AB	CG	10 YR 5/3	10 YR 3/2	30	sandy clay loam
	45-55+	B	---	10 YR 5/4	10 YR 3/3	20	sandy clay loam
108B	0-1	Oi	AS				
	1- 1.5	A	AS	10 YR 3/2.5	10 YR 2/1.5	27	sandy loam
	1.5- 22.5	AB	CG	10 YR 4/5	10 YR 3/3	20	sandy loam
	22.5- 47	B1	AS	10 YR 4/4	10 YR 3/3	20	sandy loam
	47- 57+	B2	---	10 YR 4/5	10 YR 3/5	12	sandy loam
Wow	0-4	O	AC				
	4-8	A	CW	10 YR 3/2	10 YR 2/2	20	sandy loam
	8-48+	B	---	2.5 Y 5/3	10 YR 3/1.5	40	sandy loam
143	0-1	O	SG				
	1-5	A	AI	10 YR 2/2	10 YR 2/1	40	sand
	5-45+	B	---	7.5 YR 3/4	7.5 YR 3/3	18	sandy loam

Table 3 continued. Soil pedon descriptions, colors, and textures for basaltic sites

Site	Depth cm	Horizon	Boundary	Color (dry)	Color (moist)	Redness Rating	Texture
NFT	0-1	Oi	AS				
	1-2	A	AS	10 YR 5/4	10 YR 3/3	20	silty clay loam
	2-22	B	CS	10 YR 5/4	10 YR 3/3.5	17	silty clay loam
	22-46+	Bt	---	10 YR 5/4	7.5 YR 3/4	13	silty clay loam
19	H1	Oi	AS				
	H2	A	GS	10 YR 4.5/4	10 YR 3.5/3.5	20	sand
	H3	AB	AI	10 YR 5/4	10 YR 3/3	20	sandy loam
	H4	B1	AS	10 YR 4/5	10 YR 3/3.5	17	sandy loam
	H5	B2	---	10 YR 5/5	10 YR 4/4	20	loamy sand
14B	0-2	Oi	AS				
	2-4	A	AS	10 YR 3/4	10 YR 3/2	30	loamy sand
	4-34	Bt1	GW	10 YR 4/6	10 YR 3/4	15	sandy clay loam
	34-64+	Bt2	---	10 YR 5/6	10 YR 3/6	10	sandy clay loam
Jensen	0-1	Oi	AS				
	1-30	Bt1	AS	7.5 YR 3/4	7.5 YR 2.5/3	15	silty clay loam
	30-41+	Bt2	---	7.5 YR 3/4	7.5 YR 2.5/3	15	silty clay
Stein	0-1	Oi	AS				
	1-2	A	CS	10 YR 3/4	7.5 YR 2.5/7.5	6	sandy loam
	2-20	B	CS	10 YR 4/4	7.5 YR 3/3	18	silty clay loam
	20-55+	Bt	---	10 YR 4/5	7.5 YR 4/5	14	sandy clay loam
WP	0-2	Oi	AS				
	2-12	A	CS	10 YR 3/4	10 YR 2/2	20	sand
	12-64+	AB	---	7.5 YR 4/6	7.5 YR 3/4	13	sandy loam

Table 3 continued. Soil pedon descriptions, colors, and textures for basaltic sites

Site	Depth cm	Horizon	Boundary	Color (dry)	Color (moist)	Redness Rating	Texture
8	0-1	Oi	SR				
	1-6	A	AS	10 YR 3/2	10 YR 2/2	20	loamy sand
	6-24.5	B1	CW	10 YR 3/3	7.5 YR 2.5/2	22	loamy sand
	24.5-41	B2	AW	10 YR 3/3	7.5 YR 2.5/2	22	loamy sand
	41-63+	B3	---	10 YR 3/4	10 YR 2/2	20	sandy loam
Hoag	0-1	Oi	CS				
	1-4	A	AS	10 YR 4/4	10 YR 2/2	20	sandy loam
	4-28	B	CS	10 YR 4/4	10 YR 3/2	30	sandy loam
	28-67+	Bt	---	10 YR 5/6	7.5 YR 3/3	18	sandy clay loam
60	0-2	Oi	AS				
	2-48+	A	---	2.5 Y 3/3	2.5YR 3/2.5	27	sand
RR1	0-2	Oi	AS				
	2-65+	Bt	CS	10 YR 5/3	10 YR 3/3	20	sandy loam
BC1	0-3	Oi	AS				
	3-8	A	CW	7.5 YR 3/2	5 YR 2.5/1	38	sandy loam
	8-40	AB	SG	10 YR 4/4	10 YR 3/2	30	sandy loam
	40-56+	B	---	10 YR 4/4	10 YR 3/2	30	sandy loam

Table 4. Exchangeable soil chemical properties, Ca/Sr ratios, and $^{87}Sr/^{86}Sr$ ratios of < 2 mm in diameter soil fraction for sedimentary sites. Dashed lines indicate $^{87}Sr/^{86}Sr$ not measured in 20-30 and 30-40 cm.

Site	Depth	Na	K	Mg	Ca	Sr	Acidity	Al	ECEC	Base Sat.	Ca/Sr	$^{87}Sr/^{86}Sr$
	cm	μg g^{-1}, exchangeable					cmol(+)/kg			%	molar	
Lake	0-10	18.7	542	612	2084	25.5	0.07	0.00	17.0	99.6	179	0.70872
	10-20	20.5	453	609	1702	21.9	1.37	0.90	16.1	91.5	170	0.70875
	20-30	17.4	322	532	1320	16.6	1.62	2.84	13.5	88.0	174	---
	30-40	21.4	308	587	1366	17.6	3.88	3.20	16.4	76.3	169	---
	40-50	19.8	223	495	1301	19.1	4.83	4.32	16.1	69.9	149	0.70880
Devitt	0-10	17.2	454	369	1549	10.0	1.45	0.85	13.5	89.2	339	0.70942
	10-20	16.7	372	333	1096	8.2	3.71	3.18	12.9	71.3	292	0.70933
	20-30	17.1	352	412	973	8.0	6.86	6.33	16.1	57.4	267	---
	30-40	14.8	250	288	519	4.7	10.67	11.63	16.3	34.7	242	---
	40-50	11.0	198	157	339	3.5	15.20	13.94	18.7	18.9	210	0.70956
Steere	0-10	14.9	316	158	508	5.6	7.88	6.81	12.6	37.4	197	0.70890
	10-20	12.8	224	50	113	1.6	11.18	10.46	12.8	12.5	152	0.70900
	20-30	15.8	177	59	129	1.5	11.33	10.83	13.0	12.7	191	---
	30-40	10.3	174	55	142	1.6	10.54	10.04	12.2	13.6	189	---
	40-50	7.2	123	7	22	0.5	10.62	10.59	11.1	4.6	101	0.71022
7	0-10	33.0	574	609	2019	11.4	3.67	3.36	20.4	82.0	388	0.70904
	10-20	29.8	335	492	1423	9.3	9.02	8.19	21.2	57.4	333	0.70884
	20-30	26.8	326	593	1445	8.8	10.22	10.03	23.3	56.1	360	---
	30-40	26.3	258	574	1395	8.3	10.21	9.67	22.7	55.0	366	---
	40-50	25.4	169	373	1061	7.4	12.19	12.02	21.1	42.2	315	0.70895

Table 4 continued. Exchangeable soil chemical properties, Ca/Sr ratios, and $^{87}Sr/^{86}Sr$ ratios of < 2 mm in diameter soil fraction for sedimentary sites.

Site	Depth	Na	K	Mg	Ca	Sr	Acidity	Al	ECEC	Base Sat.	Ca/Sr	$^{87}Sr/^{86}Sr$
	cm	μg g^{-1}, exchangeable					cmol(+)/kg			%	molar	
56	0-10	15.2	421	341	1850	12.6	2.24	1.89	15.4	85.5	321	0.70880
	10-20	16.6	388	225	890	8.7	7.82	7.55	15.2	48.5	225	0.70885
	20-30	14.4	275	178	518	5.5	12.22	12.43	17.0	28.3	206	---
	30-40	16.2	242	222	581	5.6	11.20	10.24	16.6	32.6	227	---
	40-50	13.5	185	83	261	3.8	12.73	12.04	15.2	16.5	150	0.70898
43	0-10	15.3	243	94	426	5.7	4.18	4.13	7.8	46.2	164	0.70803
	10-20	13.6	137	32	111	2.0	6.40	6.12	7.6	16.1	123	0.70815
	20-30	15.9	179	81	368	4.5	5.87	5.37	8.9	34.1	178	---
	30-40	17.8	183	127	401	5.1	5.60	5.16	9.2	39.1	171	---
	40-50	12.1	136	22	73	1.4	5.05	4.73	6.0	15.8	114	0.70812
Trask	0-10	17.7	235	133	216	2.00	18.3	17.1	21.1	13.5	237	0.70837
	10-20	13.0	118	31.6	26.8	0.45	20.8	19.8	21.6	3.5	130	0.70910
	20-30	12.6	72.1	51.9	40.0	0.61	21.0	20.0	21.9	4.0	143	---
	30-40	14.9	69.7	62.6	68.2	0.87	19.5	18.7	20.6	5.3	172	---
	40-50	11.3	51.7	14.5	15.9	0.31	17.7	17.4	18.1	2.1	113	0.70928
HC1	0-10	11.5	189	41.6	110	0.98	9.55	10.48	11.0	13.0	245	0.70891
	10-20	10.0	123	11.0	27.8	0.35	11.6	11.2	12.2	4.81	174	0.70929
	20-30	6.03	83.6	15.8	34.8	0.38	10.0	9.62	10.5	5.15	203	---
	30-40	13.6	87.6	24.3	63.1	0.59	8.14	7.49	8.94	8.92	234	---
	40-50	7.04	70.0	2.7	10.5	0.19	7.82	7.88	8.11	3.51	119	0.70996

Table 4 continued. Exchangeable soil chemical properties, Ca/Sr ratios, and $^{87}Sr/^{86}Sr$ ratios of < 2 mm in diameter soil fraction for sedimentary sites.

Site	Depth	Na	K	Mg	Ca	Sr	$Acidity_{TOT}$	Al	ECEC	Base Sat.	Ca/Sr	$^{87}Sr/^{86}Sr$
	cm	μg g^{-1}, exchangeable					cmol(+)/kg			%	molar	
108B	0-10	19.7	349	312	948	6.11	17.3	16.7	25.6	32.4	339	0.70749
	10-20	16.9	236	172	593	4.09	20.4	18.9	25.4	19.9	317	0.70750
	20-30	17.2	201	194	612	3.84	18.4	17.2	23.7	22.1	348	---
	30-40	15.6	192	164	550	3.33	17.3	16.3	21.9	21.2	361	---
	40-50	13.8	191	83.7	362	2.56	16.4	16.1	19.4	15.7	309	0.70787
Wow	0-10	19.0	128	23.4	65.7	0.92	15.3	14.2	16.2	5.74	156	0.70924
	10-20	16.9	96.4	6.16	9.70	0.29	12.8	12.2	13.2	3.17	73.0	0.70952
	20-30	13.8	76.4	10.4	15.8	0.37	11.0	10.4	11.4	3.68	92.0	---
	30-40	11.0	72.0	7.57	13.4	0.29	8.98	8.44	9.34	3.86	103	---
	40-50	10.9	86.0	1.70	2.80	0.11	8.16	7.94	8.46	3.49	58.3	0.71083
143	0-10	9.24	96.8	15.2	33.0	0.42	16.0	15.1	16.6	3.48	173	0.70922
	10-20	7.22	73.1	2.29	6.32	0.09	10.23	9.88	10.49	2.56	148	0.70952
	20-30	6.50	61.4	5.39	11.9	0.18	8.04	7.63	8.33	3.47	148	---
	30-40	7.93	51.8	5.78	10.8	0.23	7.28	6.94	7.55	3.56	101	---
	40-50	5.98	50.3	0.74	1.87	0.04	6.28	6.03	6.45	2.63	106	0.71036

Table 4 continued. Exchangeable soil chemical properties, Ca/Sr ratios, and $^{87}Sr/^{86}Sr$ ratios of < 2 mm in diameter soil fraction for basaltic sites.

Site	Depth	Na	K	Mg	Ca	Sr	Acidity	Al	ECEC	Base Sat.	Ca/Sr	$^{87}Sr/^{86}Sr$
	cm	μg g^{-1}, exchangeable					cmol(+)/kg			%	molar	
NFT	0-10	12.6	332	167	1089	6.01	1.43	1.40	9.14	84.4	396	0.70628
	10-20	9.26	184	94.5	480	3.58	3.64	3.43	7.32	50.3	293	0.70622
	20-30	9.80	107	152	528	3.77	3.97	3.82	8.17	51.4	306	---
	30-40	10.5	116	105	371	2.55	4.74	4.39	7.79	39.2	318	---
	40-50	10.4	106	67.9	375	3.27	5.49	5.15	8.24	33.4	251	0.70663
Jensen	0-10	15.1	503	316	1596	7.75	0.54	0.64	12.5	95.7	450	0.70748
	10-20	10.5	228	266	893	5.43	2.99	2.72	10.3	70.9	359	0.70756
	20-30	10.7	246	402	917	6.24	3.91	3.52	12.5	68.6	321	---
	30-40	11.6	231	385	803	5.97	3.49	2.97	11.3	69.1	294	---
	40-50	8.88	189	278	638	5.04	3.62	3.54	9.6	62.3	277	0.70768
Stein	0-10	14.9	393	278	1183	9.38	3.2	3.1	12.4	74.6	276	0.70703
	10-20	11.4	290	172	606	4.17	6.8	6.5	12.0	43.6	318	0.70709
	20-30	11.6	295	173	477	3.23	8.73	8.35	13.3	34.6	323	---
	30-40	11.9	193	146	357	2.57	9.41	9.30	12.9	27.3	304	---
	40-50	10.7	145	115	395	4.09	10.2	10.2	13.5	24.6	212	0.70753
19	0-10	36.1	345	1040	1379	30.5	8.01	7.63	24.5	67.3	98.8	0.70663
	10-20	36.6	200	756	979	22.7	6.62	6.09	18.4	64.0	94.4	0.70663
	20-30	29.8	184	948	936	19.7	6.19	6.82	19.3	67.9	104	---
	30-40	27.4	131	624	687	14.5	8.79	8.25	17.8	50.6	104	---
	40-50	19.4	75.4	195	177	4.82	10.61	10.24	13.38	20.7	80.2	0.70719

Table 4 continued. Exchangeable soil chemical properties, Ca/Sr ratios, and $^{87}Sr/^{86}Sr$ ratios of < 2 mm in diameter soil fraction for basaltic sites.

Site	Depth	Na	K	Mg	Ca	Sr	Acidity	Al	ECEC	Base Sat.	Ca/Sr	$^{87}Sr/^{86}Sr$
	cm	μg g^{-1}, exchangeable					cmol(+)/kg			%	molar	
WP	0-10	25.1	192	475	1394	17.2	4.43	4.22	15.9	72.1	177	0.70529
	10-20	22.2	113	311	417	6.65	8.97	7.94	14.0	35.9	137	0.70518
	20-30	20.3	82.4	416	486	6.60	9.36	7.74	15.5	39.6	161	---
	30-40	20.6	65.9	407	398	5.58	8.98	8.54	14.6	38.4	156	---
	40-50	17.2	47.2	452	472	6.19	8.57	7.78	14.8	42.2	167	0.70518
14B	0-10	23.8	439	455	1069	23.2	15.29	14.82	25.6	40.3	101	0.70534
	10-20	19.4	263	317	734	18.1	19.01	18.35	26.0	27.0	88.8	0.70530
	20-30	19.9	220	399	822	18.5	21.7	20.0	29.7	27.0	97.1	---
	30-40	25.3	236	541	1004	23.0	21.2	20.2	31.3	32.5	95.4	---
	40-50	24.8	169	433	970	25.0	20.56	19.42	29.5	30.3	84.8	0.70527
Hoag	0-10	15.2	213	118	491	6.02	5.71	5.46	9.75	41.4	178	0.70562
	10-20	13.3	156	62.4	222	3.32	6.03	5.57	8.11	25.6	146	0.70579
	20-30	13.8	130	61.2	187	3.78	5.54	4.99	7.37	24.8	108	---
	30-40	19.5	97.4	76.2	274	5.16	1.42	4.57	3.75	62.2	116	---
	40-50	17.8	71.1	23.3	96.8	2.53	3.7	3.47	4.6	20.37	83.5	0.70578
60	0-10	47.2	475	618	2090	31.5	15.62	14.57	32.6	52.0	145	0.70501
	10-20	46.2	415	598	2011	33.1	15.78	14.86	32.0	50.7	133	0.70495
	20-30	38.7	341	681	2005	31.6	14.8	14.5	31.4	52.9	139	---
	30-40	43.9	379	934	2898	39.4	12.7	11.7	36.0	64.7	161	---
	40-50	47.5	258	565	2136	37.2	8.90	8.55	25.1	64.5	125	0.70510

Table 4 continued. Exchangeable soil chemical properties, Ca/Sr ratios, and $^{87}Sr/^{86}Sr$ ratios of < 2 mm in diameter soil fraction for basaltic sites.

Site	Depth	Na	K	Mg	Ca	Sr	Acidity	Al	ECEC	Base Sat.	Ca/Sr	$^{87}Sr/^{86}Sr$
	cm	μg g^{-1}, exchangeable					cmol(+)/kg			%	molar	
8	0-10	26.5	422	1213	2856	20.7	5.3	4.8	30.7	82.8	302	0.70781
	10-20	24.1	380	1106	2316	17.2	6.9	6.5	28.6	75.9	295	0.70779
	20-30	28.1	203	920	1485	10.4	12.1	11.7	27.8	56.3	311	---
	30-40	27.9	218	930	1453	10.3	12.3	12.0	27.8	56.0	310	---
	40-50	11.0	107	477	678	5.94	13.13	12.47	20.8	36.7	249	0.70786
RR1	0-10	22.1	104	104	185	1.88	10.72	10.57	12.9	16.7	215	0.70832
	10-20	14.3	47.0	13.0	13.8	0.23	11.0	10.32	11.3	3.17	134	0.70857
	20-30	12.8	34.5	13.1	15.1	0.32	6.42	5.94	6.75	4.85	102	---
	30-40	12.2	35.6	13.1	18.3	0.40	5.59	5.20	5.94	5.79	100	---
	40-50	8.05	27.3	1.11	1.44	0.07	4.30	3.62	4.42	2.74	45.8	0.70919
BC1	0-10	22.1	216	123	287	3.40	11.1	10.48	14.2	21.7	184	0.70816
	10-20	16.6	162	33.7	71.2	1.14	8.28	8.13	9.40	11.9	137	0.70823
	20-30	15.7	130	74.0	144	2.01	6.34	5.70	8.07	21.4	156	---
	30-40	17.8	101	67.5	122	1.83	5.72	5.23	7.22	20.8	146	---
	40-50	16.1	84.1	17.3	17.6	0.45	4.92	4.76	5.43	9.5	85.6	0.70857

Table 4 continued. Exchangeable soil chemical properties, Ca/Sr ratios, and $^{87}Sr/^{86}Sr$ ratios of < 2 mm in diameter soil fraction for mixed lithology sites (sedimentary and basaltic).

Site	Depth	Na	K	Mg	Ca	Sr	$Acidity_{TOT}$	Al	ECEC	Base Sat.	Ca/Sr	$^{87}Sr/^{86}Sr$
	cm	μg g^{-1}, exchangeable					cmol(+)/kg			%	molar	
54	0-10	26.5	269	245	690	7.0	6.42	6.13	12.7	49.4	215	0.70732
	10-20	20.1	268	114	259	3.2	6.45	6.13	9.45	31.8	179	0.70723
	20-30	20.3	70.3	51.2	56.7	0.8	7.24	5.76	8.21	11.8	159	---
	30-40	23.2	67.5	78.4	111	1.0	7.58	7.03	9.05	16.3	247	---
	40-50	16.1	116	94.5	105	2.3	9.46	9.18	11.1	15.0	99.0	0.70728
GV1	0-10	27.7	181	66.2	111	1.0	19.5	18.3	21.2	7.94	238	0.70856
	10-20	23.4	104	34.8	46.7	0.7	18.8	17.9	19.7	4.51	156	0.70876
	20-30	21.0	218	188	288	4.1	16.8	15.7	20.4	17.8	153	---
	30-40	19.3	155	150	216	3.4	16.6	15.7	19.4	14.4	140	---
	40-50	18.2	47.7	13.9	12.7	0.3	15.1	14.7	15.5	2.44	99.0	0.70908

Table 5. Residual soil chemical properties, Ca/Sr ratios, and $^{87}Sr/^{86}Sr$ ratios for sedimentary sites.

Site	Depth	Na	K	Mg	Ca	Al	Fe	P	Sr	Nb	Ca/Sr	$^{87}Sr/^{86}Sr$
	cm	mg g^{-1}						µg g^{-1}			molar	
Lake	0-10	10.1	18.0	8.28	5.04	81.2	28.2	543	188	16.9	58.7	0.71218
	10-20	10.3	18.9	9.03	5.09	89.9	30.9	433	187	18.3	59.6	0.71248
	20-30	11.0	18.8	7.99	4.55	87.7	32.7	461	189	18.8	52.5	---
	30-40	11.2	19.1	7.95	4.61	87.2	31.7	415	195	17.9	51.7	---
	40-50	10.2	18.3	7.98	4.53	86.1	34.0	441	186	18.1	53.3	0.71249
Devitt	0-10	3.75	15.33	6.32	2.50	80.1	39.5	1097	85.0	17.0	64.2	0.71633
	10-20	3.36	16.03	7.25	2.24	94.0	39.5	787	88.5	18.1	55.3	0.71732
	20-30	3.81	15.95	6.75	1.49	98.3	41.5	741	87.7	19.2	37.2	---
	30-40	3.33	15.65	6.88	1.24	102.6	43.2	646	83.7	19.8	32.4	---
	40-50	3.46	15.15	7.41	1.23	105.0	41.7	500	83.3	17.6	32.2	0.71647
Steere	0-10	5.55	15.2	7.74	2.31	82.6	36.9	719	85.7	16.5	59.0	0.71500
	10-20	5.90	15.5	8.08	2.40	90.8	40.5	681	93.5	18.1	56.1	0.71475
	20-30	6.44	15.7	8.03	2.20	98.4	44.5	700	97.1	21.0	49.5	---
	30-40	6.44	15.7	8.18	2.25	98.0	44.2	651	98.1	21.1	50.2	---
	40-50	6.41	14.0	8.41	2.17	88.8	43.7	562	86.7	19.5	54.8	0.71501
7	0-10	1.23	7.00	7.39	2.12	92.0	60.9	1331	35.3	13.6	132	0.71940
	10-20	0.96	7.45	8.17	1.72	105.8	67.8	1101	36.9	17.1	102	0.72050
	20-30	1.47	7.69	7.08	1.11	105.7	73.2	1105	34.3	17.0	70	---
	30-40	1.27	7.54	6.92	1.00	105.1	74.2	1078	33.2	16.9	66	---
	40-50	1.56	11.53	10.24	1.58	150.5	79.5	884	69.3	15.7	50	0.72177

Table 5 continued. Residual soil chemical properties, Ca/Sr ratios, and $^{87}Sr/^{86}Sr$ ratios for sedimentary sites.

Site	Depth	Na	K	Mg	Ca	Al	Fe	P	Sr	Nb	Ca/Sr	$^{87}Sr/^{86}Sr$
	cm	mg g^{-1}						µg g^{-1}			molar	
56	0-10	7.6	17.1	9.4	4.2	88.2	35.3	687	131.4	16.3	70.1	0.71462
	10-20	8.1	17.3	8.8	4.0	88.7	36.9	696	135.4	17.0	65.2	0.71386
	20-30	8.6	17.9	8.4	3.3	93.3	39.0	631	140.3	19.5	51.1	---
	30-40	8.7	17.8	8.5	3.3	92.1	38.6	608	141.6	19.0	51.3	---
	40-50	8.0	15.7	7.1	2.9	75.5	36.9	540	117.1	17.6	55.1	0.71407
43	0-10	10.5	14.5	6.9	5.9	69.6	30.1	1151	187	12.3	68.6	0.71092
	10-20	10.9	15.9	7.7	5.7	80.8	34.9	1136	194	13.1	64.3	0.71098
	20-30	11.8	16.2	7.6	5.8	81.4	37.9	1287	205	14.7	62.0	---
	30-40	11.5	16.3	7.7	5.6	82.5	37.1	1292	199	15.0	61.2	---
	40-50	11.4	17.4	8.1	5.8	92.5	38.0	1200	220	14.1	58.0	0.71109
Trask	0-10	2.67	7.24	8.65	2.35	82.1	60.3	1053	46.5	18.2	111	0.71333
	10-20	2.05	9.04	10.88	1.51	105.8	76.3	1102	41.6	22.4	79	0.71690
	20-30	2.64	7.90	9.07	1.46	97.3	77.9	1039	44.4	25.0	72	---
	30-40	2.58	6.97	7.90	1.59	87.4	76.7	1110	42.4	23.9	82	---
	40-50	2.86	7.87	9.50	1.70	99.6	74.8	1017	47.9	23.0	77	0.71620
HC1	0-10	4.34	10.63	6.48	2.10	76.2	38.9	1942	76.4	15.4	60	0.71535
	10-20	4.28	11.44	7.18	2.07	88.2	41.9	1707	81.4	17.2	56	0.71558
	20-30	5.06	12.63	7.38	2.07	97.5	46.6	1680	91.1	19.3	50	---
	30-40	4.97	12.59	7.48	2.05	97.7	47.2	1501	89.7	19.5	50	---
	40-50	5.13	12.52	7.78	1.94	93.9	45.9	1320	87.0	19.5	49	0.71619

Table 5 continued. Residual soil chemical properties, Ca/Sr ratios, and $^{87}Sr/^{86}Sr$ ratios for sedimentary sites.

Site	Depth	Na	K	Mg	Ca	Al	Fe	P	Sr	Nb	Ca/Sr	$^{87}Sr/^{86}Sr$
	cm	mg g^{-1}						µg g^{-1}			molar	
108B	0-10	1.66	7.69	10.44	2.00	83.8	64.3	1974	35.0	16.0	125	0.71596
	10-20	1.38	6.81	10.83	2.08	88.2	72.9	2105	36.8	20.1	123	0.71512
	20-30	1.48	6.15	7.98	1.12	71.3	75.5	1875	26.4	21.0	93	---
	30-40	1.58	6.78	8.09	1.18	83.0	75.6	1637	30.2	19.4	86	---
	40-50	1.93	7.04	9.20	1.34	89.4	73.6	1539	34.1	18.4	86	0.71772
Wow	0-10	3.03	7.54	4.56	1.69	61.7	30.8	845	57.2	13.8	65	0.71519
	10-20	3.09	9.53	6.31	1.81	90.3	40.7	806	71.7	17.2	55	0.71529
	20-30	4.17	10.70	6.49	1.79	98.7	46.5	868	78.3	19.4	50	---
	30-40	4.14	10.64	6.30	1.80	97.9	46.3	744	79.9	18.5	49	---
	40-50	4.28	9.83	5.67	1.65	81.5	43.0	597	72.8	20.2	50	0.71611
143	0-10	NA	NA	NA	NA	NA	NA	NA	NA	NA	NA	0.71545
	10-20	NA	NA	NA	NA	NA	NA	NA	NA	NA	NA	0.71603
	20-30	2.41	5.66	4.17	1.30	111	79.1	1046	45.5	24.7	63	---
	30-40	2.23	5.42	4.11	1.16	109	77.5	937	44.1	23.1	57	---
	40-50	NA	NA	NA	NA	NA	NA	NA	NA	NA	NA	0.71600

Table 5 continued. Residual soil chemical properties, Ca/Sr ratios, and $^{87}Sr/^{86}Sr$ ratios for basaltic sites.

Site	Depth	Na	K	Mg	Ca	Al	Fe	P	Sr	Nb	Ca/Sr	$^{87}Sr/^{86}Sr$
	cm	mg g^{-1}						μg g^{-1}			molar	
NFT	0-10	8.66	9.57	8.24	7.00	86.5	68.0	576	129.9	18.9	117.8	0.71213
	10-20	8.53	10.77	8.41	5.95	94.6	75.1	528	131.4	20.6	99.1	0.71391
	20-30	9.03	11.1	7.90	5.65	95.0	79.9	560	135.0	22.2	91.5	---
	30-40	8.29	10.2	7.60	5.15	90.9	73.8	491	122.2	20.2	92.1	---
	40-50	8.05	10.48	8.26	5.30	96.7	80.3	520	123.5	21.6	93.8	0.71383
Jensen	0-10	1.66	3.38	7.57	3.22	98.2	119	1090	33.8	25.8	208.6	0.71152
	10-20	1.48	4.49	9.35	2.88	122.1	128	890	34.8	28.5	181.4	0.71187
	20-30	1.85	4.82	7.91	2.04	120	135	920	30.3	32.1	147.4	---
	30-40	2.17	4.22	7.72	2.33	118	140	930	35.5	30.2	143.5	---
	40-50	1.07	2.60	6.30	2.00	91.5	125	707	28.4	27.4	153.8	0.71123
Stein	0-10	4.53	4.53	13.6	8.95	97.6	93.3	1130	79.0	12.7	247.7	0.70971
	10-20	4.15	4.56	15.6	9.38	108.2	104.3	933	69.3	12.9	295.9	0.71074
	20-30	4.53	4.29	14.6	8.66	105	110	963	66.1	15.7	286.7	---
	30-40	4.31	4.21	14.6	7.84	105	109	838	63.4	15.0	270.0	---
	40-50	4.60	4.41	16.1	8.47	102.6	111	807	68.6	14.7	269.7	0.71114
19	0-10	2.19	10.79	19.6	3.02	97.8	99.3	1302	102.3	47.2	64.6	0.70737
	10-20	2.95	10.28	18.1	3.78	106.8	105.8	1260	100.8	51.7	81.9	0.70849
	20-30	3.07	10.4	18.4	2.98	110	115	1507	90.1	55.9	72.4	---
	30-40	2.98	9.13	15.0	2.26	97.0	108	1225	72.7	51.0	68.1	---
	40-50	2.86	10.42	15.7	2.07	113.0	111.6	1147	78.5	52.6	57.7	0.71004

Table 5 continued. Residual soil chemical properties, Ca/Sr ratios, and $^{87}Sr/^{86}Sr$ ratios for basaltic sites

Site	Depth	Na	K	Mg	Ca	Al	Fe	P	Sr	Nb	Ca/Sr	$^{87}Sr/^{86}Sr$
	cm	mg g^{-1}						μg g^{-1}			molar	
WP	0-10	2.70	2.82	39.3	28.6	64.1	81.0	1749	86.5	24.8	722	0.70467
	10-20	2.53	3.08	42.1	38.3	71.6	93.7	1859	84.7	34.0	990	0.70445
	20-30	2.44	3.47	48.4	35.0	72.0	102.2	2040	78.2	35.1	978	---
	30-40	2.80	3.62	51.2	37.9	73.9	108.2	2080	83.4	35.0	993	---
	40-50	2.65	3.10	50.7	38.4	69.9	102.6	1706	79.9	NA	1050	0.70443
14B	0-10	1.73	6.73	16.6	1.99	89.8	88.9	1561	58.8	40.8	73.9	0.71000
	10-20	1.86	7.01	17.0	1.73	96.3	98.2	1571	56.2	45.5	67.3	0.71107
	20-30	2.29	7.08	16.9	1.34	96.5	102.0	1662	51.1	45.3	57.3	---
	30-40	2.12	6.78	17.9	1.19	96.3	104.0	1477	49.9	47.4	52.2	---
	40-50	2.11	6.40	18.5	1.30	95.8	99.8	1380	53.2	45.9	53.5	0.71092
Hoag	0-10	6.92	6.20	13.72	14.1	65.8	79.4	2457	100.9	44.3	305	0.70513
	10-20	8.12	7.39	16.07	15.4	85.2	105.5	2913	111.4	46.3	302	0.70502
	20-30	9.81	8.46	18.06	16.6	95.2	120.1	3050	127.5	55.6	284	---
	30-40	9.85	9.01	18.79	17.5	100.7	125.9	3025	125.4	55.8	305	---
	40-50	9.41	8.34	17.83	16.3	95.0	126.3	2794	122.3	54.9	291	0.70499
60	0-10	1.85	4.00	26.9	3.28	95.5	83.4	1003	54.2	9.7	132	0.70645
	10-20	1.72	4.50	30.0	4.25	107.4	97.5	1106	57.2	13.2	162	0.70611
	20-30	2.14	4.64	28.8	3.10	100.4	95.1	1308	49.1	14.4	138	---
	30-40	1.82	4.81	31.2	3.52	103.2	99.5	1202	51.2	14.1	150	---
	40-50	2.57	4.07	29.7	3.88	101.9	96.6	1161	56.1	12.9	151	0.70657

Table 5 continued. Residual soil chemical properties, Ca/Sr ratios, and $^{87}Sr/^{86}Sr$ ratios for basaltic sites.

Site	Depth	Na	K	Mg	Ca	Al	Fe	P	Sr	Nb	Ca/Sr	$^{87}Sr/^{86}Sr$
	cm	mg g^{-1}						μg g^{-1}			molar	
8	0-10	0.50	9.99	26.67	3.96	74.5	91.3	2253	107	34.2	81	0.70643
	10-20	0.58	11.73	29.18	3.88	88.5	107.9	2369	117	38.1	72	0.70613
	20-30	1.08	12.46	29.51	2.45	90.0	114.1	2237	120	41.4	44	---
	30-40	1.00	12.57	32.36	2.55	93.8	119.3	2158	121	43.4	46	---
	40-50	1.30	13.12	32.67	2.70	97.0	120.0	1817	125	42.0	47	0.70634
RR1	0-10	3.01	6.14	7.10	2.95	78.2	69.2	1461	64.3	34.1	100	0.71078
	10-20	4.07	7.98	9.43	3.31	106.3	92.5	1734	78.2	38.9	92	0.71127
	20-30	4.53	8.11	8.81	3.21	107.5	95.6	1683	80.4	42.9	87	---
	30-40	4.79	8.49	9.23	3.49	110.3	97.7	1453	86.8	42.5	88	---
	40-50	4.87	9.12	10.13	3.49	113.8	98.1	1389	88.6	42.4	86	0.71114
BC1	0-10	3.07	6.33	9.80	2.67	72.0	65.8	1452	72.5	30.7	80	0.71052
	10-20	3.90	8.06	13.35	2.55	101.4	87.9	1527	80.4	35.4	69	0.71114
	20-30	4.35	6.80	11.54	2.13	80.0	94.0	1590	67.2	41.6	69	---
	30-40	4.53	6.81	11.54	2.35	88.9	91.4	1505	71.7	39.4	72	---
	40-50	4.71	8.33	14.12	2.38	105.3	95.3	1408	82.1	42.4	63	0.71178

Table 5 continued. Residual soil chemical properties, Ca/Sr ratios, and $^{87}Sr/^{86}Sr$ ratios for mixed lithology sites.

Site	Depth	Na	K	Mg	Ca	Al	Fe	P	Sr	Nb	Ca/Sr	$^{87}Sr/^{86}Sr$
	cm	mg g^{-1}						µg g^{-1}			molar	
54	0-10	1.30	3.97	8.31	2.58	85.3	79.2	1337	41.5	15.2	136	0.71221
	10-20	1.18	4.75	10.57	1.92	112.1	97.7	1254	37.8	20.1	111	0.71439
	20-30	1.91	4.39	8.27	1.44	98.1	105	1335	35.0	21.4	90	---
	30-40	1.83	3.56	6.83	1.34	78.8	101	1281	32.0	20.7	91	---
	40-50	1.30	4.67	9.87	1.29	100.0	83.5	909	31.9	17.1	88	0.71523
GV1	0-10	1.41	4.11	4.29	1.51	71.3	55.6	733	36.0	16.9	92	0.71381
	10-20	NA	NA	NA	NA	NA	NA	NA	NA	NA	NA	0.71333
	20-30	2.48	5.18	4.85	1.81	95.2	77.6	819	47.8	20.5	83	---
	30-40	2.17	4.71	4.43	1.60	88.3	72.1	772	42.3	18.7	83	---
	40-50	NA	NA	NA	NA	NA	NA	NA	NA	NA	NA	0.71357

Table 6. Soil physical properties and chemical indices of soil formation for fine (<2 mm diameter) and coarse (>2 mm diameter) soil fractions, and on a whole soil basis from 0-50 cm depth for sedimentary sites.

Site	Soil Pool	Depth	Bulk Density	Coarse Soil Fragments	CIA	WIP	τCa	τAl	τFe
		cm	g cm^{-3}	%, by mass			Nb normalized, molar		
Lake	Residue	0-10	0.65	22.9	80.1	27.6	8.17	-0.50	0.59
	Residue	10-20	1.00	8.23	80.7	28.9	6.50	-0.51	0.57
	Residue	20-30	1.01	6.84	80.5	28.9	9.40	0.46	0.88
	Residue	30-40	1.09	4.63	79.9	29.4	10.09	0.52	0.91
	Residue	40-50	1.11	4.05	80.8	27.9	6.27	-0.33	0.76
	Coarse Soil	40-50	---	---	82.0	25.4	6.27	-0.33	0.76
	Whole Soil	0-50	---	---	80.6	28.3	7.92	-0.06	0.76
Devitt	Residue	0-10	0.73	8.99	89.0	19.3	-0.87	-0.21	0.03
	Residue	10-20	0.77	20.8	89.4	19.8	-0.89	-0.12	-0.03
	Residue	20-30	0.78	16.4	89.9	19.8	-0.93	-0.14	-0.04
	Residue	30-40	0.50	33.0	90.6	19.2	-0.95	-0.12	-0.03
	Residue	40-50	0.72	22.9	90.5	18.9	-0.94	0.01	0.06
	Coarse Soil	40-50	---	---	88.7	14.9	-0.94	-0.31	0.10
	Whole Soil	0-50	---	---	89.6	18.5	-0.92	-0.16	0.02
Steere	Residue	0-10	0.38	46.9	86.9	20.8	0.10	0.02	0.25
	Residue	10-20	0.51	31.4	87.4	21.5	0.04	0.02	0.25
	Residue	20-30	0.67	17.9	88.0	22.0	-0.18	-0.05	0.18
	Residue	30-40	0.79	27.7	87.8	22.0	-0.16	-0.05	0.17
	Residue	40-50	0.93	25.6	87.3	20.5	-0.13	-0.08	0.25
	Coarse Soil	40-50	---	---	80.1	25.0	0.75	-0.06	0.35
	Whole Soil	0-50	---	---	85.4	22.4	0.15	-0.04	0.25
7	Residue	0-10	0.51	15.3	98.4	9.5	3.82	-0.24	-0.33
	Residue	10-20	0.59	9.61	97.9	9.8	2.11	-0.30	-0.40
	Residue	20-30	0.71	8.71	97.9	10.1	1.02	-0.30	-0.35
	Residue	30-40	0.76	11.6	98.0	9.7	0.83	-0.29	-0.34
	Residue	40-50	0.82	17.4	96.1	14.5	2.12	0.09	-0.23
	Coarse Soil	40-50	---	---	99.1	8.4	6.46	-0.23	0.19
	Whole Soil	0-50	---	---	97.8	10.6	2.44	-0.20	-0.26

Table 6 continued. Soil physical properties and chemical indices of soil formation for fine (<2 mm diameter) and coarse (>2 mm diameter) soil fractions, and on a whole soil basis from 0-50 cm depth for sedimentary sites.

Site	Soil Pool	Depth	Bulk Density	Coarse Soil Fragments	CIA	WIP	τCa	τAl	τFe
		cm	g cm^{-3}	%, by mass			Nb normalized, molar		
56	RES	0-10	0.52	34.3	84.1	24.9	3.06	0.13	0.30
	RES	10-20	0.48	14.5	84.0	25.3	2.72	0.08	0.30
	RES	20-30	0.61	12.8	84.2	26.2	1.64	0.00	0.20
	RES	30-40	0.71	10.6	84.0	26.1	1.74	0.01	0.22
	RES	40-50	0.85	6.21	82.8	23.2	1.63	-0.11	0.26
	CRF	40-50	---	---	75.2	23.0	2.28	-0.39	0.34
	Whole Soil	0-50	---	---	82.4	24.7	2.09	-0.06	0.27
43	RES	0-10	0.45	37.0	80.9	24.5	-0.38	0.04	0.36
	RES	10-20	0.41	32.3	82.2	26.2	-0.43	0.14	0.49
	RES	20-30	0.42	31.8	82.0	27.3	-0.49	0.02	0.43
	RES	30-40	0.42	32.2	82.5	27.1	-0.52	0.01	0.38
	RES	40-50	0.49	31.0	83.2	28.2	-0.46	0.21	0.50
	CRF	40-50	---	---	72.9	27.4	-0.46	-0.27	0.20
	Whole Soil	0-50	---	---	79.1	26.9	-0.46	-0.03	0.35
Trask	RES	0-10	0.41	28.0	95.4	11.1	39.07	1.88	1.64
	RES	10-20	0.34	41.6	96.5	12.6	19.92	2.01	1.71
	RES	20-30	0.36	39.1	96.2	11.6	17.12	1.49	1.48
	RES	30-40	0.42	36.2	96.7	10.5	19.59	1.34	1.56
	RES	40-50	0.46	36.6	96.0	11.9	21.89	1.77	1.59
	CRF	40-50	---	---	95.2	11.8	7.28	2.45	2.72
	Whole Soil	0-50	---	---	95.8	11.6	17.76	1.97	2.00
HC1	RES	0-10	0.57	8.30	95.5	15.2	0.72	-0.05	0.31
	RES	10-20	0.59	3.03	94.7	16.1	0.52	-0.01	0.27
	RES	20-30	0.78	4.23	93.8	17.8	0.35	-0.03	0.26
	RES	30-40	0.60	4.28	93.3	17.7	0.33	-0.03	0.27
	RES	40-50	0.76	7.16	92.4	17.8	0.26	-0.07	0.23
	CRF	40-50	---	---	89.4	18.1	0.24	-0.26	0.44
	Whole Soil	0-50	---	---	93.6	17.1	0.41	-0.05	0.28

Table 6 continued. Soil physical properties and chemical indices of soil formation for fine (<2 mm diameter) and coarse (>2 mm diameter) soil fractions, and on a whole soil basis from 0-50 cm depth for sedimentary sites.

Site	Soil Pool	Depth	Bulk Density	Coarse Soil Fragments	CIA	WIP	τCa	τAl	τFe
		cm	g cm^{-3}	%, by mass			Nb normalized, molar		
108B	RES	0-10	0.45	42.4	100.5	11.0	3.17	-0.27	-0.08
	RES	10-20	0.48	28.1	101.9	10.0	2.45	-0.39	-0.17
	RES	20-30	0.51	37.6	102.6	8.8	0.78	-0.53	-0.17
	RES	30-40	0.50	33.8	100.4	9.5	1.03	-0.41	-0.11
	RES	40-50	0.51	37.4	99.3	10.2	1.45	-0.32	-0.08
	CRF	40-50	---	---	98.1	12.2	0.90	-0.46	-0.19
	Whole Soil	0-50	---	---	99.9	10.7	1.43	-0.41	-0.15
Wow	RES	0-10	0.33	21.5	92.8	10.8	0.26	0.07	0.52
	RES	10-20	0.52	11.7	93.4	13.1	0.08	0.27	0.62
	RES	20-30	0.66	11.0	92.8	15.1	-0.05	0.23	0.64
	RES	30-40	0.65	11.0	92.4	15.0	0.00	0.28	0.71
	RES	40-50	0.75	14.0	90.9	14.1	-0.16	-0.03	0.46
	CRF	40-50	---	---	92.3	12.0	-0.65	-0.09	0.69
	Whole Soil	0-50	---	---	92.3	13.7	-0.09	0.13	0.61
143	RES	0-10	0.38	3.95	NA	NA	NA	NA	NA
	RES	10-20	0.45	2.45	NA	NA	NA	NA	NA
	RES	20-30	0.54	2.24	98.2	8.3	-0.93	-0.15	0.40
	RES	30-40	0.51	2.41	98.1	7.9	-0.93	-0.10	0.46
	RES	40-50	0.63	1.30	NA	NA	NA	NA	NA
	CRF	40-50	---	---	96.2	7.6	-0.93	-0.41	0.70
	Whole Soil	0-50	---	---	NA	NA	NA	NA	NA

Table 6 continued. Soil physical properties and chemical indices of soil formation for fine (<2 mm diameter) and coarse (>2 mm diameter) soil fractions, and on a whole soil basis from 0-50 cm depth for basaltic sites.

Site	Soil Pool	Depth	Bulk Density	Coarse Soil Fragments	CIA	WIP	τCa	τAl	τFe
		cm	g cm^{-3}	%, by mass			Nb normalized, molar		
NFT	Residue	0-10	0.62	9.12	85.1	18.8	-0.96	-0.41	-0.61
	Residue	10-20	0.83	12.8	86.1	19.7	-0.97	-0.41	-0.60
	Residue	20-30	0.89	6.55	86.0	20.2	-0.97	-0.45	-0.61
	Residue	30-40	0.87	5.67	86.5	18.6	-0.97	-0.42	-0.60
	Residue	40-50	1.01	10.2	87.2	18.9	-0.97	-0.42	-0.59
	Coarse Soil	40-50	---	---	50.8	15.3	-0.90	-0.84	-0.48
	Whole Soil	0-50	---	---	83.1	18.9	-0.96	-0.46	-0.59
Jensen	Residue	0-10	0.48	34.1	99	6.6	-0.97	-0.04	-0.16
	Residue	10-20	0.75	19.6	98	7.8	-0.98	0.08	-0.18
	Residue	20-30	0.85	14.4	98.2	7.9	-0.99	-0.06	-0.23
	Residue	30-40	0.95	10.3	98.2	7.6	-0.98	-0.02	-0.15
	Residue	40-50	1.09	8.35	98.9	4.9	-0.98	-0.16	-0.17
	Coarse Soil	40-50	---	---	87.3	12.2	-0.83	-0.03	0.04
	Whole Soil	0-50	---	---	96.6	7.7	-0.96	-0.05	-0.14
Stein	Residue	0-10	0.50	17.3	92.3	12.2	-0.91	-0.17	-0.33
	Residue	10-20	0.65	13.9	92.3	12.3	-0.90	-0.09	-0.26
	Residue	20-30	0.76	4.98	92.5	12.0	-0.93	-0.27	-0.36
	Residue	30-40	0.85	4.34	92.8	11.6	-0.93	-0.24	-0.34
	Residue	40-50	0.99	3.61	91.9	12.4	-0.92	-0.24	-0.32
	Coarse Soil	40-50	---	---	92.4	14.3	-0.88	-0.17	-0.11
	Whole Soil	0-50	---	---	92.3	12.3	-0.92	-0.21	-0.30
19	Residue	0-10	0.38	39.9	94.8	16.3	-0.97	-0.11	-0.16
	Residue	10-20	0.40	39.3	94.4	16.3	-0.97	-0.11	-0.18
	Residue	20-30	0.44	32.9	95.7	16.4	-0.98	-0.15	-0.18
	Residue	30-40	0.37	42.7	95.4	14.3	-0.98	-0.18	-0.15
	Residue	40-50	0.47	32.8	95.3	15.6	-0.98	-0.07	-0.15
	Coarse Soil	40-50	---	---	87.5	26.6	-0.94	-0.25	-0.10
	Whole Soil	0-50	---	---	92.3	19.8	-0.96	-0.17	-0.14

Table 6 continued. Soil physical properties and chemical indices of soil formation for fine (<2 mm diameter) and coarse (>2 mm diameter) soil fractions, and on a whole soil basis from 0-50 cm depth for basaltic sites.

Site	Soil Pool	Depth	Bulk Density	Coarse Soil Fragments	CIA	WIP	τCa	τAl	τFe
		cm	g cm^{-3}	%, by mass			Nb normalized, molar		
WP	RES	0-10	0.29	53.9	78.3	17.8	0.72	0.98	1.37
	RES	10-20	0.24	58.1	74.4	20.3	0.69	0.61	1.00
	RES	20-30	0.26	68.3	76.9	21.1	0.49	0.57	1.11
	RES	30-40	0.35	63.3	75.5	22.6	0.62	0.62	1.24
	RES	40-50	0.36	62.2	73.4	22.0	NA	NA	NA
	CRF	40-50	---	---	60.4	35.0	0.95	0.21	0.81
	Whole Soil	0-50	---	---	66.5	29.5	0.83	0.40	0.96
14B	RES	0-10	0.47	24.8	99.2	11.3	-0.96	0.30	0.07
	RES	10-20	0.35	28.2	99.3	11.7	-0.97	0.25	0.06
	RES	20-30	0.40	26.1	99.6	12.0	-0.98	0.26	0.11
	RES	30-40	0.38	30.9	99.2	11.7	-0.98	0.20	0.08
	RES	40-50	0.42	27.3	99.0	11.5	-0.98	0.24	0.07
	CRF	40-50	---	---	94.7	14.6	-0.94	0.78	0.32
	Whole Soil	0-50	---	---	98.0	12.4	-0.96	0.40	0.14
Hoag	RES	0-10	0.34	33.1	87.5	16.6	-0.85	-0.24	-0.42
	RES	10-20	0.32	29.8	89.4	19.4	-0.85	-0.06	-0.26
	RES	20-30	0.40	20.4	88.6	22.3	-0.86	-0.13	-0.30
	RES	30-40	0.50	24.9	88.2	23.2	-0.86	-0.08	-0.26
	RES	40-50	0.50	27.5	88.2	21.8	-0.86	-0.12	-0.25
	CRF	40-50	---	---	66.7	33.2	-0.44	-0.09	-0.01
	Whole Soil	0-50	---	---	82.5	24.3	-0.75	-0.11	-0.21
60	RES	0-10	0.18	71.0	97.7	10.9	-0.81	3.94	2.26
	RES	10-20	0.19	57.0	97.5	12.0	-0.82	3.05	1.78
	RES	20-30	0.20	69.3	98.5	12.1	-0.88	2.48	1.49
	RES	30-40	0.20	72.8	98.0	12.5	-0.86	2.65	1.66
	RES	40-50	0.25	65.0	97.5	12.1	-0.83	2.96	1.83
	CRF	40-50	---	---	85.5	22.5	-0.33	2.24	1.69
	Whole Soil	0-50	---	---	89.5	19.1	-0.50	2.48	1.72

Table 6 continued. Soil physical properties and chemical indices of soil formation for fine (<2 mm diameter) and coarse (>2 mm diameter) soil fractions, and on a whole soil basis from 0-50 cm depth for basaltic sites.

Site	Soil Pool	Depth	Bulk Density	Coarse Soil Fragments	CIA	WIP	τCa	τAl	τFe
		cm	g cm^{-3}	%, by mass			Nb normalized, molar		
8	RES	0-10	0.38	37.0	99.3	15.7	-0.84	1.98	1.87
	RES	10-20	0.38	34.7	98.7	17.9	-0.86	2.18	2.05
	RES	20-30	0.43	27.6	98.4	18.8	-0.92	1.98	1.96
	RES	30-40	0.43	25.1	98.0	19.4	-0.92	1.96	1.95
	RES	40-50	0.48	22.4	96.1	20.2	-0.91	2.16	2.07
	CRF	40-50	---	---	92.5	21.0	-0.75	2.00	2.03
	Whole Soil	0-50	---	---	96.4	19.2	-0.85	2.04	2.00
RR1	RES	0-10	0.37	11.3	97.1	10.1	-0.93	0.50	-0.02
	RES	10-20	0.40	8.67	96.9	13.2	-0.93	0.79	0.15
	RES	20-30	0.51	8.26	96.4	13.6	-0.94	0.64	0.08
	RES	30-40	0.55	6.10	95.2	14.3	-0.93	0.70	0.11
	RES	40-50	0.64	9.10	94.8	15.1	-0.93	0.76	0.12
	CRF	40-50	---	---	95.2	15.5	-0.91	0.01	0.21
	Whole Soil	0-50	---	---	95.8	13.7	-0.93	0.63	0.10
BC1	RES	0-10	0.38	18.5	96.9	10.8	-0.88	2.21	1.30
	RES	10-20	0.45	16.4	96.5	13.7	-0.90	2.92	1.67
	RES	20-30	0.51	13.0	96.9	12.5	-0.93	1.63	1.43
	RES	30-40	0.56	16.5	96.5	12.7	-0.92	2.09	1.49
	RES	40-50	0.61	8.89	95.7	14.7	-0.92	2.40	1.42
	CRF	40-50	---	---	92.5	21.0	-0.75	2.00	2.03
	Whole Soil	0-50	---	---	95.9	14.2	-0.89	2.21	1.55

Table 6 continued. Soil physical properties and chemical indices of soil formation for fine (<2 mm diameter) and coarse (>2 mm diameter) soil fractions, and on a whole soil basis from 0-50 cm depth for mixed lithology sites.

Site	Soil Pool	Depth	Bulk Density	Coarse Soil Fragments	CIA	WIP	τCa	τAl	τFe
		cm	g cm^{-3}	%, by mass			Nb normalized, molar		
54	RES	0-10	0.34	26.6	100.0	6.9	-0.81	-0.30	-0.14
	RES	10-20	0.48	14.5	99.8	7.8	-0.89	-0.31	-0.20
	RES	20-30	0.58	13.7	100.2	7.5	-0.93	-0.43	-0.19
	RES	30-40	0.65	13.9	100.8	6.4	-0.93	-0.53	-0.20
	RES	40-50	0.74	10.9	98.8	7.6	-0.92	-0.27	-0.20
	CRF	40-50	---	---	99.2	10.8	-0.94	-0.32	0.09
	Whole Soil	0-50	---	---	99.8	7.8	-0.91	-0.37	-0.15
GV1	RES	0-10	0.48	5.60	97.6	6.1	-0.61	-0.42	-0.11
	RES	10-20	0.24	7.94	NA	NA	NA	NA	NA
	RES	20-30	0.42	2.55	96.8	8.2	-0.61	-0.36	0.03
	RES	30-40	0.43	3.39	97.1	7.4	-0.62	-0.35	0.05
	RES	40-50	0.56	5.50	NA	NA	NA	NA	NA
	CRF	40-50	---	---	NA	NA	NA	NA	NA
	Whole Soil	0-50	---	---	NA	NA	NA	NA	NA

Table 7. Coarse soil fragment chemical properties, Ca/Sr ratios, and $^{87}Sr/^{86}Sr$ ratios (40-50 cm depth)

Site	Na	K	Mg	Ca	Al	Fe	P	Sr	Nb	Ca/Sr	$^{87}Sr/^{86}Sr$
	mg g^{-1}						µg g^{-1}			molar	
Sedimentary											
Lake	11.71	18.71	8.34	6.24	77.8	76.4	1222	219.5	15	62.1	---
Devitt	3.43	11.15	7.01	1.26	68.8	41.7	425	64.1	17	42.8	---
Steere	9.15	16.23	8.86	3.40	70.6	36.8	470	114.7	15	64.7	---
7	0.97	5.65	9.07	2.82	79.6	92.3	1392	31.8	12	194	---
56	9.21	14.78	5.27	3.65	51.4	39.0	418	121.7	17	65.5	---
43	12.95	15.55	6.43	6.10	58.1	31.6	520	187.4	15	71.2	---
Trask	0.88	9.12	12.36	0.42	85.7	74.1	604	14.7	16	63.2	---
HC1	5.39	12.74	7.27	1.74	68.1	48.7	1283	78.8	18	48.2	---
108B	1.41	8.21	16.04	1.36	93.3	84.2	1348	24.5	24	121	---
Wow	2.45	9.22	5.78	0.64	70.2	46.0	557	44.6	19	31.5	---
143	1.50	5.49	5.17	1.11	66.6	83.6	691	28.8	21	84.4	0.71749
Basaltic											
NFT	11.0	3.8	5.0	11.1	16.3	63.2	657	92	13	263	---
Jensen	3.7	2.9	15.9	18.1	94.8	139.6	1016	51	25	774	---
Stein	5.0	4.1	21.6	12.5	104.7	133.7	1698	71	14	385	---
19	1.5	18.2	33.4	9.0	101.2	131.3	1188	173	59	113	0.70464
WP	7.7	5.5	61.1	62.6	74.1	103.8	1633	178	38	770	---
14	2.0	8.1	25.1	2.6	93.6	83.9	836	95	31	61	---
Hoag	8.9	7.6	48.2	50.7	74.4	126.7	2890	126	42	883	---
60	2.7	7.1	53.3	18.8	102.3	112.4	757	127	16	324	0.70517
8 & BC1	0.3	9.3	55.6	7.9	92.6	119.2	1121	107	42	161	0.70571
RR1	3.1	8.4	19.1	7.2	106.2	171.6	1871	50	69	313	0.70590
Mixed											
54	0.94	6.17	21.52	1.01	106.4	130.3	1113	21	20	107	---
GV1	NA	NA	NA	NA	NA	NA	NA	NA	NA	NA	NA

Table 8. Foliar chemistry, Ca/Sr ratios, and $^{87}Sr/^{86}Sr$ ratios.

Site	C	N	C/N	P	Na	K	Mg	Ca	Sr	Ca/Sr	$^{87}Sr/^{86}Sr$
Sedimentary	%		molar	μg g-1						molar	
Lake	50.7	1.45	40.8	1381	13.0	5862	1187	2426	10.2	519	0.70858
Devitt	51.2	1.43	41.9	1281	12.2	5500	946	2143	3.0	1563	0.70941
Steere	51.1	1.47	40.4	1132	20.9	5662	969	1374	3.3	922	0.70895
7	49.6	1.39	41.6	1389	18.5	5978	978	2099	1.9	2436	0.70955
56	51.3	1.65	36.3	1476	17.3	7271	957	2748	15.6	385	0.70916
43	52.5	1.68	36.4	1533	53.1	7927	823	1330	5.1	565	0.70802
Trask	51.0	1.44	41.2	1157	13.1	5153	1036	1767	4.2	915	0.70819
HC1	52.2	1.86	32.7	1718	18.0	6048	1283	1709	4.3	868	0.70911
108B	49.4	1.28	44.9	783	23.3	3331	714	1389	2.4	1292	0.70871
Wow	51.0	1.77	33.5	1196	33.7	5807	962	1256	1.2	2283	0.70896
143	52.6	1.69	36.3	1096	16.4	6634	880	1547	2.9	1154	0.70907
Basaltic											
NFT	50.3	1.4	42.6	1309	13.1	5740	1018	2595	4.7	1199	0.70617
Jensen	50.4	1.2	48.6	1027	16.7	6537	1313	2649	4.3	1336	0.70714
Stein	49.8	1.4	42.7	1405	9.5	5063	1008	2178	3.2	1485	0.70713
19	50.5	1.5	38.8	1142	28.7	4393	1024	2399	14.4	365	0.70669
WP	50.5	1.4	42.5	1548	6.9	5294	1046	1967	23.6	182	0.70460
14B	50.7	1.4	41.1	989	9.6	4143	932	1515	7.5	441	0.70579
Hoag	49.4	1.2	47.5	1176	9.7	4766	804	1407	2.7	1136	0.70549
60	51.2	1.6	37.9	1239	17.2	5061	864	2022	15.5	284	0.70453
8	51.3	1.6	37.2	1704	28.2	4922	786	1700	3.1	1202	0.70819
RR1	51.2	1.6	37.4	1277	19.1	4466	894	1472	2.8	1168	0.70815
BC1	50.9	1.5	39.9	1106	30.6	5052	941	1493	5.9	553	0.70844
Mixed											
54	50.21	1.49	39.4	1193	16.2	4203	757	1214	1.8	1506	0.70752
GV1	50.90	1.68	35.3	1263	37.3	4406	1073	1955	3.1	1399	0.70828

Table 9. Whole rock chemistry, Ca/Sr ratios, and $^{87}Sr/^{86}Sr$ ratios.

Site	Na	K	Mg	Ca	Al	Fe	P	Sr	Nb	Ca/Sr	$^{87}Sr/^{86}Sr$
	mg g^{-1}						µg g^{-1}			molar	
Sedimentary											
Lake	2.14	11.91	9.48	0.59	103.7	19.5	215	50.3	18.8	25.6	0.71937
Devitt	16.2	21.1	12.32	16.6	84.8	32.2	590	397	14.3	92	0.70872
Steere	7.61	24.1	9.45	2.22	86.0	31.4	428	107.1	17.5	45.4	0.71584
7	0.43	9.88	10.80	0.37	101.4	75.9	721	10.7	11.5	75.7	0.75260
56	4.13	23.3	12.25	1.29	97.0	33.5	475	100.5	20.1	28.0	0.71843
43	15.7	21.1	6.81	10.56	74.5	24.6	399	335	13.7	68.9	0.70968
Trask	0.26	4.79	13.0	0.18	85.4	68.5	1174	6.2	54.5	62.2	0.72324
HC1	4.88	20.9	12.64	1.43	93.7	34.6	606	81.0	18.0	38.5	0.72045
108B	1.06	11.35	9.63	0.38	91.4	55.2	588	22.2	12.7	37.4	0.73115
Wow	6.08	15.5	9.58	2.05	87.4	30.8	339	98.5	21.1	45.5	0.71532
143	15.1	17.97	11.52	11.19	79.5	34.6	631	341	15.1	71.7	0.70975
Basaltic											
NFT	18.2	1.76	38.4	84.8	77.1	90.8	668	218	9.9	852	0.70319
Jensen	18.6	3.02	36.7	82.3	75.4	104	1154	254	19.0	708	0.70337
Stein	11.5	2.17	45.1	64.6	78.1	93.2	737	181	8.5	779	0.70701
19	14.9	3.33	35.8	84.1	79.6	85.6	1497	526	34.4	350	0.70317
WP	23.7	7.33	24.1	42.5	82.2	88.4	2777	1744	64.0	53	0.70339
14	21.78	6.33	30.1	65.2	81.0	98	2119	852	47.9	167	0.70354
Hoag	11.5	4.08	63.2	74.4	67.0	105	1680	249	34.2	653	0.70410
60	24.8	5.39	34.5	73.5	82.5	109	2021	666	41.2	241	0.70349
8 & BC1	15.3	22.4	39.7	73.0	72.1	91.8	2004	564	98.6	283	0.70379
RR1	23.8	9.25	25.8	60.8	79.5	107	2180	473	52.1	281	0.70351
Mixed											
54	4.15	7.80	16.1	12.4	109.5	83.0	2200	508	13.6	53	0.70615
GV1	2.15	7.97	8.18	2.85	91.5	46.3	419	67	12.5	92	0.70777

Table 10. 1 M HNO_3 rock leachate chemistry, Ca/Sr ratios, and $^{87}Sr/^{86}Sr$ ratios.

Site	P	Na	K	Mg	Ca	Sr	Ca/Sr	$^{87}Sr/^{86}Sr$
	µg g^{-1}						molar	
Sedimentary								
Lake	128	36	779	811	86	2.8	67.8	0.71516
Devitt	481	329	1930	5081	4413	65.7	146.8	0.70805
Steere	116	83	1439	2623	547	19.3	62.1	0.71158
7	<IDL	44	794	1983	205	3.2	141.4	0.71347
56	211	50	1348	2418	739	30.9	52.3	0.71141
43	158	198	1110	3437	1723	39.1	96.4	0.70811
Trask	251	28	585	3936	109	1.6	146.7	0.71399
HC1	239	58	1161	1696	525	12.7	90.4	0.71223
108B	103	29	866	849	258	2.5	229.5	0.71478
Wow	132	71	1111	2245	131	4.0	71.1	0.71723
143	350	211	878	5286	2717	64.9	91.5	0.70797
Basaltic								
NFT	528	1965	149	7110	8308	38	472	0.70384
Jensen	1087	1500	153	7307	7632	29	576	0.70326
Stein	537	1058	95	11052	9485	24	864	0.70374
19	1284	1491	177	9424	14737	94	342	0.70365
WP	2513	18249	283	13420	20107	1224	36	0.70357
14	<IDL	108	22	22171	3098	59	115	0.70719
Hoag	1487	552	279	14265	4611	30	332	0.70380
60	1651	6702	447	4725	10860	251	94	0.70400
8 & BC1	1426	11637	253	15094	25844	195	290	0.70402
RR1	1965	809	378	3530	5774	27	473	0.70372
Mixed								
54	1327	197	623	5490	7379	195	83	0.70569
GV1	207	85	784	1812	5053	51	216	0.70679

Table 11. Open rainfall base cation concentrations, Ca/Sr ratios, and $^{87}Sr/^{86}Sr$ ratios.

Site	Sampling Date	Na	K	Mg	Ca	Sr	Ca/Sr	$^{87}Sr/^{86}Sr$
			μM			nM	molar	
143a	2/21/13	131	4.42	15.1	3.94	26.8	147	0.70916
143b	2/21/13	135	4.42	15.7	4.05	27.7	147	0.70918
143a	4/4/13	56.4	2.59	5.90	2.12	12.7	167	0.70904
143b	4/4/13	57.9	2.09	5.94	1.96	12.5	156	0.70920
143a	6/22/13	9.80	0.76	1.04	0.60	3.08	196	0.70903
143b	6/22/13	9.10	0.54	1.08	0.46	3.18	144	0.70871
7a	2/21/13	115	3.54	12.8	3.45	22.8	151	0.70919
7b	2/21/13	115	3.58	12.9	3.71	22.9	162	0.70922
7a	4/4/13	51.0	1.85	5.28	2.35	11.6	203	0.70892
7b	4/4/13	50.5	1.68	5.35	2.88	11.6	249	0.70898
7a	6/22/13	5.19	0.80	0.75	0.69	3.15	218	0.70861
7b	6/22/13	5.11	1.93	0.86	0.56	3.51	159	0.70901
GV1a	2/21/13	121	4.28	13.8	4.04	24.4	166	0.70921
GV1b	2/21/13	133	4.58	16.0	4.26	27.7	154	0.70919
GV1a	4/4/13	60.3	2.65	7.92	2.61	14.0	185	0.70924
GV1b	4/4/13	35.9	1.72	3.81	1.29	8.13	159	0.70925
GV1a	6/22/13	12.4	1.20	1.38	0.90	3.67	245	0.70897
GV1b	6/22/13	13.2	0.87	1.37	0.88	3.51	252	0.70906
						Weighted Average*	171	0.70916
						Seawater	118	0.7092

* - Average Ca/Sr weighted by average monthly precipitation for the 3 months of observation (February, April, and March: 10.86, 6.34, and 2.75 in, respectively (Western Regional Climate Center)). Average $^{87}Sr/^{86}Sr$ weighted by the monthly flux of Sr in precipitation (i.e. measured Sr conc. x average monthly precip).

Table 12. Percent atmospheric Sr and Ca of foliage.

Site	Rock Endmember	Atmospheric Sr (%) min	Atmospheric Sr (%) max	Atmospheric Ca (%) min	Atmospheric Ca (%) max
Sedimentary					
Lake	Rock Leachate	101	111	100	105
Devitt	**Soil Residue**	90	98	98	99
Steere	Rock Leachate	89	113	97	106
7	Rock Leachate	81	93	87	93
56	Rock Leachate	80	104	95	102
43	**Calcite Average**	-3	-2	-8	-2
Trask	Rock Leachate	108	122	105	125
HC1	Rock Leachate	86	105	94	103
108B	Rock Leachate	98	110	99	118
Wow	Rock Leachate	96	104	99	102
143	**Soil Residue**	92	104	98	101
Basaltic					
NFT	Rock Leachate	49	43	32	18
Jensen	Rock Leachate	73	65	52	30
Stein	Rock Leachate	70	61	38	20
19	Rock Leachate	61	54	52	32
WP	Rock Leachate	21	18	63	46
14B	**Ave. Tillamook Basalt**	42	37	65	47
Hoag	Rock Leachate	35	31	28	15
60	Rock Leachate	11	10	24	14
8	Rock Leachate	91	80	89	65
RR1	Rock Leachate	91	80	83	53
BC1	Rock Leachate	96	84	95	72
Mixed Lithology					
54	Rock Leachate	63	51	83	63
GV1	Rock Leachate	82	61	83	49

* - We used soil residue (40-50 cm depth) as the rock weathering endmember at sites Devitt and 143 because a calcite signal dominated the rock leach but was not reflected in plant or soil exchangeable pools, likely due to deep weathering below the rooting zone. A calcite signal also dominated the rock leach at site 143 and was reflected in plant and soil exchangeable pool. For this reason we used the $^{87}Sr/^{86}Sr$ ratio of Phanerozoic seawtaer (0.7078, Peterman 1970), which is the source of calcite in OCR sedimentary rocks, as our rock-weathering endmember. Lastly, our rock sample from site 14B displayed clear signs of weathering, so we used average $^{87}Sr/^{86}Sr$ and Sr/Ca ratios from the Tillimook Formation as our rock weathering endmember at this site.

Table 13. Correlations between soil N (%, 0-10 cm depth) and state factors of soil formation and ecosystem development

Table 10. Correlations between soil state factors and soil N concentration separated by rock type

	Basaltic Soil N (%, 0-10 cm)		Sedimentary Soil N (% 0-10 cm)	
Climate Factors	r	p-value	r	p-value
MAP (cm)	0.24	0.48	0.08	0.82
MAT (°C)	0.16	0.65	0.39	0.24
Distance from the Coast (km)	-0.79	**< 0.01**	-0.66	0.03
Organisms				
Stand Age (years)	0.43	0.24	-0.05	0.90
$\delta^{15}N$ (0-10 cm depth only)	-0.33	0.33	-0.76	**< 0.01**
Relief				
Slope (degrees)	0.37	0.26	0.24	0.48
Rock Depth (m)	0.56	0.15	0.32	0.34
Coarse Rock Fragments (mass %)	-0.10	0.77	-0.27	0.42
Parent Material				
Whole Rock Ca Conc. (mg/g)	-0.21	0.54	0.08	0.81
Rock-Leach Ca Conc. (mg/g)	0.53	0.09	< 0.01	0.99
Time				
Soil Redness Rating	0.85	**< 0.01**	-0.10	0.79
Effective cation exchange capacity	0.11	0.74	-0.16	0.65
Soil Residue Ca Conc. (mg/g, 0-10 cm depth)	-0.16	0.63	-0.43	0.18
Chemical index of alteration (CIA)	0.28	0.41	0.4	0.25
Weathering index of Parker (WIP)	-0.05	0.88	-0.49	0.15
Coarse rock fragment Ca Conc. (mg/g, 40-50 cm depth)	-0.02	0.95	-0.11	0.77
τ Ca	-0.23	0.5	-0.57	0.07

* - Bold values indicate statistical significance at the p = 0.01 level or less.

APPENDICES

Appendix A. Site characteristics of our fifty-four sampling sites in 2012

Site	Latitude	Longitude	Elevation	Distance from the Coast	MAP[1]	MAT[1]	Slope	Soil				Foliage			
								C	N	C/N	δ15N	C	N	C/N	δ15N
			(m)	(km)	(mm)	(°C)	(degrees)	(%)	(%)	(molar)	(‰)	(%)	(%)	(molar)	(‰)
Sedimentary															
Lake Creek	44.5698	-123.6933	298	30.1	1838	10.9	33	2.48	0.17	14.2	3.72	50.7	1.45	40.8	-1.12
77	44.7045	-123.6585	240	31.6	1878	10.5	19	4.30	0.25	17.4	3.17	51.9	1.74	34.8	-1.47
Steere	44.7287	-123.6359	374	33.3	2642	10.3	14	4.93	0.27	18.2	2.08	51.1	1.47	40.5	-1.97
Devitt	44.6413	-123.5348	230	41.9	1837	10.7	13	6.38	0.29	21.7	3.21	51.2	1.43	41.9	-0.66
5	44.6256	-123.8011	285	20.8	2070	10.9	14	5.20	0.31	16.9	2.41	51.1	1.68	35.4	-0.63
7	45.1261	-123.6439	286	26.7	2217	10.5	14	8.89	0.34	26.2	3.18	49.6	1.39	41.7	-1.92
Borba	45.2895	-123.7392	122	17.6	2440	11.0	20	5.42	0.35	15.5	1.89	49.9	1.30	44.7	-2.83
49	45.1295	-123.6927	281	22.7	2627	10.5	25	6.62	0.35	19.1	3.63	50.2	1.45	40.3	-1.73
58	44.7215	-123.8103	107	19.5	2119	11.0	16	6.44	0.36	17.8	2.89	50.4	1.81	32.4	-1.43
HC-2	44.6971	-123.8190	178	18.8	2046	10.7	13	5.97	0.36	16.5	2.75	52.2	1.96	31.1	-1.18
56	44.6997	-123.7386	333	25.2	2038	10.2	32	5.49	0.36	15.1	2.72	51.3	1.65	36.3	-1.48
54	45.1628	-123.6834	277	22.7	3227	10.6	17	7.98	0.39	20.5	2.40	50.5	1.55	38.1	-1.99
108B	45.3015	-123.6920	232	21.3	2740	10.9	43	7.55	0.45	17.0	2.61	49.4	1.28	44.9	-2.49
76	44.5798	-123.7999	228	21.5	1974	11.2	23	6.90	0.45	15.5	2.72	51.1	1.59	37.4	-1.00
Trask River	45.4620	-123.6222	303	26.8	2712	10.0	16	8.91	0.46	19.2	1.92	51.0	1.44	41.2	-1.87
32	45.1242	-123.7948	319	14.7	2869	10.5	6.6	12.1	0.50	24.0	3.03	51.1	1.44	41.4	-1.19
122	44.6944	-123.6551	209	31.9	1849	10.7	11	7.92	0.51	15.5	2.54	51.2	1.67	35.7	-1.71
30	45.8582	-123.7332	240	17.6	3019	9.70	10	11.5	0.54	21.5	2.69	50.8	1.40	42.3	-0.85
101	45.2969	-123.8113	232	11.9	2304	10.4	29	8.59	0.54	15.9	1.92	50.8	1.37	43.1	-1.85
HC-1	44.6760	-123.7908	126	21.2	1959	10.9	9.1	9.53	0.54	17.6	2.39	52.2	1.86	32.7	-1.38
6	45.2757	-123.6358	373	25.8	2936	10.6	21	10.7	0.60	17.9	0.87	50.7	1.36	43.3	-1.94
43	44.6927	-123.8531	117	16.1	2037	10.9	15	10.8	0.64	17.0	2.13	52.5	1.68	36.4	-1.48
NR-1	44.6904	-123.7087	307	27.6	1831	10.2	12	12.7	0.64	19.8	2.13	51.5	1.68	35.8	-0.77
Wow	44.6173	-123.8092	95	20.3	2050	11.7	32	11.6	0.68	17.2	2.00	51.0	1.77	33.5	-1.04
143	44.6890	-123.7977	224	20.5	2014	10.5	25	14.0	0.80	17.6	1.42	52.6	1.69	36.3	-1.89

Appendix A Continued. Site characteristics of our fifty-four sampling sites in 2012

Site	Latitude	Longitude	Elevation	Distance from the Coast	MAP[1]	MAT[1]	Slope	Soil				Foliage			
								C	N	C/N	δ15N	C	N	C/N	δ15N
			(m)	(km)	(mm)	(°C)	(degrees)	(%)	(%)	(molar)	(‰)	(%)	(%)	(molar)	(‰)
Basaltic															
NFT	45.4274	-123.3684	517	46.4	2160	9.20	6.3	3.81	0.20	19.2	4.12	50.3	1.38	42.5	-2.01
Jensen	44.5362	-123.4743	371	48.0	1927	10.6	17	4.31	0.23	19.1	5.12	50.4	1.21	48.6	-0.20
Steinberg Mnt.	45.4426	-123.3982	537	43.8	2275	9.20	14	4.95	0.24	20.8	2.27	49.8	1.36	42.7	-3.06
19	45.4380	-123.6300	241	25.6	2804	10.5	29	5.35	0.30	17.6	0.81	50.6	1.52	38.8	-2.00
Stone-B	45.4424	-123.6290	286	25.7	2778	10.2	50	6.34	0.32	20.1	2.66	52.0	1.58	38.4	-2.90
Bark Shanty	45.4443	-123.5661	158	30.6	2866	11.0	15	5.68	0.31	18.2	1.64	51.2	1.33	44.9	-3.13
WP	45.5817	-123.6201	592	25.7	3832	9.10	30	8.16	0.34	24.2	2.88	50.5	1.39	42.4	-3.33
Hoag Pass	45.2691	-123.4908	761	37.2	2559	8.90	14	7.98	0.38	20.8	2.85	49.4	1.21	47.6	-1.32
14B	45.3041	-123.6993	189	20.7	2737	11.1	17	7.20	0.48	15.0	2.55	50.7	1.44	41.0	-1.95
8	44.9995	-123.8698	265	11.2	2503	10.2	20	9.81	0.60	16.4	2.58	51.3	1.61	37.2	-1.81
RR1	45.7756	-123.7003	517	20.2	3171	8.70	23	16.9	0.68	24.9	1.84	51.2	1.60	37.4	-1.37
BC1	45.0030	-123.8776	173	10.5	2476	10.7	23	14.4	0.74	19.5	2.50	50.9	1.49	39.8	-2.01
27	45.7681	-123.7088	607	19.3	3192	8.3	24	17.9	0.82	21.8	1.91	52.1	1.41	43.1	-2.44
Chopping Block	45.3818	-123.7725	80	15.2	2506	10.9	3.8	14.4	0.82	17.6	2.35	51.4	1.56	38.4	-1.84
60	45.8050	-123.7038	204	20.2	3137	10.1	27	14.2	0.85	16.7	1.75	51.2	1.58	37.8	-2.15
GV1	45.7657	-123.7961	246	12.5	2866	9.90	9.9	18.2	0.85	21.4	3.13	50.9	1.68	35.3	-0.38
Mixed Lithology															
E. Beaver	45.2938	-123.8143	122	11.7	2276	10.9	24	5.27	0.36	14.8	2.45	50.6	1.43	41.3	-2.37
NF12	45.0699	-123.8108	346	14.6	2735	10.2	3.7	11.2	0.50	22.5	2.47	50.9	1.44	41.1	-0.54
RR-2	45.7654	-123.7359	419	17.1	3231	9.30	25	13.6	0.70	19.3	1.40	51.3	1.54	38.9	-2.41
SRC-1	44.9884	-123.8429	220	13.5	2866	10.4	12	14.7	0.76	19.3	2.50	50.6	1.41	41.8	-1.14
Rock Type Not Confirmed from Hand Sample															
S-1	44.5361	-123.7433	221	26.5	1934	11.3	18	4.41	0.25	17.3	2.93	52.2	2.12	28.7	-0.97
128	45.0948	-123.7424	207	19.5	2608	10.8	2.8	9.10	0.34	27.1	3.09	50.5	1.34	44.1	-1.13
S-1	44.5361	-123.7433	222	26.5	1936	11.3	18	6.96	0.41	17.1	3.29	51.4	1.66	36.2	-1.41
S-1	44.4967	-123.6740	463	32.2	2672	10.6	22	8.14	0.44	18.7	2.13	51.8	1.74	34.7	-2.02
Music Road	45.7984	-123.4128	480	43.1	2649	9.10	5.8	13.8	0.49	28.3	3.94	50.3	1.25	46.8	-2.82
35	45.8517	-123.7317	219	17.7	3007	9.80	0.0	13.1	0.64	20.6	3.89	50.6	1.64	35.9	-0.72

Appendix B. Quality control summary for NIST SRM2709a by ICP-OES

	Na	K	Mg	Ca	Al	Fe	Ti	P	Sr	Mn
				mg g^{-1}					µg g^{-1}	
Published	**11.6**	**20.3**	**15.1**	**18.9**	**75.0**	**34.9**	**3.40**	**620**	**231**	**538**
Average	**11.7**	**18.8**	**14.4**	**18.7**	**69.2**	**32.0**	**3.2**	**606**	**228**	**496**
2*SD	2.5	2.2	1.9	1.1	6.0	1.5	0.2	92	12	24
Date										
2/15/13	11.6	20.5	13.0	18.2	66.1	31.4	3.16	641	224	490
2/15/13	11.8	20.6	13.0	18.3	66.2	31.6	3.21	627	225	494
2/15/13	11.6	20.7	13.1	18.3	66.9	31.6	3.17	640	224	493
2/15/13	11.7	20.5	12.9	18.2	65.7	31.3	3.17	637	224	490
3/1/13	13.1	20.4	14.1	18.9	69.9	32.8	3.30	NA	228	501
3/1/13	13.1	20.5	14.0	18.9	69.7	32.8	3.31	NA	228	503
3/1/13	13.0	20.3	14.0	18.8	69.7	32.6	3.29	NA	227	501
3/1/13	13.1	20.4	14.0	18.9	69.6	32.9	3.32	NA	228	505
3/1/13	13.0	20.5	14.1	18.8	69.9	32.7	3.29	NA	228	500
4/19/14	13.2	16.7	13.2	18.9	61.9	31.5	3.18	633	211	503
4/19/14	13.7	17.9	14.5	19.5	67.2	32.8	3.32	617	230	522
4/19/14	12.7	16.9	13.9	18.3	64.2	30.6	3.09	585	217	485
4/19/14	12.9	17.5	14.5	19.0	66.5	31.2	3.11	658	219	498
4/19/14	13.4	18.9	16.1	19.7	72.4	32.6	3.24	678	236	517
4/19/14	13.1	18.4	15.8	19.1	70.9	31.6	3.16	637	232	501
4/19/14	13.2	17.3	14.0	19.1	64.9	31.8	3.21	637	219	507
4/19/14	13.3	16.7	13.3	18.7	62.3	31.5	3.20	587	214	503
8/23/13	12.0	18.6	14.0	18.4	68.6	32.0	3.16	532	228	492
8/23/13	11.9	18.5	14.0	18.3	68.3	31.8	3.15	529	227	489
8/23/13	12.0	18.8	14.1	18.5	69.2	32.2	3.17	533	229	491
8/23/13	12.0	18.6	14.0	18.4	68.5	32.0	3.16	539	228	492
8/23/13	11.9	18.6	14.0	18.4	68.5	31.9	3.15	526	228	490
10/31/13	11.3	17.9	14.4	18.0	68.9	31.0	3.10	622	226	484
10/31/13	11.5	18.1	14.7	18.3	69.6	31.6	3.14	620	228	491
10/31/13	11.6	18.0	14.9	18.4	70.1	31.9	3.17	630	230	495
10/31/13	11.3	17.9	14.7	18.0	69.2	31.3	3.08	616	227	481
10/31/13	11.5	18.0	14.5	18.1	69.1	31.3	3.12	632	226	488
10/31/13	11.4	18.0	14.4	18.1	69.2	31.2	3.12	617	226	488
6/19/14	11.3	18.8	14.4	18.7	70.6	31.9	3.06	635	229	487
6/19/14	10.6	18.9	14.4	18.7	70.6	31.8	3.07	625	229	491
6/19/14	10.6	19.0	14.4	18.8	70.5	31.7	3.07	595	231	491
6/19/14	10.4	18.8	14.6	18.9	71.0	32.0	3.10	579	232	495
6/19/14	10.7	19.1	14.3	18.5	70.6	32.0	3.08	612	231	488
6/19/14	10.3	18.9	14.3	18.6	70.2	31.6	3.05	591	227	485
6/19/14	10.1	18.7	14.2	18.4	69.7	31.6	3.02	563	226	482
6/19/14	10.0	18.5	14.3	18.5	70.0	31.8	3.05	592	227	484
7/30/14	12.0	18.9	15.5	19.6	72.0	32.1	3.14	661	241	500
8/26/14	11.1	18.5	14.0	18.3	69.8	31.2	2.97	563	225	476
8/26/14	10.9	18.4	14.0	18.1	68.7	31.3	2.95	482	225	477
9/19/14	11.8	19.6	16.8	20.0	75.9	34.1	3.24	652	240	515
9/19/14	8.6	19.8	16.7	20.1	76.1	33.7	3.29	676	240	522
9/19/14	8.2	19.0	16.7	20.3	75.6	34.0	3.28	630	236	529

Appendix C. Calculation for dust deposition flux to the Pacific Northwest during the last glacial maximum

1.5 g m^{-2} yr^{-1}	Dust deposition rate during the LGM (Mahowald et al., 1999)
x 68.8 mg g^{-1}	Average Ca conc. of China Plateau loess (Jahn et al., 2001)*
x 2000 yrs	Period of peak dust conc. in ice cores (Svensson et al., 2000)
x 10^{-6} kg mg^{-1}	Conversion factor
x 10^{4} m^{2} ha^{-1}	Conversion factor
= 2.06 Mg Ca ha^{-1}	

* Average of loess samples only (XN-2, XN-4, XN-6, XN-10, XF-2, XF-4, XF-6, XF-10, JX-2, JX-4, JX-6, and JX-10).

Appendix D. Calculation for Mazama ash flux to coastal Oregon forests

1.5 cm	Thickness of ash layer in OCR lakes (Long et al., 2007, 1998)
x 0.18	Ratio of Lost Lake to total catchment area (Long et al., 2007)
x 0.45 g cm^{-3}	Bulk density of volcanic ash (Sarna-Wojcicki et al., 1981)
x 21.4 mg g^{-1}	Average Ca conc. in pre-Mazama rocks (Bruggman et al., 1993)
x 10^{-6} kg mg^{-1}	Conversion factor
x 10^{8} cm^{2} ha^{-1}	Conversion factor
= 260 kg Ca ha^{-1}	